CORTICAL MECHANISMS OF VISUAL TARGET MEMORY AND MOVEMENT PLANNING AND EXECUTION FOR REACHES AND SACCADES IN HUMANS

DAVID CHRISTOPHER CAPPADOCIA

A DISSERTATION SUBMITTED TO THE FACULTY OF GRADUATE STUDIES IN PARTIAL FULFILLMENT OF THE REQUIREMENTS FOR THE DEGREE OF DOCTOR OF PHILOSOPHY

GRADUATE PROGRAM IN KINESIOLOGY AND HEALTH SCIENCE

YORK UNIVERSITY

TORONTO, ONTARIO, CANADA

APRIL 2018

Abstract

The cortical mechanisms for reach have been studied extensively, but directionally selective mechanisms for visuospatial target memory, movement planning, and movement execution have not been clearly differentiated in the human. It is also unclear how effector-specificity evolves in the human brain across these three phases for reaches and saccades. To study these phenomenon, an event-related fMRI design with three key phases was used to break apart a movement into target memory, movement planning and movement execution phases. In the first experimental chapter (chapter 2) directionally selective mechanisms were studied in a memory-guided reach task that informed the subject to perform a pro- or anti-reach after the target memory phase. Using the pro/anti instruction to differentiate visual and motor directional selectivity during planning, we found that one occipital area showed contralateral *visual* selectivity, whereas a broad constellation of left hemisphere occipital, parietal, and frontal areas showed contralateral *movement* selectivity. Temporal analysis of these areas through the entire memory-planning sequence revealed early visual selectivity in most areas, followed by movement selectivity in most areas, with *all* areas showing a stereotypical visuo-movement transition. Cross-correlation of these spatial parameters through time revealed separate spatiotemporally correlated modules for visual input, motor output, and visuo-movement transformations that spanned occipital, parietal, and frontal cortex. In the second experimental chapter (Chapter 3), effector-specific activation for reaches and saccades was studied using a similar design that informed subjects of the effector after the target memory phase. Our analysis revealed more medial (pIPS, mIPS, M1, and PMd) activity during both *reach planning* and *execution*, and more lateral (mIPS, AG, and FEF) activity only during *saccade execution*. These motor activations were bilateral, with a left (contralateral) preference for reach. Apart from right FEF, effector-specific contrasts comparing reach and saccade activation revealed significantly more parietofrontal activation for reaches than saccades during both planning and execution. Cross-correlation of reach, saccade, and reach-saccade activation through time revealed spatiotemporally correlated activation both within and across effectors in each hemisphere, but with higher correlations in the right hemisphere. Taken together, these results demonstrate highly distributed, coordinated occipital-parietal-frontal networks for both reach and saccade, with effector-specific activation.

Dedication

This dissertation is dedicated to my wife Valen and my son Sebastian

Table of Contents

List of Tables

List of Figures

Chapter One: General Introduction

To effectively interact with the world, a person takes in sensory information and uses it to interact with their environment in a meaningful way. Two of the most common cases of this are goal-directed eye movements (E.g., looking for your coffee mug on your desk or looking at a person when they enter the room) and goal-directed arm movements (E.g., reaching to and grasping a cup of coffee, pushing a doorbell, or working on a computer). These common, everyday tasks may seem simple at first glance, but the computations required for the brain to effectively use sensory information to guide meaningful actions are rather complex. Information from several sensory systems (E.g., vision, proprioception, & vestibular), movement control systems (eye, head, & arm), and cognitive factors (E.g. attention & memory) must be integrated to plan and perform an appropriate movement (Desmurget et al., 1998; Sabes 2000; Cohen and Andersen, 2002; Crawford et al., 2004, 2011; Goodale 2011).

Many studies in both humans and non-human primates have implicated regions of the brain in the visuomotor transformations required to plan eye and arm movements to visual targets (Monkey: Kalaska et al., 1997; Colby and Goldberg, 1999; Andersen and Buneo, 2002; Johnston and Everling, 2008; Andersen and Cui, 2009; Schall, 2013; Human: Goodale and Milner, 1992; Culham and Kanwisher, 2001; Rossetti et al., 2003; Culham and Valyear, 2006; McDowell et al., 2008; Pisella et al., 2009; Filimon, 2010; Crawford et al., 2011; Medendorp et al., 2011; Vesia and Crawford, 2012). When typical visually-guided reach and saccade studies are performed in humans, subjects are initially shown an object that they are instructed to look at or reach towards. It disappears, and after a memory delay they move towards the remembered location of that object. In patient studies, patients with focal brain damage to a region of interest

(E.g., parietal cortex) perform a similar task to infer the contributions of that brain region to saccade or motor planning (Khan et al., 2005, Granek et al., 2012, Ptak and Muri, 2013). In transcranial magnetic stimulation (TMS) experiments, magnetic pulses are applied over areas of interest during the memory delay period to causally investigate the role of these regions in movement planning (van Donkelaar et al., 2000, 2002; Vesia et al., 2006, 2008, 2010; Striemer et al., 2011). In event-related functional magnetic resonance imaging (fMRI) experiments, the memory delay is much longer and the blood oxygen level dependent (BOLD) response collected during this period is used as an indication of movement planning activity (DeSouza et al., 2000; Connolly et al., 2003; Medendorp et al., 2003, 2005a, 2005b; Fernandez-Ruiz et al., 2007; Beurze et al., 2007, 2009, 2010; Gallivan et al., 2011).

While it is known that several brain areas in parieto-frontal reach and saccade networks are involved in using remembered visual information for planning a reach or saccade to a goal, the fundamental question of how, where, and when visual information becomes action in the brain remains unanswered. Put another way, when moving to the remembered location of a visual target, the involvement of brain areas in the visual working memory representation of target position, movement planning, and movement execution remains unclear, as do any effector-specific aspects of movement planning and execution coding.

An important aspect of this that has not been studied for reach is the temporal evolution of visuospatial information into motor coordinates. The input to the brain for visually guided arm movements is retinotopic, as light initially hits a specific location on the human retina. The output from the system is the arm movement, which is coded in primary motor cortex (M1) in the preferred motor direction (Georgopoulos et al., 1982). It remains unclear how, where, and when the visuomotor transformation from retinotopic “visual” direction coordinates to motor “movement” direction coordinates required for visually-guided reach evolves in the brain.

This dissertation uses functional magnetic resonance imaging (fMRI) brain imaging to investigate: (1) The brain areas involved in visual target representation, motor planning, and motor execution for visually-guided reaching, (2) the evolution of visual and movement directional coding over time for visually-guided reaching, (3) brain areas involved in visual target representation, motor planning, and motor execution for visually-guided saccades, and (4) effector specificity in movement planning and execution for saccades and reaches.

1.1 Perception and Action

Darwin’s theory of evolution by natural selection states that given the genetic variation observed in populations of organisms, a heritable trait that increases the survival and reproduction of an organism can be selected over time and drive evolution (Darwin, 1859). Two key traits that have increased the survival and reproduction of many species including human beings (and our ancestors) are vision and movement. Our ability to use vision to guide movements provides clear advantages in hunting, protection, navigating, and child rearing among many other activities. In humans, visual information initially is encoded in two dimensions on the retina of both eyes. This information is then relayed from the eye to primary visual cortex (V1) in occipital cortex via the lateral geniculate nucleus (LGN).

In cortex, Ungerleider and Mishkin (1982) found evidence in non-human primates for two distinct visual pathways. One of these pathways extended ventrally from V1, interconnecting the striate, prestriate, and inferior temporal areas. This pathway processed perceptual information about the properties and identity of objects and was dubbed the ‘what’ stream. The other visual pathway extended dorsally from V1, interconnecting the striate, prestriate, and inferior parietal areas. This pathway processed spatial information about object and was dubbed the ‘where’ stream.

In humans, Goodale and Milner (1992) found evidence for two similar visual streams. By testing neuropsychological patients with damage to their ventral and dorsal visual streams using a dual dissociation design, they found evidence for a ventral ‘what’ perceptual stream projecting from primary visual cortex (V1) to inferotemporal cortex (similar to Ungerleider and Mishkin’s animal model). In the dorsal stream however, they found a key difference. In humans, the dorsal stream (which projects from V1 to posterior parietal cortex (PPC)) was not dependent on the input of spatial information as proposed by Ungerleider and Mishkin, but rather was defined by the output requirements of the motor system. The main evidence for this shift came from testing D.F., a visual form agnosia patient with damage to her ventral stream (lateral occipital and parasagital occipitoparietal regions). D.F. could not identify the size, shape, or orientation of objects, she could accurately grasp them. The guidance of both her hand and finger towards an object were not affected by the damage to her ventral stream (Goodale and Milner, 1992). They thus renamed the dorsal stream the ‘how’ stream, as it is responsible for using visual information to guide motor actions. While this theory has been challenged by Schenk (2006), who suggested that the deficits found in patient D.F. can be better explained as a deficit in world-centred target (allocentric) representations rather than purely perceptual, this framework remains influential and has been clarified to account for Schenk’s findings, as well as communication between these streams (Milner and Goodale, 2008; Goodale, 2011). This ‘action-perception’ model provides an account for the cortical processing of vision for perception and action (Figure 1). The next question to answer is how the spatial aspects of that information are coded in the brain.

1.2 Reference Frames and Transformations

As was mentioned earlier, the input to the visual system is the retina. Light hits the retina in each eye and is initially spatially coded in two dimensions (2-D). This information in each eye is used to perform complex three-dimensional actions (4-D if we want to consider time as an axis as the world tends to be more dynamic that the static

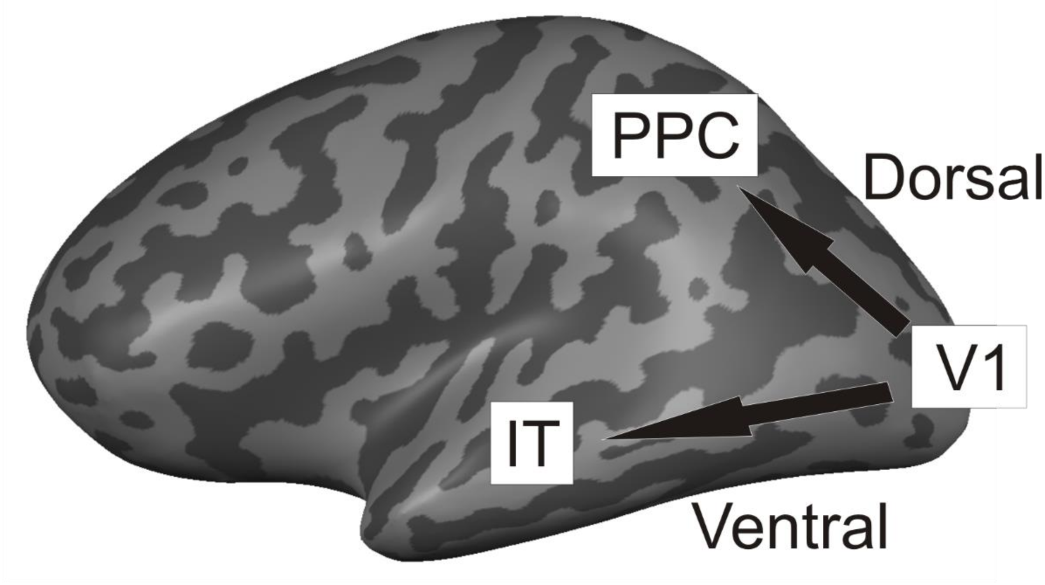

Figure 1. An illustration of the Goodale-Milner ventral and dorsal visual processing streams in human cortex (Adapted from Goodale and Milner 1992, 2008; Goodale 2011). The dorsal stream projects from primary visual cortex (V1) to posterior parietal cortex (PPC), and the ventral stream projects from V1 to inferotemporal cortex (IT). This framework is overlaid on the inflated brain on one representative subject. This is the medial view of the left hemisphere. The light grey areas represent gyri and the dark grey areas represent sulci.

representations found in many papers). How is this information spatially encoded in the brain and what transformations are required to move from a 2-D retinal representation to complex goal-directed movements? Before jumping in to answer questions about spatial coding and transformations it is useful to define a reference frame. For an object to be coded in space, it requires a reference frame. A reference frame is a rigid body with coordinate axes that can be used to define directions of rotation and translation of an object (Soechting and Flanders, 1992; Crawford et al., 2011). In the case of a retinotopic reference frame (also referred to as an eye-centred reference frame), the head is the rigid body that is used (E.g., the eye is moving 5º to the right). Head position is often reported with shoulder/torso as the reference frame. This is also used for gaze (eye-in-head).

To plan an eye or arm movement, the brain has to code a movement vector so that the eye and/or the arm can move from the current position towards the desired position (the goal). This can be done using feedforward mechanisms, which are internal models within the brain that can generate movement commands based on the initial state of both the external and internal environments (Soechting and Flanders, 1992; Crawford et al., 2011). Feedforward models are more useful than feedback models as they are faster (do not require the input of additional afferent sensory information to correct a movement) and predictive (in case the target is no longer visible, such as a rabbit that has run into the bushes). For a feedforward model to be useful, however, it requires accurate information about the position of the target (this information can be multisensory, and in real life most often is), the position of the effector acting on the target, and the spatial relationship between the two.

When coding the movement vector guiding a gaze shift to a visual target, the initial position of the effector is the same as the centre of gaze. Because of this, the movement vector can simply be calculated based on the target position relative to the retina. This becomes more complicated if fixation and the target are not in the same plane of depth. Recordings from neurons in the primate LIP have shown activity for both the difference in depth between fixation and the target and modulation for fixation position in depth, implying that neurons in LIP may account for this (Genovesio and Ferraina, 2004).

Unlike saccades, the relationship between the current and desired hand location for a visually guided reach is not fixed. It is therefore very important for the brain to have an accurate internal representation of the location of the effector. This can be done using visual information about the location of the hand, or proprioception of the hand position based on joint angles. Since a reach is a change in location, vector subtraction can be used to plan the translational movement. Sober and Sabes (2003) used models of feedforward motor planning to investigate how the initial hand position is coded for reach. By dissociating visual and proprioceptive feedback and measuring the resulting error patterns. They found that movement vector planning relies primarily on visual information. In contrast, computation of the intrinsic motor command relied more on proprioception. In another study, however, they found that the sensory modality of the target and content of visual feedback (the presence of joint angles) can affect these weightings (Sober and Sabes, 2005).

Once the movement vector coding a gaze shift or arm movement has been computed, the brain needs to send out a motor signal to guide the required action. Klier and Crawford (1998) investigated how the brain takes visual information about the distance between current and desired gaze position (referred to as the retinal error) and produces the motor command used by the saccade burst neurons that drive saccades (referred to as motor error). There were two proposed mechanisms. The first was a direct mapping of retinal error to motor error using a look-up table. The second was a reference frame transformation that transformed the eye-centred retinal error into head-centred coordinates. The former mechanism predicted gaze-dependent errors in the final gaze direction of up to 19.8 degrees, while the later did not. The behavioural data supported the reference frame transformation model. If the initial eye-centred target location is transformed into a head-centred representation, one must question where this happens. As mentioned in the section on spatial updating, Andersen and Mountcastle (1983) found gain fields in primate areas 7a and the lateral intraparietal sulcus (LIP). In a follow up study, Zipser and Andersen (1988) used a neural network model to transform target position from an eye-centred to a space-centred reference frame. They found that the artificial neurons from their study produced gain fields similar to those seen in parietal cortex. When these artificial neurons were viewed at the population level, placing more weighting on neurons with stronger gain fields and summing their outputs downstream could produce a novel spatial code downstream that may serve as the basis for the reference frame transformation. A neural network study was run my Smith and Crawford (2005) to model the 3-D reference frame transformation. In the study, 2-D gaze-centred visual receptive fields and efference copies of proposed eye movements were input into the model and an eye orientation displacement command similar to the one that drives the 3-D brain stem burst neurons was the output. In the model, the hidden units developed eye-centred visual receptive fields and were sensitive to eye position using representations similar to gain fields.

For arm movements, the brain must take in visual information about the location of the desired target and the initial position of the hand in a retinotopic reference frame (target: Batista et al., 1999; Crawford et al., 2004; hand: Buneo et al., 2002) and later use a shoulder-centred reference frame (Kalaska et al., 1997; Scott, 2002) to accurately plan the reach. Blohm and Crawford (2007) created a feed-forward model of the transformations required to perform the transformation from 2-D retinotopic information to an accurate 3-D reach, and compared the predictions of their model to experimental data. An important aspect of their model was accommodating for the rotations and translations (offsets in centres of rotations) between the eyes, head, and shoulder. The experimental data best matched the model that accounted for rotations and translations, indicating that before the brain has access to other sources of information (such as proprioception), a feed-forward plan of a desired reach that accounts for the 3-D linkage geometry between the eye to the shoulder is most likely utilized. In another study, Blohm et al. (2008) showed that when reaching to a target in depth, the brain must utilize 3-D eye and head orientation signals in addition to retinal disparity to perform accurate reaches in depth.

1.3 Visuospatial Working Memory

While saccades and reaches are often performed towards objects that are still visible, they are also often performed to objects that are no longer visible, and thus require memory of the object's position. When visual information must be stored for use in future target selection, visual working memory is involved.

1.3.1 Behaviour

One of the first modes of what we now refer to as visual working memory was put forth by Atkinson and Smith (1968). Their model, referred to as the multi-store or modal model of memory, sensory information was first maintained in the ‘sensory store’. This information was stored very briefly (less than a second), unless it was selected by visual attention to be maintained in short-term memory. Short-term memory lasted several seconds, and to be further maintained information had to be rehearsed or moved into long-term memory.

This model was later rethought by Baddeley and colleagues (Baddeley and Hitch, 1974; Baddeley, 1986), who retitled short-term memory as working memory to focus on the immediate storage function rather than the temporal duration. Baddeley proposed a multicomponent model of working memory, with separate stores for visual working memory and verbal working memory, both of which were controlled by another component of the model called the central executive.

One of the central experimental topics investigated to understand visual working memory (VWM) it its capacity. Luck and Vogel (1997; Vogel et al., 2001) came up with a very influential series of experiments looking at the capacity of VWM for objects defined by different (non-verbal) visual features. By leveraging a change detection task with a different number of objects with multiple visual features, they found that subjects could retain the features for roughly 4 items in VWM. Any more lead to significantly worst performance in the change detection task. Interestingly, subjects could remember up to 4 different objects defined by 4 features, suggesting that VWM stores integrated objects, referred to as the object file theory. Subsequent investigations (Olson and

Jiang, 2002; Alvarez and Cavanagh, 2004) found that both the number of objects and the number of visual features affect VWM capacity for object files.

Bays and Husain (2008) took a different approach to study VWM capacity. Instead of measuring how many objects subjects could remember, they tested the precision of item memory as a function of the number of objects present. By using a continuous scale to measure precision (object orientation, colour), they found that performance decreased when two items were shown instead of one. This led to a resource sharing model, where resources are shared between objects rather than all of the features being remembered for the limited objects that could be remembered.

In addition to the amount of information that can be stored in VWM and how that may be grouped, researchers have also investigated decay over time in VWM. Previous research has shown that information in working memory is lost rapidly (Posner and Keele, 1967). The nature of representation decay in VWM was thought to decay gradually over time (Cornelissen and Greenlee, 2000; Lee and Harris, 1996), but recent research by Zhang and Luck (2009) has shown that VWM of colours and shapes are held for 4 seconds without a significant loss in quality or quantity. After this time, there was a sharp decline, which they interpreted as a 'sudden death' of VWM.

1.3.2 Human Neuroscience

The neural basis of visual working memory has been studied extensively. In general terms, the right hemisphere has been linked to spatial working memory and the left hemisphere has been linked to non-spatial / object working memory by neuroimaging (Jonides et al., 1993,1998; D'Esposito et al., 1998; Smith et al., 1998). Within these hemispheres, spatial working memory has been linked by neuroimaging to prefrontal, premotor, parietal, and occipital brain regions (Jonides et al., 1998; Smith et al., 1998), while inferotemporal and parietal regions in the left hemisphere have been linked to non-sptatial / object working memory (Fuster et al., 1982; Smith et al., 1998).

Several specific frontal regions have been linked to visual working memory. For example, fMRI has shown that the right middle frontal gyrus shows increased activity for both spatial and non-spatial working memory tasks (D’Esposito et al., 1998). In another study, prefrontal region 8 (near the Frontal Eye Fields) showed increased activity during VWM maintenance, while the dorsolateral prefrontal cortex was shown to be involved in selection (Rowe et al., 2000). Also, the FEF shows sustained activity for spatial working memory information (Srimal and Curtis, 2008). Finally, the FEF has been shown to be involved in transsaccadic memory causally with TMS (Prime et al., 2010).

Parietal cortex has an interesting and important role in feature memory. Imaging data (fMRI) has shown that the posterior parietal cortex shows different activation when the feature capacity or VWM capacity is altered (Song and Jiang, 2006). Studies by Todd and Marois have shown that PPC activity is correlated to the scene information in VWM (2004), and that the level of activation in PPC indicates the VWM capacity across subjects (2005). There is thus a link between PPC activation and information / capacity. The superior parietal lobe also shows increased fMRI BOLD activity when more complex objects are remembered (Xu and Chun, 2006). The BOLD activity in this area has also been shown to correspond to the total amount of feature information to be remembered, rather than representing whole objects with feature integration occurring upstream (Xu, 2007). It should be noted that like the oculomotor system, there is a great amount of overlap in the neuroanatomy of working memory and attention (LaBar et al., 1999).

1.4 Visual and Memory-Guided Saccades

Humans can only view a small spotlight (the fovea) of the environment in high detail at any given point in time (Riggs, 1965). To scan an environment and obtain useful information, it is therefore critical that people perform eye movements. These include small eye movements such as slow drifts (Ditchburn, 1955), microsaccades (Ditchburn and Foley-Fisher, 1967), and tremors (Steinman et al., 1967), as well as larger eye movements. One type of larger eye movement is smooth pursuit, which allow people to track a moving object by moving the eyes at roughly the same speed and direction. This allows the object to be tracked with a stable image on the retina across the eye movement (Fuchs, 1967; Lisberger et al., 1987).

The other type of larger eye movement is used to foveate spatially separated targets and is called a saccade. Saccades are very important, as they allow a person to immediately foveate an object of interest, and they are performed about 3-5 times every second (Rayner, 1998).

In order to perform a visually-guided saccade, a person must select a visual target. This process relies on visual attention. Attention, a process by which a location in the visual field receives increased processing, can be shifted either overtly (with a gaze shift) or covertly (with fixation maintained) (Posner, 1980). Several studies have shown that that spatial attention shifts towards the location of a saccade prior to saccade onset (Shepherd et al., 1986; Crawford and Muller, 1992; Hoffman and Subramaniam, 1995; Kowler et al., 1995; Deubel and Schneider, 1996).

Once visual information is attended to, how is the goal of a saccade selected? Visual information necessary for object recognition can be accessed in peripheral vision if close enough to fixation (Geisler et al., 2006). When at fixation, items located between 5-6 degrees around fixation are well considered (Findlay et al., 2001; Kotowicz et al., 2010). Importantly, Kotowicz et al. (2010) showed that during free-viewing conjunction search, subjects can identify a target object before foveating it. Foveating the target increases selection confidence rather than performance. When the distance between fixation and a stimulus is much greater than that, motor performance tends to suffer in both single feature (Viviani and Swensson, 1982) and multiple feature conjunction search tasks (Carrasco et al., 1995). Unsurprisingly, there is also evidence that saccade target selection is faster when peripheral objects are very dissimilar from the target, as indicated by lower fixation duration in visual search (Hooge and Erkelens, 1999).

When a saccade is performed in the presence of distractors, the distractors seem to influence the saccade under certain circumstances. For example, Ottes et al. (1985) showed that when subjects performed a saccade to a colour-defined target near a distractor, the first saccade was generally at an averaged position (consistent with Findlay, 1995). If, however, subjects delayed their response, an accurate saccade was made. He and Kowler (1989, 1991) expanded on this by having people make a saccade to a predesignated location on a triangle. The accuracy of those saccades was only slightly worse then a saccade to a single point. This was taken as evidence that a voluntary selection process weighs information at different spatial locations and uses that information to compute the saccade output, with separate selection and targeting stages (also supported by Findlay and Blythe, 2009).

1.4.1 Animal Neurophysiology

The neurophysiology of saccades has been extensively studied and focused on three key areas: the lateral intraparietal area (LIP), the frontal eye fields (FEF), and the superior colliculus (SC).

The lateral intraparietal area (LIP) is located in the parietal cortex, and as such is a part of the dorsal visual processing stream (Ungerleider and Mishkin, 1982; Goodale and Milner 1992). The LIP takes up a large portion of the lateral wall of the intraparietal sulcus. It receives input from V2, V3, V3a, V4, MT, MST, and IT (Baizer et al., 1991; Blatt et al., 1990; Distler et al., 1993; Lewis and Van Essen, 2000). It also projects to FEF, the anterior cingulate cortex, and thalamic nuclei (Baizer et al., 1991; Blatt et al., 1990). High current /microstimulation of LIP can produce saccades (Thier and Andersen, 1998). LIP was initially termed a saccade planning area (Gnadt and Andersen, 1988). In a typical memory-guided saccade, LIP neurons show a visual burst of activity when a peripheral target is shown, elevated firing during the memory delay, and a small increase in activity at saccade onset (Barash et al., 1991). LIP neurons code the locations of stimuli in retinotopic coordinates (Andersen et al., 1990), and display predictive remapping prior to saccade onset (Duhamel et al., 1992).

The frontal eye field is located in the prefrontal cortex along the rostral bank of the arcuate sulcus. The FEF has strong anatomical connections with LIP (Andersen et al. 1985; Ferraina et al., 2002; Schall et al., 1995b) and is topographically organized (Tehovnik et al., 2000). The information sent from LIP to the FEF contains visual, delay, and saccadic activity. Compared to projections to SC, the activity in LIP-FEF projections are less dependent on saccadic generation and more dependent on the presence of visual stimuli (Ferraina et al., 2002). The FEF receives input from V4 and temporal cortex and has saccade related connections to both the SC (Sommer and Wurtz, 2000; Schall et al., 1995b) and the oculomotor regions of the pons (Segraves 1992). Sufficient electrical stimulation of the FEF generates fixed vector saccades (Bruce et al., 1985). The FEF contains visual motor and visuomotor neurons (Bruce and Goldberg, 1985).

The FEF has been found to be highly involved in saccade target selection, which is essentially an overt attentional mechanism. Schall and colleagues have performed a series of experiments investigating this in the FEF. Their experiments involve visual search and selection of an oddball stimulus. In a simple detection task, FEF neurons are only active when the stimulus appeared in its receptive field. In a search task, neurons are initially active if the target or a distracter is in its receptive field. After the initial activation, if the stimulus was the target, activity peaked. If the stimulus was a distant distracter, the activity remained similar. If the stimulus was a distracter near the target, the activity was then suppressed until the saccade was performed (Schall and Hanes, 1993).

The superior colliculus is located in the primate midbrain. Like the FEF, the SC is topographically organized, is comprised of both movement and visual cells, and microstimulation elicits a saccade. Unlike the FEF, the SC contains a map of motor goals that represent target position rather than saccade trajectory (Krauzlis et al., 97; Port and Wurtz, 2003). This motor map plots the end points for saccadic eye movements. The SC has connections to both the FEF (Sommer and Wurtz, 2000, Schall et al., 1995b) and LIP (Pare and Wurtz, 1997; Pare and Wurtz, 2001).

The SC contributes to target selection before a clear movement goal can be selected. In experiments by Basso and Wurtz (1997; 1998), monkeys were presented with a variable number of targets that could potentially be the saccade goal. As the number of targets increased the probability that any one target would be the saccade goal decreased. This was reflected in neuronal activity as an increase in the number of targets decreased neuronal activity in the receptive field of SC neurons representing the targets. This lower activity was predictive of increased saccadic latency. In a gap task, where the fixation point disappears before the targets appear, neurons with receptive fields representing potential target sites showed low frequency preparatory activity in preparation for a saccade. At the same time, fixation neurons show a decrease in activity. This created a preparatory set to allow for a saccade to occur faster (Dorris et al. 1997). In another experiment, Dorris and Munoz (1998) altered the probability that a stimulus in a neuronal receptive field would be the saccade target systematically between blocks. Pre-target recordings from intermediate SC showed that as the likelihood of a stimulus being the saccade goal increased, so did neuronal activity. This led to motor preparation, as the saccadic reaction time decreased when pre-target neuronal activity was higher.

1.4.2 Human Neuroscience

In humans, a functional human homologue to the parietal eye fields has been found and is referred to as the human parietal eye fields (hPEF). With fMRI, a cluster of activation medial to the IPS called the midposterior IPS (mIPS) has been linked to saccade planning (Astafiev et al., 2003; Merriam et al., 2003; Schluppeck et al., 2005; Tosoni et al., 2008), both eye movements and attention (Corbetta et al., 1998; Astafiev et al., 2003), eye movements and visual working memory (Curtis et al, 2004; Curtis and Connelly, 2008; Srimal and Curtis, 2008) and all three processes (Jerde et al., 2012). Many TMS experiments on saccades have targeted a nearby region under P3/P4 that is around the angular gyrus (Ryan et al., 2006) and found various saccade effects (Elkington et al., 1992; Oyachi and Ohtsuka, 1995; Muri et al., 1996; Kapoula et al., 2005). It has been suggested that this region is a human homologue of monkey LIP (Koyama et al., 2004).

Research has also identified a human homologue to the FEF. This region has been found to encode saccade targets in gaze-centered reference frames and show a preference for left/right topography (Van Pelt et al., 2010). This was found using repetition suppression, a fMRI technique that assumes a non-novel feature presented a second time will create a lower BOLD signal than a novel feature (location, colour, etc…). The FEF has been found to be involved in the selection and coding of saccade goals (Curtis and D'Esposito, 2006) and is involved in the preparatory set for saccades (DeSouza et al., 2003). The FEF has also been found to be involved in saccade planning in a delayed-reach task (Gallivan et al., 2011), and TMS to the FEF was shown to inhibit trans-saccadic integration of visual information (Prime et al., 2009).

1.5 Visual and Memory-Guided Reach

To meaningfully interact with the environment, people need to be able to use visual information to reach out and interact with objects. This process involves the coordination of the eye and the arm, as visual information is first encoded on the retina.

Extensive literature has shown the eye and arm to be closely connected (Fisk and Goodale, 1985; Neggers and Bekkering, 2000; Engel et al., 2002). Eye movements typically precede hand movements to a given location (Prablanc et al., 1979), and foveated targets show higher reach accuracy (Prablanc et al., 1979; Henriques et al., 1998). Even though there are significant linkages between the eye and arm for visually guided reach, eye and arm movements can be decoupled (Gorbet and Sergio, 2009) and people can reach to remembered peripheral target locations approximately as accurately as previously foveated locations using retinotopic remapping (Henriques et al., 1998).

1.5.1 Animal Neurophysiology

There is a considerable amount of evidence that has linked the posterior parietal cortex (PPC) to reach planning. The PPC sits at the termination of the dorsal stream of visual processing, which processes information relevant for planning actions (Goodale and Milner, 1992). Many studies in non-human primates have implicated sub-regions of the PPC along the intraparietal sulcus (IPS) in the visuomotor transformations required to plan eye and arm movements to visual targets. Neurons in the lateral intraparietal area (LIP) have been linked to planning saccadic eye movements (Andersen et al., 1990; Colby et al., 1996), as well as working memory (Pesaran et al., 2002) and visuospatial attention (Colby et al., 1996; Bisley and Goldberg, 2003). Another functionally specific region along the IPS is the anterior intraparietal area (AIP), where neurons show activity related to hand pre-shaping, object-directed grasping, and encoding 3D visual properties of objects in a way suitable to guide grasping

(Mountcastle et al., 1975; Gallese et al., 1994; Jeannerod et al., 1995; Murata et al., 2000; Baumann et al., 2009).

For reaching, several areas including the medial intraparietal area (MIP) (Johnson et al., 1996; Eskandar and Assad, 1999), area 5 (Kalaska, 1996; Ferraina et al., 2001), area 7A (MacKay, 1992; Johnson et al., 1996; Battaglia-Mayer et al., 2000), V6A (Fattori et al., 2001, 2009; Galletti et al., 2003), and the parietal reach region, which overlaps MIP and V6A (Snyder et al., 1997; Batista et al., 1999; Buneo et al., 2002; Chang et al., 2008; Andersen and Cui, 2009) have been identified. The PRR is also known to encode reach goals in eye-centred coordinates (Batista et al., 1999; Buneo et al., 2002) and it has been suggested that the PRR and LIP share a common reference frame (Cohen and Andersen, 2002). It should be noted that the dissociation between reach- and saccade-related regions in PPC is relative, to absolute (Snyder et al., 1997, 2000; Calton et al., 2002).

In frontal cortex, both primary motor cortex (M1) and non-primary motor areas (the premotor, supplementary motor, and cingulate motor areas) influence and/or produce the motor commands required to produce a reaching movement (Picard and Strick, 1996, 2001). The PMd has been shown to receive projections from the PRR and area 5 (Kalaska et al., 1997; Wise et al., 1997). PMd neurons are active during the delay period preceding an instructed movement and are tuned for the direction and distance of reaches with either hand (Weinrich and Wise, 1982; Caminiti et al., 1991; Messier and Kalaska, 2000; Cisek et al., 2003). The final stage of cortical process occurs in primary motor cortex (M1), where the reach is encoded in muscle-centred coordinates and the forces and torques required for a reach are computed (Scott and Kalaska, 1997; Sergio and Kalaska, 1998; Kakei et al., 1999; Sergio and Kalaska, 2003)

1.5.2 Human Neuroscience

Two reach-related regions have been identified in humans PPC with fMRI. The first one is around the mIPS and encodes pointing and reaching activity (DeSouza et al., 2000; Medendorp et al., 2003, 2005a; Prado et al., 2005; Beurze et al., 2007, 2009, 2010; Fernandez-Ruiz, 2007; Tosoni et al., 2008; Filimon et al., 2009). This area also codes activity when a person points with a joystick (Grefkes et al., 2004; Bedard et al., 2011) has been shown to be involved in spatial updating (Medendorp et al., 2003) and is equally active with or without visual feedback, suggesting that activity in this area is not visually driven (Filimon et al., 2009). TMS to this region increases variance in initial movement direction for contralateral reaches (Davare et al., 2012) and shows deficits related to planning and programming movements rather than online control (Striemer et al., 2011). Reaching related TMS studies to the nearby P3/P4 sites have shown that TMS disrupts the integration of saccade information for reach planning (Van Donkelaar et al., 2000), increases errors in contralateral reach planning (Smyrnis et al., 2003; Vesia et al., 2006), and inhibits the internal representation of hand position used to compute the reach vector (Vesia et al., 2008). They have also shown that this area codes in motor coordinates (Vesia et al., 2006) [consistent with the fMRI motor coordinate AG activity found in Fernandez-Ruiz et al., 2007].

The other parietal reach-related region codes contralateral arm movements and is located near the parieto-occipital junction and often referred to as the superior parietal occipital cortex (SPOC) (Astafiev et al., 2003; Connolly et al., 2003; Prado et al., 2005;

Fernandez-Ruiz et al., 2007; Tosoni et al., 2008; Beurze et al., 2009; Gallivan et al., 2009, 2011; Bernier and Grafton, 2010; Cavina-Pratesi et al., 2010; Monaco et al., 2011). It shows preferential activation for peripheral targets (Prado et al., 2005), graspable objects within reaching distance (Gallivan et al., 2009), is more active for visually guided reaching, suggesting its activity is more visually driven (Filimon et al., 2009). It has been shown to encode the transport component of a react-to-grasp movement (Cavina-Pratesi et al., 2010) and codes hand orientation during grasping (Monaco et al., 2011). A recent study found that SPOC was equally active for pointing with the hand and foot, suggesting that it may be functionally specific to visually guiding pointing movements with limbs, not just the arms (Heed et al., 2011). TMS to SPOC increases reaction times in reaching tasks for either arm (Busan et al., 2009a, 2009b) that are time dependent (Busan et al., 2009c), and increases spatial variance in manual interception (Dessing et al., 2013).

A recent TMS experiment by Vesia et al. (2010) investigated the effector specificity of three PPC regions (AG, mIPS, and SPOC) using TMS. Subjects had to perform a saccade or a reach-to-touch arm movement to the remembered location of a target. TMS (3 pulses, 10 Hz, 60% stimulator output) was applied in the interval following the extinguishing of the target stimulus and the execution of the reach or saccade. It was found that for saccades, the TMS over AG and mIPS decreased saccade accuracy for contralateral targets, while TMS over SPOC had no effect. For reaches, TMS over AG and mIPS increased reach end-point variability, while TMS over SPOC deviated reach endpoints towards fixation (termed ‘magnetic reaching’). Contralateral limb specificity was higher for AG and mIPS than SPOC. Vision of the hand eliminated the variability effects for AG and mIPS, but magnetic reaching effects were still seen for TMS over SPOC. These results led Vesia and colleagues to conclude that SPOC is specialized in encoding peripheral reach goals, while AG and mIPS are involved in saccade and reach planning and are more involved in planning the motor aspects of contralateral reaches such as planning reach vectors. Using multi-voxel pattern analysis (MVPA), recent studies by both Haar et al. (2015) and Gertz et al. (2017) have studied processes that a traditional subtraction analysis may not be sensitive to. Haar et al. (2015) found evidence for direction coding for reach in visual, frontal (PMd, SMA, M1), and pariental cortex (SPOC, mIPS). Gertz et al. (2017) found movement goal encoding in both left PMd, as well as bilateral SPL for normal reaches, but those with an unspecified goal found the PMd encoded the visual cue position (not SPL).

In addition to studies on healthy patients, research on optic ataxia patients with PPC damage has implicated the region to reach planning. Unilateral damage impairs reaching in the contralateral visual field, while bilateral damage impairs reaches to both visual fields. Unilateral OA patients can have deficits related to reaching within a particular visual field (called a field effect), or reaching with a particular hand (called a hand effect) (Perenin and Vighetto, 1988). Interestingly, these deficits tend to interact such that reaching with the contralesional hand in the contralesional visual field has the most errors (Perenin and Vighetto, 1988; Blangero et al., 2007). Reach deficits in what is referred to as non-foveal OA are limited to reaches to peripheral targets, as they can perform accurate reaches toward objects in central vision (Perenin and Vighetto, 1988, Buxbaum and Coslett, 1997).

In frontal cortex, fMRI research has shown PMd to encode the reach goal of an effector during reach planning, with hemispheric lateralization encoding for the arm contralateral to the hemisphere (Medendorp et al., 2005; Beurze et al., 2007; 2009). PMd has also been linked to the planning of both pro-reaches towards a target and anti-reaches away from a target (Connolly et al., 2003; Gertz et al., 2015).

1.6 Effector Specificity for Saccade and Reach

In humans, reach and saccade signals in the PPC have been very difficult to dissociate. Several studies have shown large amounts of overlap during the planning of eye and arm movements (Medendorp et al., 2003; Beurze et al., 2007, 2009). There is, however, evidence for effector specificity in human PPC. With fMRI, a cluster of activation medial to the IPS called the midposterior IPS (mIPS) has been linked to saccade planning (Astafiev et al., 2003; Merriam et al., 2003; Schluppeck et al., 2005; Tosoni et al., 2008), both eye movements and attention (Corbetta et al., 1998; Astafiev et al., 2003), eye movements and visual working memory (Curtis et al, 2004; Curtis and Connelly, 2008; Srimal and Curtis, 2008) and all three processes (Jerde et al., 2012). Many TMS experiments on saccades have targeted a nearby region under P3/P4 that is around the angular gyrus (Ryan et al., 2006) and found various saccade effects (Elkington et al., 1992; Oyachi and Ohtsuka, 1995; Muri et al., 1996; Kapoula et al., 2005). It has been suggested that this region is a human homologue of monkey LIP (Koyama et al., 2004). A grasping related region in the human PPC with functions similar to monkey AIP has been identified by fMRI in the anterior intraparietal sulcus (aIPS) (Binkofski et al., 1998; Culham et al., 2003; Cavina-Pratesi, 2010). TMS to this area has been shown to inhibit online grip adjustments (Glover et al., 2005, Rice et al., 2006, 2007) and online reach control (Desmurget et al., 1999).

In frontal cortex, researchers have struggled to dissociate reach from saccade regions as well. As both the FEF and PMd are functionally defined areas, there is often overlap in their activation and the regions are classified based on the effector being used in a given task (Culham et al., 2006; Medendorp et al., 2005; Gallivan et al., 2011; 2015).

Additional fMRI techniques with stronger temporal sensitivity than fMRI have also been used to study saccades and reaches. Van Der Werf et al. (2008, 2009, 2010, 2013) has a series of studies examining the evolution of MEG signals during reach tasks. These studies found synchronised activation (50-100Hz) in PPC during saccades, and directionally selective synchronization in the 70-90 Hz gamma frequency band in PPC for reaches.

1.7 Functional Magnetic Resonance Imaging (fMRI)

Functional Magnetic Resonance Imaging (fMRI) is a non-invasive neuroimaging technique that leverages MRI technology to measure changes in blood oxygenation over time in neural structures (Kwong et al., 1992; Ogawa et al., 1992). fMRI measures changes in the blood oxygenation level dependent (BOLD) signal over time, which quantifies the different magnetic properties of oxygenated and deoxygenated blood in the brain in units called voxels (Bandettini et al., 1992; Disbrow et al., 2000; Ances et al., 2008; Logothetis, 2008). Earlier fMRI studies relied on blocked designs, where activation was measured over an interval of time (typically 10-30 seconds) and experimental and control runs were compared to examine the neural correlates of a phenomenon (Belliveau et al., 1991; Kwong et al., 1992; Ogawa et al., 1992). More recent studies have relied on event-related designs, where changes in the BOLD signal are measured within a trial and lined to events occurring during a single trial (Buckner et al., 1996; Dale and Buckner, 1997; Bandettini and Cox, 2000). Analysis of fMRI data can be performed either on the whole brain using a voxelwise analysis, or on a subset of voxels using a region of interest (ROI) design. Voxelwise analyses are more common when examining systematic activation in the whole brain over time and when a newer, less well understood phenomenon is being examined (although it is necessary for these examinations to be hypothesis-driven). ROI designs are more frequently used when the role of a previously defined region is being examined in a new task.

1.8 Overall Objectives for this Dissertation

This general introduction has outlined fundamental neuroscience studies that have greatly expanded our understanding of both saccades and reaches. Given the extensive research into these fields, there remains several key questions regarding how the human brain takes the visual inputs to the system and processes this information to produce either saccadic or reach outputs. In cortex, several steps must occur to produce a visually-guided movement, including representation of the target, planning of the movement itself, and the neural signals associated with the execution of the movement. Some fMRI studies have isolated planning from execution, but slow BOLD dynamics did not allow a distinction between visual target memory and movement planning (Connolly et al., 2000; Fernandez-Ruiz et al. 2007; Beurze et al., 2007, 2009).

In other studies, target memory was separated from movement planning, but did not distinguish planning from execution (Connolly et al., 2000; Chen et al., 2014). When comparing between effectors, studies have reported considerable overlap between saccade and reach activity, perhaps due to the spatial resolution limits of fMRI (Connolly et al, 2007; Curtis et al, 2008; Beurze et al., 2009; Gallivan et al, 2011).

However, one thing that has not be fully accounted for in the design of these studies is the limited temporal resolution of fMRI. As a result of this limitation, studies where the visual stimulus and movement cues overlap closely in time could result in the conflation of these different signals. This is particularly important for distinguishing between the spatial selectivity of visual working memory responses versus motor planning responses, and effector-independent visual/memory inputs to various cortical regions as opposed to their effector specific motor outputs.

The overall objective of this dissertation was to overcome some of these former limitations with the use of an event-related cue-separation fMRI paradigm that clearly disentangles visual memory, motor planning, and motor execution signals. This allowed me to examine the following key concepts: (1) The brain areas involved in visual target representation, motor planning, and motor execution for visually-guided reaching (chapters 2 and 3) and saccades (chapters 3), (2) the evolution of visual and movement directional coding over time for visually-guided reaching (chapter 2), (3) effector specificity in movement planning and execution for saccades and reaches (chapter 3).

Chapter Two: Temporal Evolution of Target Representation, Movement Direction Planning, and Reach Execution in Occipital-Parietal-Frontal Cortex: An fMRI Study

AUTHORS: David C. Cappadocia, Simona Monaco, Gunnar Blohm, and J. Douglas Crawford

PUBLISHED IN *CEREBRAL CORTEX*:

Cappadocia DC, Monaco S, Chen Y, Blohm G, Crawford JD. 2017. Temporal Evolution of Target Representation, Movement Direction Planning, and Reach Execution in Occipital–Parietal–Frontal Cortex: An fMRI Study. Cerebral Cortex. 27(11):5242–5260.

2.1 Abstract

The cortical mechanisms for reach have been studied extensively, but directionally selective mechanisms for visuospatial target memory, movement planning, and movement execution have not been clearly differentiated in the human. We used an event-related fMRI design with a visuospatial memory delay, followed by a pro-/anti-reach instruction, a planning delay, and finally a ‘go’ instruction for movement. This sequence yielded temporally separable preparatory responses that expanded from modest parieto-frontal activation for visual target memory to broad occipital-parietal-frontal activation during planning and execution. Using the pro/anti instruction to differentiate visual and motor directional selectivity during planning, we found that one occipital area showed contralateral *visual* selectivity, whereas a broad constellation of left hemisphere occipital, parietal, and frontal areas showed contralateral *movement* selectivity. Temporal analysis of these areas through the entire memory-planning sequence revealed early visual selectivity in most areas, followed by movement selectivity in most areas, with *all* areas showing a stereotypical visuo-movement transition. Cross-correlation of these spatial parameters through time revealed separate spatiotemporally correlated modules for visual input, motor output, and visuo-movement transformations that spanned occipital, parietal, and frontal cortex. These results demonstrate a highly distributed occipital-parietal-frontal reach network involved in the transformation of retrospective sensory information into prospective movement plans.

2.2 Introduction

In order to effectively interact with the world, human beings take in sensory information and use it to produce meaningful actions. One of the most commonly studied cases of this is visually-guided reach-to-touch movements (e.g., ringing a doorbell or pushing the power button on a laptop computer). Often visual information is no longer available by the time one makes a movement, or gaze has been re-directed to another location by the time one initiates a movement (Henriques et al., 1998; Flanagan & Johansson, 2003). To perform such movements, the brain must retain information about the spatial location of a target in working memory, use this information to form a motor plan, and then execute that motor plan to reach towards the goal. Neurophysiological studies in awake behaving non-human primates have shown a progression from visual-to-motor (visuomotor) coding within and between neurons in the occipital-parietal-frontal cortical axis (Picard and Strick, 2001; Andersen and Buneo, 2002; Gail and Andersen, 2006; Cisek and Kalaska, 2010; Westendorff et al., 2010; Kravitz et al., 2011), and spatially-selective networks for memory, attention, and planning that span parietal and frontal cortex (Berman and Colby, 2009; Rawley and Constantinidis, 2009). However, human imaging studies have not clearly differentiated spatial selectivity for reach plans in cerebral cortex from visuospatial target representation and/or movement execution, or tracked visual and movement directional selectivity through the entire sequence of events leading up to reach execution.

Previous human neuroimaging studies investigating visual-to-movement (visuo-movement) transformations have identified several key regions in the parietal-frontal reach planning network. In parietal cortex, both the midposterior intraparietal sulcus (mIPS) (DeSouza et al., 2000; Medendorp et al., 2003, 2005; Prado et al., 2005; Beurze et al., 2007, 2009, 2010; Fernandez-Ruiz, 2007; Tosoni et al., 2008; Filimon et al., 2009; Chen et al., 2014) and the superior parietal occipital cortex (SPOC) (Astafiev et al., 2003; Connolly et al., 2003; Prado et al., 2005; Fernandez-Ruiz et al., 2007; Tosoni et al., 2008; Beurze et al., 2009; Gallivan et al., 2009, 2011; Bernier and Grafton, 2010; Cavina-Pratesi et al., 2010; Monaco et al., 2011; Chen et al., 2014) show activation related to reach planning and execution. These areas encode this information with a contralateral left–right topography (Beurze et al., 2007; Vesia et al., 2010; 2012). In frontal cortex, human dorsal premotor cortex (PMd) also encodes pointing and reaching (Connolly et al., 2000, 2007; Astafiev et al., 2003; Prado et al., 2005; Beurze et al., 2007, 2009, 2010; Bernier et al., 2010, 2012; Chen et al., 2014), as well as contralateral spatial selectivity (Beurze et al., 2007, 2009, 2010; Bernier et al., 2012; Chen et al. 2014).

An important question in vision-memory-motor transformations is whether spatial locations and reach plans are specified in visual or movement selective coordinates, i.e., whether sustained spatial activity codes retrospective sensory information or prospective motor plans (Curtis, 2006). One strategy scientists have used to study this question is dissociating the visual target from the movement goal. Some studies have used anti-reaching tasks, where subjects view a target and must perform a reach in the opposite direction (Connolly et al., 2000; Chen et al., 2014; Gertz and Fiehler, 2015). Using this type of paradigm, Chen et al. (2014) found contralateral visual coding in left occipital cortex during the target representation period and contralateral movement directional coding in parieto-frontal cortex during movement execution. In another study, contralateral movement directional coding was observed in the left precuneus during movement planning (Gertz and Fiehler, 2015). Fernandez-Ruiz et al. (2007) studied visual and movement selective coding using reversing prisms, which reverse the visual input such that a leftward reach target appears to be in the right visual field. They found that most regions in the left posterior parietal cortex (PPC) encoded the visual direction of the goal during movement execution (with the exception of the angular gyrus, which encoded the movement direction).

What all of these imaging studies lacked, leading to the current study, was a clear separation between target memory, movement planning, and movement execution for reach. Some fMRI studies have isolated reach planning from execution, but slow BOLD dynamics did not allow a distinction between visual target memory and movement planning (Connolly et al., 2000; Fernandez-Ruiz et al. 2007; Beurze et al., 2007, 2009). In other studies, target memory was separated from movement planning, but did not distinguish planning from execution (Connolly et al., 2000; Chen et al., 2014). Based on these studies, one might predict that parieto-frontal cortex should show contralateral directional tuning for reach plans, especially in the hemisphere contralateral to the hand (Connolly et al., 2003; Fernandez-Ruiz, 2007; Bernier et al., 2012; Gertz and Fiehler, 2015). However, one cannot clearly differentiate this spatial tuning for planning from coding target direction (and/or movement execution signals), especially in occipital cortex that might show tuning for either visual direction or an imaginary goal. Further, one cannot track visual versus movement directional tuning through a separate sequence of visual memory, planning, and execution events, or use this information to construct functional networks of sensory, motor, and sensorimotor codes for reach.

The current study uses an event-related fMRI paradigm that explicitly separates visually-guided reaching into three phases in time (visual target representation, movement planning, and movement execution), by introducing a pro / anti-reach instruction between visual target memory and planning phases, and a ‘go signal’ between planning and execution times. We used this paradigm in combination with a new way of spatially analyzing combined pro- / anti-reach data, to investigate four questions: (1) which brain areas are differentially activated for visual target representation, movement planning, and movement execution, (2) which of these areas show contralateral visual and/or movement direction specificity during the planning phase, (3) at what point in the target-planning-execution coding sequence does a visual-to-movement (visuo-movement) transformation occur *within* the cortical areas involved in reach, and (4) how are these visual, movement, and visuo-movement parameters temporally and spatially distributed through the cortical networks for reach in the human?

2.3 Methods

Participants

Twelve right-handed subjects (3 males, 9 females aged 20-36) were recruited from the York University community. We chose this number of subjects based on precedents set in similar studies of visuomotor control in healthy subjects (Cavina-Pratesi et al., 2007, Gallivan et al., 2011). The resulting dataset was sufficient to yield statistically significant results that survived corrections for multiple comparisons (see Results). All subjects had normal or corrected-to-normal vision and none of the subjects had any known neurological deficits. The York University Human Participants Review Sub-committee approved all techniques used in this study and all participants gave their informed consent prior to the experiment.

Experimental stimuli and apparatus

The experimental stimuli and apparatus were the same as the setup used in Chen et al. (2014). Visual stimuli consisted of optic fibers embedded into a custom-built board with adjustable tilt. The board was mounted atop a platform whose height was also adjustable (Figure 2A). The platform was attached to the MRI scanner bed and placed over the abdomen of the subject. The height of the platform and tilt of the board were adjusted for each participant to ensure comfortable reaching movements. A translucent touchscreen (Keytec, 170 mm X 126 mm) was affixed on the board to record reach endpoints. An eye-tracking system (iView X) was used in conjunction with the MRI-compatible Avotec Silent Vision system (RE-5701) to record movements of the right eye during the experiment.

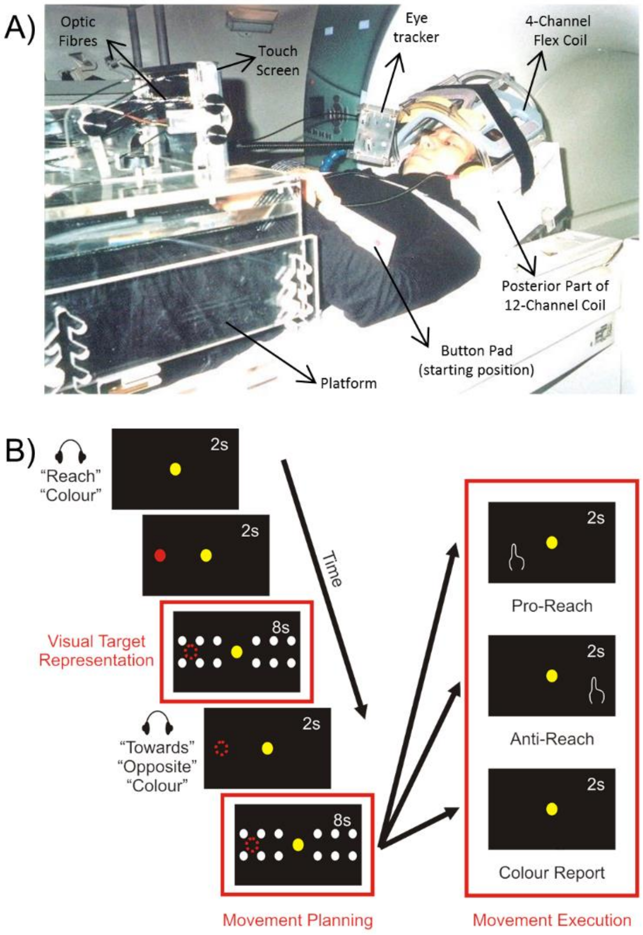

Figure 2. Experimental setup and paradigm. **A*)*** Photograph of The experimental setup.

B) Illustration of the experimental paradigm. The display of visual targets is the same for all three tasks (Pro-Reach, Anti-Reach, and Color Report). The key difference between the two reach tasks is the congruence of the visual target and movement goal. In the Pro-Reach task, subjects reach towards the remembered location of the previously displayed visual target. In the Anti-Reach task, subjects reach towards the location mirror symmetrical to the visual target in the opposite visual field. As the target presentation and pro/anti instruction are separated by an 8 second delay, this allows the task to disentangle target representation from movement planning and execution. In the

Color Report task, target color (red or green) rather than location is remembered and reported.

The head of the participant was slightly tilted (~20º) to allow direct viewing of the stimuli presented on the board (Figure 2A). The board was approximately perpendicular to gaze and approximately 60 cm from the eyes. The upper arm was strapped to the scanner bed to limit motion artifacts. Reaches were thus performed by movements of the right forearm and hand. A button pad was placed on the left side of the participants' abdomen and served as both the starting point for each trial and as the response for the color report control task (see experimental paradigm and timing). Participants wore headphones to hear auditory instructions and cues. During each trial, subjects were in complete darkness with the exception of the visual stimuli, which were not bright enough to illuminate the workspace. The hand was never visible to the subject, even during reaching.

There were 3 types of visual stimuli presented by different colors: the fixation point in yellow, targets in green or red, and masks in white. All stimuli were presented horizontally on the touchscreen, and had the same diameter of 3 mm as the optic fibres. There was one central fixation location. Eight horizontal peripheral targets (4 on each side of the touchscreen) were used (Figure 2B), and twenty "mask" LEDs were located above and below the target line (ten on each side with five above and five below the targets). The visual mask was used during the delay periods to control for visual afterimages. The distance between the eyes of the subject and the center of the touchscreen was approximately 60 cm. The target LEDs were located approximately 4°, 5°, 6° or 7° to the left or right of the fixation LED.

Experimental paradigm and timing

We used an event-related design, with each trial lasting 38 seconds (including an inter-trial interval of 12 seconds). The paradigm included 3 tasks: pro-reach, anti-reach, and color report as a control (Figure 2B). Each trial began with the presentation of the yellow fixation LED (this was displayed for 24 seconds before the first trial in each run). Concurrently, subjects were given the auditory instruction “reach” or “color” to indicate the task they had to perform at the end of that trial. The important distinction between these two instructions is that while remembering the spatial location of the target LED (the visual target) was required for the reaching trials, this information could be ignored for the color report trials. After 2 seconds, a green or red target LED was illuminated for 2 seconds, followed by an 8 second delay period (the ‘visual target representation’ phase) during which the fixation LED and mask LEDs were illuminated. At the end of the delay, subjects were given one of 3 auditory instructions: For reach trials: “towards” (indicating a pro-reach trial) or “opposite” (indicating an anti-reach trial). For color report trials the instruction “color” was repeated. This took 2 seconds. The pro- or anti-reach instruction being given in the middle of the trial prevented subjects from forming their movement plan during the first delay period. The auditory instruction was followed by another 8 second delay period (the ‘movement planning’ phase) during which the fixation LED and mask LEDs were illuminated. After the mask LEDs were turned off, subjects heard a beep that served as a ‘go’ signal for subjects to reach-to-touch to: 1) the remembered location of the target in pro-reach trials, 2) the mirror location in the opposite visual hemifield in anti-reach trials, or 3) press the button once if the target LED was green or twice if it was red for the color report trials (or vice versa, this was be counterbalanced across subjects). This is referred to as the ‘movement execution’ phase. After touching the touchscreen for 2 seconds, subjects heard a beep that instructed them to return their right index finger to the starting position. The following trial started 12 seconds later.

Each functional run consisted of 12 trials presented in a random order (4 for each of the three tasks; 50% of targets presented in each visual hemifield for each task) and lasted about 8 minutes. For the purpose of analysis, target locations were collapsed together as “left” or “right”. Subjects participated in 8 functional runs in one session. They were trained to perform the required tasks 1-2 days before imaging and practiced all tasks within the MRI scanner before scanning to ensure that they were comfortable with the task.

Behavioral recordings

Following the fMRI experiments, the eye position and reach endpoints were inspected. Eye movement errors were defined as trials where subjects were unable to maintain visual fixation from target presentation until touching the touchscreen. Reaching errors were defined as reaches to the direction opposite to the instructed reach goal. Trials with behavioral errors were excluded from further analysis (4.52% of trials).

To confirm accurate reaching in the pro- and anti-reach conditions, we performed a correlation analysis comparing horizontal target location to the horizontal reach endpoint for each subject. For pro-reach trials, across-subject means of the correlation coefficients (r) were r=0.843±0.03. For anti-reach trials, across-subject means of the correlation coefficients were r=0.836±0.04. We then applied Fischer's r-to-z transformations to individual subject's r values and performed one-way t-tests to compare subjects' z scores to 0. Both t-tests were significant ($p_{pro} < 0.001$, $p_{anti} < 0.001$), indicating accurate reaching.

Imaging parameters

The experiment was conducted at the York MRI Facility at the Sherman Health Sciences Centre at York University with a 3-T whole-body MRI system (Siemens Magnetom TIM Trio). The posterior half of a 12-channel head coil (6 channels) was placed at the back of the head, with a 4-channel flex coil over the anterior part of the head (Figure 1B). The head was tilted ~20º to allow for direct viewing of the stimuli during experimental trials.

Functional data was acquired using an EPI (echo-planar imaging) sequence (repetition time [TR] = 2000 ms; echo time [TE] = 30 ms; flip angle [FA] = 90º; field of view [FOV] = 192 mm X 192 mm, matrix size = 64 X 64 leading to an in-slice resolution of 3 mm X 3 mm; slice thickness = 3.5 mm, no gap; 36 transverse slices angled at ~25º covering the whole brain). Slices were collected in ascending and interleaved order. During each experimental session, a T1–weighted anatomical reference volume was acquired using an MPRAGE sequence (TR = 1900 ms; TE = 2.52 ms; inversion time TI = 900 ms; FA = 90º; FOV = 256 mm X 256 mm X 192 mm, voxel size = 1 X 1 X 1 mm^3).

Preprocessing

All data was analyzed using BrainVoyager QX 2.2 (Brain Innovation). The first 2 volumes of each scan were discarded to avoid T1 saturation effects. For each run, slice scan time correction (cubic spline), temporal filtering (removing frequencies <2 cycles/run) and 3D motion correction (trilinear/sinc) were performed. The 3D motion correction was performed by aligning each volume of one run to the volume of the functional scan that was closest in time to the anatomical scan. 3 runs showing abrupt head movement of 1 mm or 1º were discarded. Functional runs were coregistered to the anatomical image. Functional data was then transformed into Talairach space using the spatial transformation parameters from each individual subject's anatomical scan. The voxel size of the native functional images was 3x3x3 and was not resampled to a different voxel size during the preprocessing steps. Functional data was spatially smoothed using a FWHM of 8 mm.

Data analysis

For each participant, we used a general linear model with 33 predictors. Two predictors were used for the initial auditory instruction (reach or color); four predictors were used for visual target presentation (left or right X reach or color trial); four predictors were used for visual target representation (left or right X reach or color trial); three predictors were used for the 2nd auditory instruction (pro-reach, anti-reach, or color trial); six predictors were used for motor preparation (left or right X pro-reach, anti-reach, or color trial); six predictors were used for motor execution (left or right X pro-reach, anti-reach, or color trial). In addition, six motion correction parameters and predictors for behavioral errors and inter-trial intervals were added as confound errors. Each predictor was derived from a rectangular wave function convolved with a standard hemodynamic response function using BrainVoyager QX's default double-gamma hemodynamic response function.

Voxelwise analysis

Contrasts were performed on β weights using an RFX (random effects) GLM with a percentage signal change transformation. This GLM was used to investigate the first two main questions for this study. To investigate the brain areas involved in visual target representation, reach movement planning, and reach movement execution, we performed three contrasts to find brain areas that showed higher activity for reach trials (pro and anti) than the control (color) trials during each phase.

We also performed two contrasts to test if brain areas showed contralateral directionally selective activation in visual or movement direction coordinates during movement planning (see Figure 7). The first contrast was designed to find contralateral visually selective brain areas. So for the left hemisphere, areas that showed higher activation when the target was initially presented in the right visual field (pro- and anti-reach right) than the left (pro- and anti-reach left) would be contralaterally visually selective. For the right hemisphere, areas that showed higher activation when the target was initially presented in the left visual field (pro- and anti-reach left) than the right (pro- and anti-reach right) would be contralaterally visually selective. The other contrast aimed at finding movement-direction selective brain areas. So for the left hemisphere, areas that showed higher activation when the movement direction was to the right (pro-reach right and anti-reach left) than the left (pro-reach left and anti-reach right) would be contralaterally movement selective. For the right hemisphere, these areas showed higher activation when the movement direction was to the left (pro-reach left and anti-reach right) than the right (pro-reach right and anti-reach left). For these contrasts, we limited our analysis to brain regions showing higher BOLD activation in the hemisphere contralateral to the visual target or movement goal, respectively.

Activation maps for group voxelwise results were overlaid on the inflated brain of one representative subject. To correct for multiple comparisons, cluster threshold corrections (Forman et al., 1995) were performed for each contrast using BrainVoyager QX's cluster-level statistical threshold estimator plug-in (1000 iterations). Areas that did not survive were excluded from further analysis. A Bonferroni correction was applied to the t value for each contrast to account for the two types of contrasts performed in the experiment (movement trials > control trials and contralateral directional selectivity contrasts). These two types of contrasts were planned a priori, with contrasts 1-3 being movement > control trials at three different time periods and contrasts 4 & 5 investigating contralateral visual and movement selectivity during the planning phase. ($\alpha = 0.05 / 2$ comparisons $= 0.025$ corrected for $p < 0.05$).

2.4 Results

General Reach Activation for Visual Target Representation, Movement Planning, and Movement Execution for Reach

In our first analysis, we looked at general, non-directional reach activation; combining left and right movements for both pro- and anti-reach trials. A recent fMRI study has shown that pro- and anti-reaches activate similar parietal and premotor areas (Gertz and Fiehler, 2015). We confirmed this was the case in our study by analyzing pro-reach > color, anti-reach > color, and pro-reach > anti-reach during motor planning and execution and have included these post-hoc analyses in Supplementary Figure 1 (all supplementary figures are in Appendix A at the end of this dissertation). As indicated in this figure, most of the regions of interest (ROIs) described below fall within regions of pro- / anti-reach overlap, although some additional significant ROIs appear below when one doubles the dataset by combining these two conditions.

Figure 3 (A, B, and C) plot the pro- and anti-reach data relative to our color control task in each of the three major phases of our task: visual target representation, movement planning, and movement execution, with corresponding ß-weights for these data shown in Supplementary Figure 2, and the corresponding Talairach coordinates shown in Tables 2, 3, and 4. Brain areas were labeled by comparing the Talariach coordinates from the peak voxel within a cluster and comparing it to known sites of activation in the visuomotor system. A list of ROI brain area abbreviations is provided in Table 1. It is important to note that certain effector-specific functional areas cannot be clearly distinguished in our contrasts (e.g., frontal eye fields vs. dorsal premotor cortex), in which case the reach-related label has been given. We also provided complete time

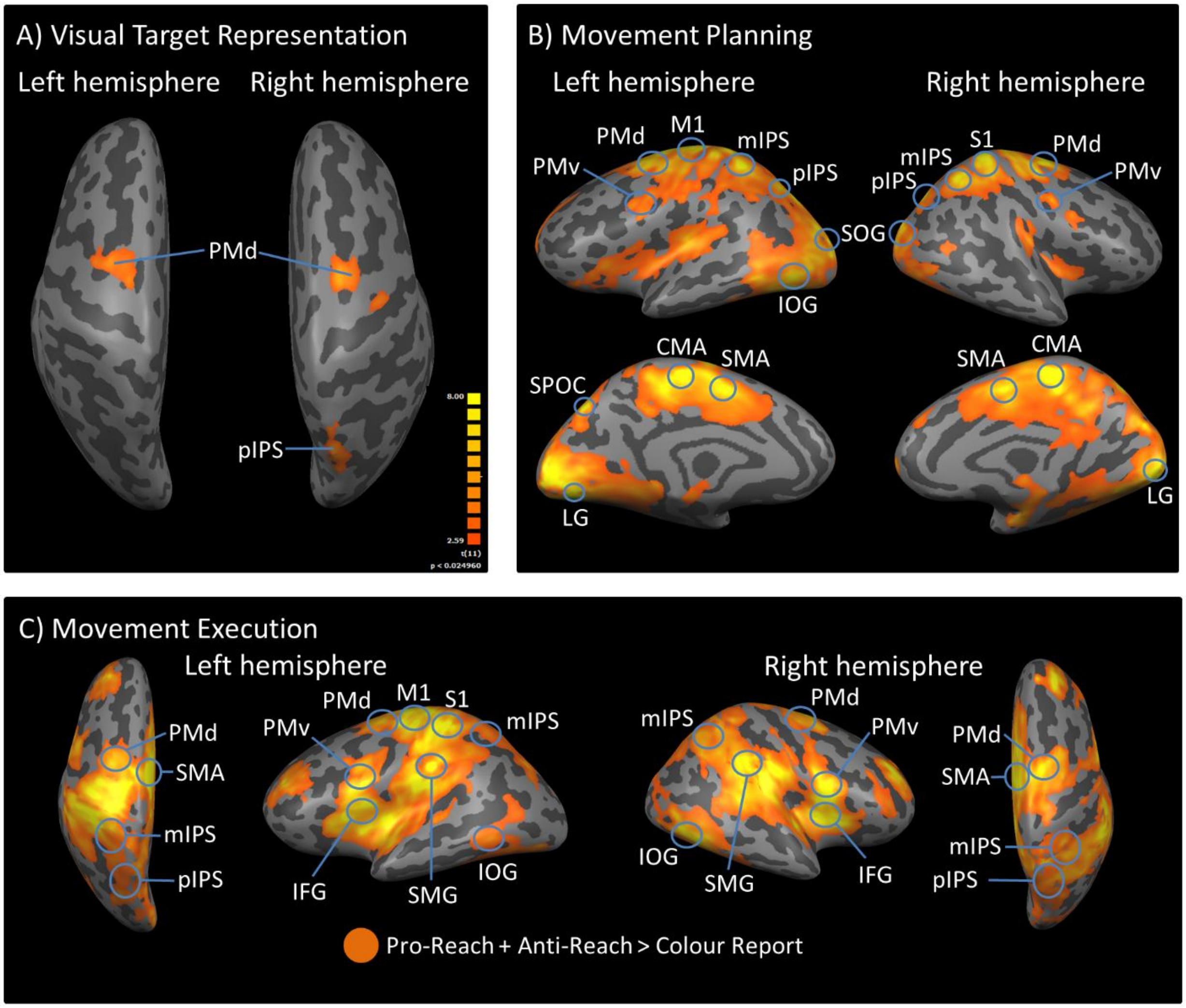

Figure 3. A) Voxelwise statistical maps obtained from the RFX GLM for the contrast Pro-Reach + Anti-Reach > Color report. Event-related group activation maps for target representation are displayed on the ‘inflated brain’ of one representative subject, where light gray represents gyri and dark gray represents sulci. The leftward inflated brain represents the left hemisphere, and the rightward brain represents the right hemisphere. Highlighted areas show significantly higher activation than control data with a $p<0.05$ with Bonferroni and cluster threshold corrections. These areas include the left and right PMd and right pIPS. B) Voxelwise statistical maps obtained from the RFX GLM for the

contrast Pro-Reach + Anti-Reach > Color report. Event-related group activation maps are displayed on the inflated brain of one representative subject for movement planning. The two leftward inflated brains represent the left hemisphere, and the two rightward brains represent the right hemisphere. Highlighted areas show significantly higher activation than control data with a $p<0.05$ with Bonferroni and cluster threshold corrections. These areas include bilateral PMd, PMv, mIPS, pIPS, and SOG. Significant activation was also observed in left M1, SPOC, and IOG, and right S1. C) Voxelwise statistical maps obtained from the RFX GLM for the contrast Pro-Reach + Anti-Reach > Color report. Event-related group activation maps are displayed on the inflated brain of one representative subject for movement execution. The two leftward inflated brains represent the left hemisphere, and the two rightward brains represent the right hemisphere. Highlighted areas show significantly higher activation than control data with a $p<0.05$ with Bonferroni and cluster threshold corrections. These areas include bilateral PMd, mIPS, SMG, IOG, SMA and IFG. Significant activation was also observed in left M1 and S1, and in right PMv. (See Table 1 for site abbreviations)

Table 1. List of ROI brain area abbreviations

Area	Abbreviation
Occipital	
Primary Visual Cortex	V1
Lingual Gyrus	LG
Superior Occipital Gyrus	SOG
Inferior Occipital Gyrus	IOG
Parietal	
Superior Parietal Occipital Cortex	SPOC
Posterior Intraparietal Sulcus	pIPS
Midposterior Intraparietal Sulcus	mIPS
Anterior Intraparietal Sulcus	aIPS
Angular Gyrus	AG
Supramarginal Gyrus	SMG
Precuneus	PCu
Primary Somatosensory Cortex	S1
Frontal	
Primary Moror Cortex	M1
Dorsal Premotor Cortex	PMd
Ventral Premotor Cortex	PMv
Cingulate Motor Area	CMA
Supplementary Motor Area	SMA
Inferior Frontal Gyrus	IFG

Table 2. Talairach coordinates and number of voxels for Target Representation regions of interest

Area	Mean X	Mean Y	Mean Z	Voxels
Left PMd	-25.43	-10.48	52.47	976
Right PMd	20.61	-9.4	51.53	976
Right pIPS	21.64	-61.84	48.21	909

Table 3. Talairach coordinates and number of voxels for Movement Planning regions of interest

Area	Mean X	Mean Y	Mean Z	Voxels
Left SOG	-13.47	-89.31	14.38	959
Right SOG	24.31	-79.24	26.31	935
Left IOG	-44.32	-79.63	-0.47	696
Left LG	-10.5	-77.5	-12.5	1000
Right LG	7.5	-74.5	-12.5	1000
Left mIPS	-24.5	-44.5	52.5	1000
Right mIPS	22.5	-46.5	44.5	1000
Left pIPS	-18.5	-68.5	38.5	1000
Right pIPS	18.5	-59.5	45.5	1000
Left SPOC	-22.41	-73.51	32.58	979
Left PMd	-15.5	-14.5	58.5	1000
Right PMd	23.5	-14.5	56.5	1000
Left PMv	-51.47	-5.51	34.47	964
Right PMv	45.51	-2.53	31.44	964
Left CMA	-7.5	-23.5	49.5	1000
Right CMA	8.5	-26.5	48.5	1000
Left SMA	-7.5	-9.5	54.5	1000
Right SMA	10.5	-4.5	45.5	1000
Right S1	16.5	-34.5	58.5	1000
Left M1	-15.51	-26.49	61.49	997

Table 4. Talairach coordinates and number of voxels for Movement Execution regions of interest

Area	Mean X	Mean Y	Mean Z	Voxels
Left IOG	-51.42	-65.21	-4.27	722
Right IOG	46.5	-60.5	-7.5	1000
Left pIPS	-8.11	-65.31	51.09	582
Right pIPS	13.78	-70.79	46.53	579
Left mIPS	-24.5	-44.5	52.5	1000
Right mIPS	22.5	-46.5	44.5	1000
Left SMG	-52.5	-23.5	19.5	1000
Right SMG	52.5	-20.5	32.5	999
Left PMd	-25.6	-6.1	55.3	1000
Right PMd	23.5	-5.5	58.5	1000
Left PMv	30.46	42.46	31.46	990
Right PMv	-34.5	41.5	25.5	1000
Left IFG	-57.85	1.84	18.67	835
Right IFG	55.44	9.53	4.56	986
SMA	-4.5	-12.5	51.5	1000
Left S1	-25.5	-23.5	61.5	1000
Left M1	-20.5	-17.5	65.5	999

series data for select areas (Figure 4). These data are described in more detail in the following sections.

Task related activation during the visual target representation phase: Contrast 1 [Target Representation Reach > Target Representation Color] investigated which brain areas showed higher activation for visuospatial coding required to plan a reach (either pro or anti) than activation related to representing the color of the target (the requirement of the control task). In this phase, only the visual target location was known (as reach direction was only specified by an auditory instruction after this delay period), and any activation revealed by this contrast may be related to any aspect of target coding (not limited to spatial location). Figure 3A shows the activation map for this contrast superimposed on inflated cortical surfaces viewed from above. The indicated areas survived a cluster threshold correction of 82 voxels. This contrast revealed modest bilateral activation near the intersection of the precentral and superior frontal sulci, consistent with the location of dorsal premotor cortex (PMd) (Monaco et al. 2011), and modest unilateral activation in the right posterior intraparietal sulcus (pIPS). At first glance it might seem odd that only areas associated with movement control (Gallivan and Culham, 2015) were activated, but recall that the control task also involves memory of a non-spatial, non-motor target type. Thus, this subtraction shows areas with memory-epoch activity *specific to spatial location or early general motor preparation for reach*.

Task related activation during the movement planning phase: Contrast 2 [Movement Planning Reach (pro + anti) > Movement Planning Color] investigated which brain areas showed higher activation for movement planning for pro- or anti-reach than

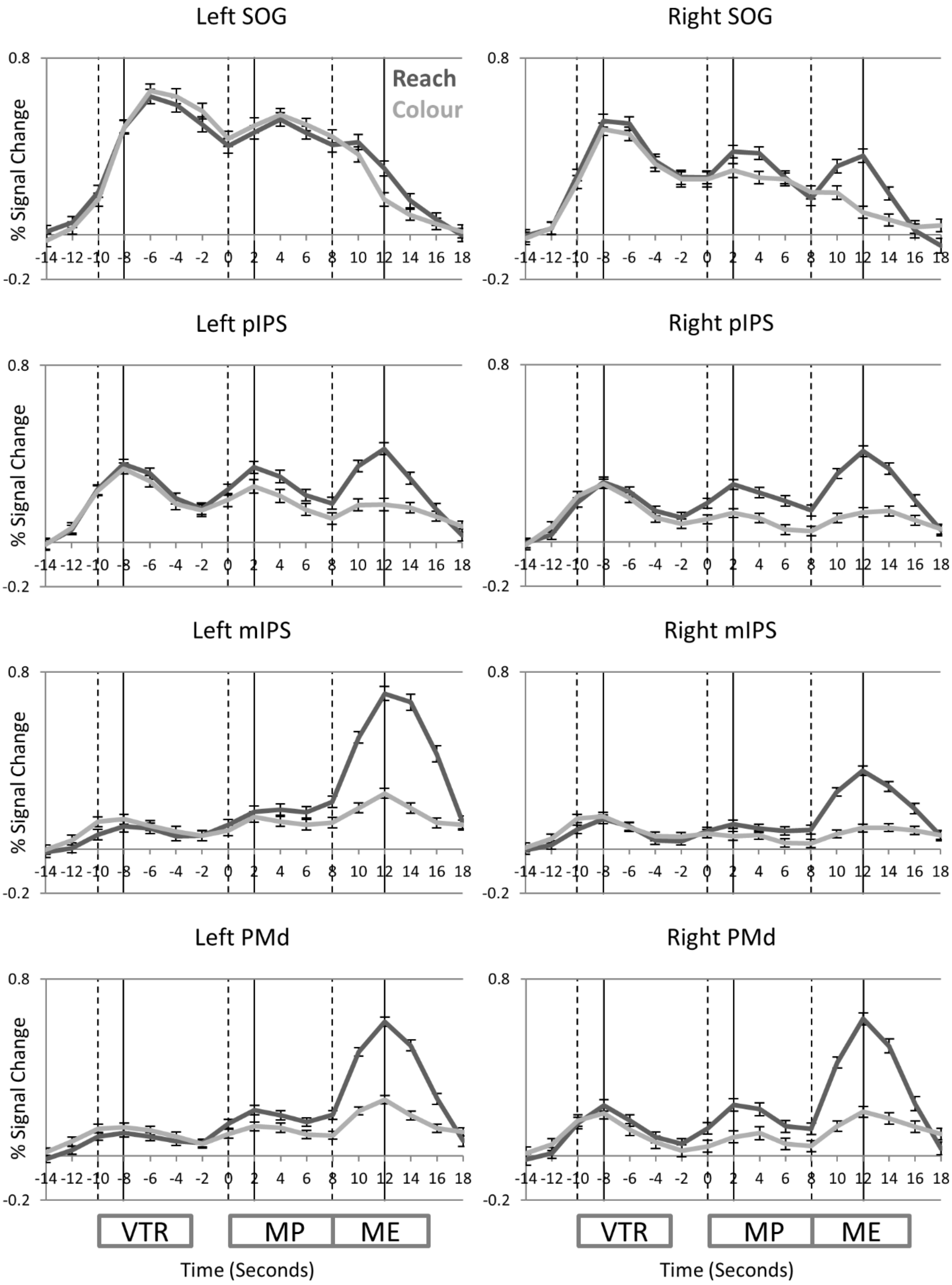
Left SOG
Right SOG
Left pIPS
Right pIPS
Left mIPS
Right mIPS
Left PMd
Right PMd
Reach
Colour
% Signal Change
0.8
-0.2
-14 -12 -10 -8 -6 -4 -2 0 2 4 6 8 10 12 14 16 18
VTR
MP
ME
Time (Seconds)

Figure 4. Time courses for four brain areas of interest (SOG, pIPS, mIPS, and PMd) that were bilaterally active from the Movement Planning Reach (pro + anti) > Movement Planning Color contrast during the movement planning phase. The dark grey line indicates activity (% signal change) from reach trials and the light grey line indicates activity from color report trials. Error bars are SEM across subjects. The x axis displays time in seconds and is time locked to the movement planning phase. The three vertical black dashed lines indicate the onset of the visual target representation (VTR), movement planning (MP), and movement execution (ME) phases (from left to right). Note that there is an activation peak corresponding to the black solid lines for all 7 time courses that contain three peaks (B-H), the only exception being left SOG.

activation related to representing the color of the target (the requirement of the control task). Activation during this phase could be related to planning a specific movement and/or general motor preparation in anticipation of an upcoming reach. The activation map for this contrast is shown on an inflated cortical surface viewed from the lateral and medial sides (Figure 3b). The marked areas survived a cluster threshold correction of 230 voxels. This contrast revealed widespread activation in bilateral dorsal premotor cortex (PMd), ventral premotor cortex (PMv), supplementary motor area (SMA), cingulate motor area (CMA), midposterior intraparietal sulcus (mIPS), posterior intraparietal sulcus (pIPS), superior occipital gyrus (SOG), lingual gyrus (LG). Activation was also found in the left hemisphere in primary motor cortex (M1), superior parietal occipital cortex (SPOC), and inferior occipital gyrus (IOG), and in right primary somatosensory cortex (S1). (For a complete list of abbreviations for regions of interest (ROI) discussed in this study, see table 1).

Task related activation during the movement execution phase: Contrast 3 [Movement Execution Reach (pro + anti) > Movement Execution Color] investigated which brain areas showed higher activation related to executing a pro- or anti-reach than activation related to indicating the color of the target with a button press (the requirement of the control task). The activation map for this contrast is shown on an inflated cortical surface (Figure 3C). The marked areas survived a cluster threshold correction of 206 voxels. This contrast revealed widespread activation in bilateral mIPS, M1, PMd, inferior frontal gyrus (IFG), supramarginal gyrus (SMG), and IOG. Activation was also found in the left hemisphere in primary somatosensory cortex (S1), in the right hemisphere in the middle frontal gyrus (MFG), and in the supplementary motor area (SMA) (could not disentangle the right and left hemisphere for SMA).

Time series data: To better understand the evolution of activation for these brain areas, we examined their time series. Figure 3 illustrates the time courses data of the reach and color conditions for 4 representative bilateral brain areas, chosen because they have been linked to visuomotor planning, including: superior occipital gyrus (SOG), posterior intraparietal sulcus (pIPS), midposterior intraparietal sulcus (mIPS), and dorsal premotor cortex (PMd). We selected these areas as SOG showed egocentric planning-related activation in a previous study (Chen et al., 2014) and pIPS, mIPS, and PMd are part of the parieto-frontal reach planning network (Culham et al., 2006; Gallivan et al., 2011, Vesia et al., 2012). The onset time for visual target representation, movement planning, and movement execution are indicated by grey vertical lines (noting that the BOLD response data have been time-corrected for estimated hemodynamic lag), with black lines indicating peak values during these 3 phases from left to right, respectively.

Looking at these representative time courses, several patterns emerge that help to understand the previous observations and provide reference events for further analysis. First, in nearly all of our regions of interests three peaks of activation were apparent, aligned closely with target representation, movement planning, and movement execution. An exception to this general trend was the lack of a distinctive third execution peak for some occipital areas, such as left SOG (Figure 4) and bilateral LG (not shown). Second, the relative heights of these peaks were dependent on the expected functional anatomy, with SOG (representing occipital cortex) showing a relatively larger target peak (although ‘planning’ and ‘execution’ peaks were present in the right cortex), pIPS showing roughly equal target, planning, and execution peaks, and mIPS and PMd showing predominant movement execution peaks. Third, the degree of reach task-specificity (gap between black vs. grey lines) generally increased both in time from visual target representation to movement execution and in cortical space from occipital cortex to parietal cortex to frontal cortex. Thus, the entire occipital-parietal-frontal axis was activated during target coding, planning, and execution, but the task-specificity of these responses increased along the antero-frontal axis and in the temporal transition from target, planning, and execution responses. We will examine this in more detail in the following sections using spatial parameters related to visual target and movement direction.

Contralateral Visual and Movement Direction Selectivity during Movement Planning

We next focused on the question of whether spatially selective activation during reach planning encodes retrospective visual location information and/or prospective movement information (Curtis, 2006). Henceforth, we will refer to these as ‘visual’ and ‘movement’ direction selectivity, respectfully, for brevity. After the pro or anti instruction, participants might hypothetically still retain memory of target location (left or right), while simultaneously planning a movement in the same or opposite direction. We took advantage of this to create contrasts that utilized all of the planning data, and either highlighted 1) visual direction selectivity where the pro-/anti-movement selectivity should cancel out (as in the right-target example shown in the left column of Figure 5A) or 2) movement direction selectivity, where left/right target direction should cancel out (as in the rightward movement example shown in the right column of Figure 5A). We focused our analysis on contralateral activation given the breadth of evidence for this type of directional selectivity in previous studies (fMRI (Medendorp et al., 2003; 2005; Filimon, 2010; Vesia and Crawford, 2012; Gertz and Fiehler, 2015), MEG (Van Der Werf et al., 2010), TMS (Vesia et al., 2010), patients (Khan et al., 2007) and primate neurophysiology (Gail and Andersen, 2006; Gail et al., 2009; Westendorff et al., 2010)). Consistent with some previous studies (Connolly et al., 2003; Fernandez-Ruiz, 2007; Bernier et al., 2012; Gertz and Fiehler, 2015) we only found contralateral directional tuning in reach-related areas located within the left hemisphere (opposite to the reaching hand). These areas are shown in Figure 5B & C (with corresponding ß-weights provided in Supplementary Figure 3 and Talairach coordinates in table 5). Some other regions of ipsilateral sensitivity appeared in both hemispheres in regions not generally associated with reach; these were eliminated from further analysis.

Visual Direction Selectivity: Contrast 4 [(pro-reach right target + anti-reach right target) – (pro-reach left target + anti-reach left target)] investigated contralateral visual selectivity during the movement planning phase in the left hemisphere, as trials where the visual target was presented in the right visual field were contrasted from trials where the visual target was presented to the left, regardless of the movement goal. The marked areas survived a cluster threshold correction of 75 voxels. In this contrast, the left cuneus was the only area to show significant contralateral activation for visual target direction (Figure 5B). A similar contrast was performed on the right hemisphere [(pro-reach left target + anti-reach left target) – (pro-reach right target + anti-reach right target)] but failed to yield significant activation that met our localizer criteria.

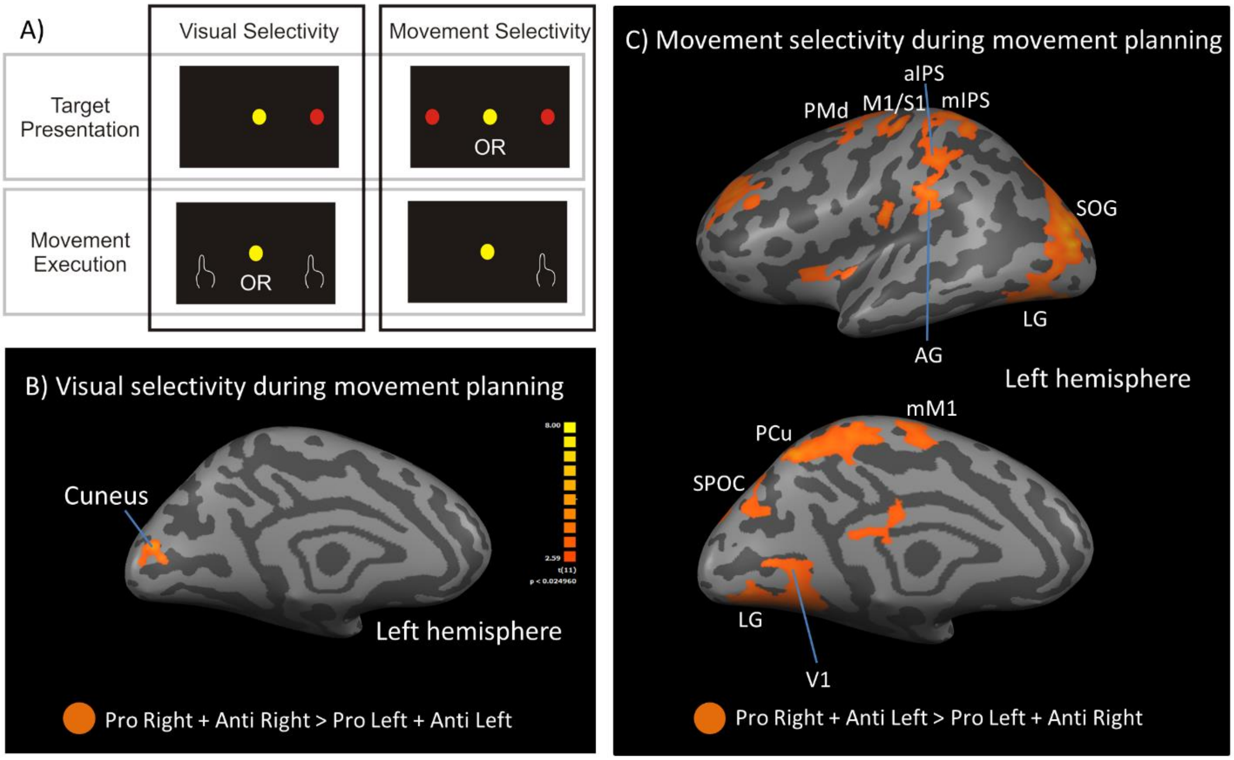

Figure 5. A visualization of the visual target and movement goal selectivity contrasts used in this experiment. For the visual selectivity contrasts, trials where the target was initially presented in the right visual field were contrasted against trials where the visual target was presented to the left, independent of the direction of the movement. For movement selectivity contrasts, the opposite was the case. Trials where the motor goal was to the right were contrasted against trials where the motor goal was to the left, independent of where the initial visual target was presented. These contrasts were used to examine activity during the movement planning phase. ***B)*** Voxelwise statistical maps obtained from the RFX GLM for the contrast Pro-Reach Right + Anti-Reach Right > Pro-Reach Left + Anti-Reach Left. Event-related group activation maps are displayed on the left hemisphere inflated brain of one representative subject for movement planning. Highlighted areas show significantly higher activation than control data with a

$p<0.05$ with Bonferroni and cluster threshold corrections. The Left cuneus met these criteria. C) Voxelwise statistical maps obtained from the RFX GLM for the contrast Pro-Reach Right + Anti-Reach Left > Pro-Reach Left + Anti-Reach Right. Event-related group activation maps are displayed on the left hemisphere inflated brain of one representative subject for movement planning. Highlighted areas show significantly higher activation than control data with a $p<0.05$ with Bonferroni and cluster threshold corrections. These areas include V1, LG, SOG, SPOC, mIPS, aIPS, PCu, AG, PMd, mM1, and an area encompassing parts of primary motor and somatosensory cortices (M1/S1). (See Table 1 for site abbreviations)

Table 5. Talairach coordinates and number of voxels for contralateral visually and motor selective areas during movement planning in the left hemisphere

Area	Mean X	Mean Y	Mean Z	Voxels
Visually Selective				
Cuneus	-2.56	-77.12	14.67	691
Motor Selective				
V1	-7.46	-76.05	-0.52	798
SOG	-28.51	-83.51	15.51	998
LG	-21.44	-74.43	-14.49	985
mIPS	-25.36	-45.39	58.35	961
SPOC	-24.6	-73.82	35.33	716
aIPS	-33.58	-27.39	50.78	902
Pcu	-4.46	-62.81	49.69	767
AG	-60.91	-36.32	24.07	823
PMd	-25.61	-3.38	58.67	671
mM1	-4.22	-17.19	63.32	859
M1/S1	-30.38	-16.12	56.13	891

Movement Direction Selectivity: Contrast 5 [(pro-reach right target + anti-reach left target) – (pro-reach left target + anti-reach right target)] investigated contralateral movement selectivity during the movement planning phase in the left hemisphere, as trials where the movement goal was to the right were contrasted from trials where the movement goal was to the left, regardless of the initial visual presentation. The marked areas survived a cluster threshold correction of 149 voxels. This contrast revealed widespread contralateral movement selectivity in occipital, parietal, and frontal areas (Figure 4C), including primary visual cortex (V1), lingual gyrus (LG), superior occipital gyrus (SOG), superior parietal occipital cortex (SPOC), midposterior intraparietal sulcus (mIPS), anterior intraparietal sulcus (aIPS), precuneus (PCu), angular gyrus (AG), dorsal premotor cortex (PMd), medial primary motor cortex (mM1), and an area bordering on primary motor and somatosensory cortex (M1/S1). This illustrates a network of reach-associated areas concerned with specifying upcoming reach direction during the planning phase. A similar contrast was performed on the right hemisphere [(pro-reach left target + anti-reach right target) – (pro-reach right target + anti-reach left target)] but failed to yield significant activation that met our localizer criteria.

Temporal Evolution of Visual and Movement Direction Coding

One of the main aims of our visual and movement direction selective voxelwise contrasts were to localize established reach-related regions for a more detailed temporal analysis on their time course data. This allowed us to understand the time course of visual and motor selectivity both within and across cortical sites. In these analyses, we traced the entire time course of visual and movement selectivity in the areas shown in Figure 4 using both the visual direction contrast (contrast 4) and the movement direction contrast (contrast 5). We also did the same for 4 sites in the left hemisphere obtained independently from the analysis in Figure 3, and obtained nearly identical results (Supplementary Figure 4).

Time Courses of Visual and Movement Direction Selectivity: Figure 6 plots the time courses of the visual directional selectivity (black lines) and movement directional selectivity (gray lines) for every region identified in Figure 5, with the exception of aIPS which showed relatively flat responses and is associated more with grasp than reach transport (Culham et al., 2006). As all of these regions are in the left hemisphere, visual direction selectivity was calculated by subtracting the time courses for trials where the visual target was presented ipsilaterally (pro-reach left and anti-reach left) from trials where the visual target was presented contralaterally (pro-reach right and anti-reach right). Movement direction selectivity for these areas was calculated by subtracting the time courses for trials with an ipsilateral reach (pro-reach left and anti-reach right) from trials with a contralateral reach (pro-reach right and anti-reach left). Supplementary figures 5, 6, and 7 show the time courses for these component signals, including % signal change for visual direction-selective activation for pro-reach left + anti-reach left, and pro-reach right + anti-reach right, as well as movement-selective activation for pro-reach left + anti-reach right and pro-reach right + anti-reach left.

Returning to figure 6, one-sample t-tests were performed to compare the % BOLD signal change at the time of the peak visual and motor activation to zero to indicate significant directional tuning in either the visual or motor domain (○). We limited our comparisons to these two points in time to indicate the presence of visual or

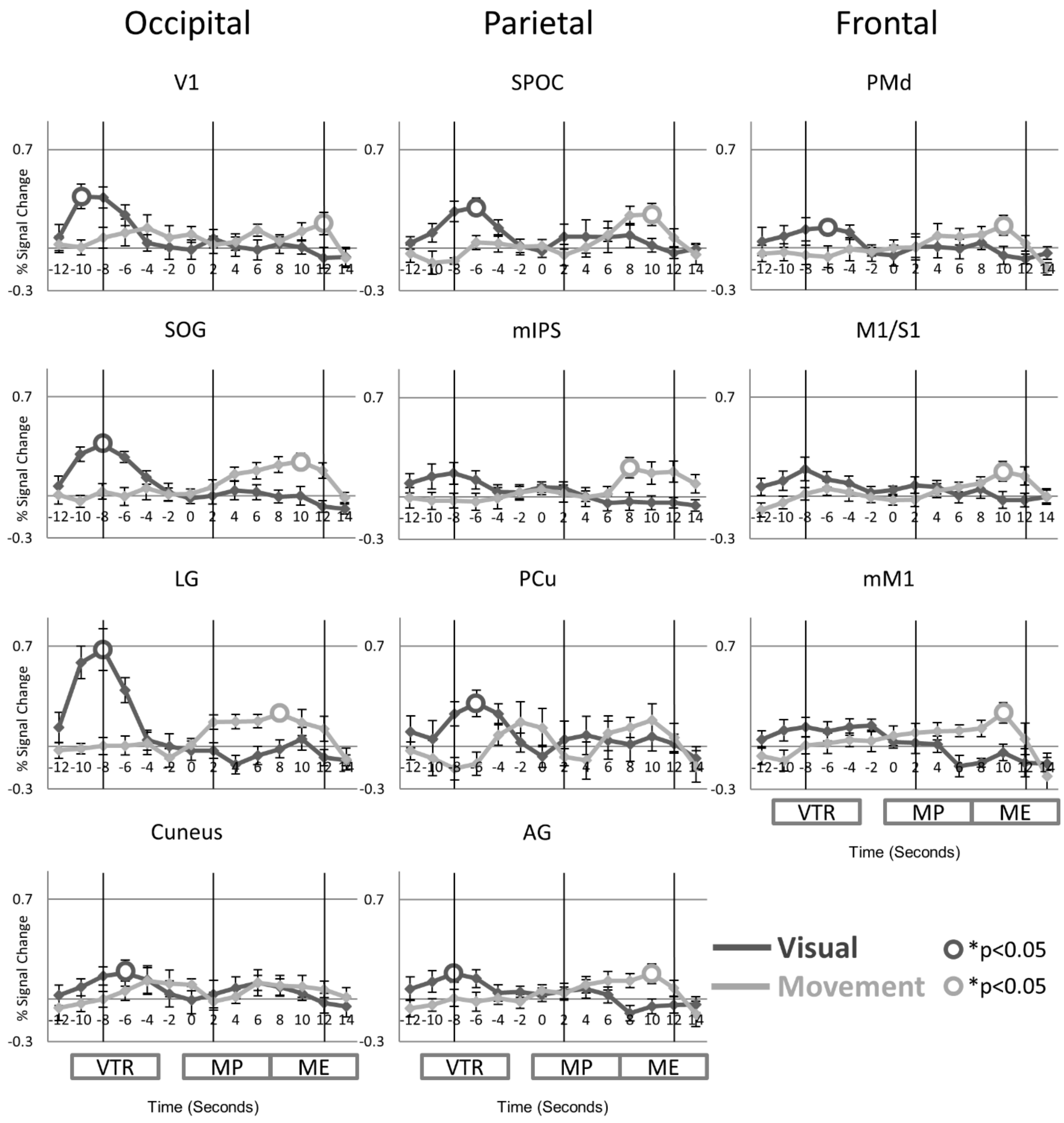

Figure 6. A plot of the time courses of visual and movement selectivity for left occipital (V1, SOG, cuneus and LG), parietal (SPOC, mIPS, PCu, and AG), and frontal (PMd, M1/S1, and M1) left hemisphere brain regions. On the x axis, time is in seconds and 0 indicates the start of the movement planning phase. The three black vertical lines indicate the times of peak activity noted in Figure 3 for the visual target representation

(VTR), movement planning (MP), and movement execution (ME) phases. The dark grey lines indicate the visually selective mean % signal change across subjects. This was calculated by subtracting the time courses for trials where the visual target was presented ipsilaterally (pro-reach left and anti-reach left) from trials where the visual target was presented contralaterally (pro-reach right and anti-reach right). The light grey lines indicate the movement direction selective mean % signal change across subjects. This was calculated by subtracting the time courses for trials with an ipsilateral motor goal (pro-reach left and anti-reach right) from trials with a contralateral motor goal (pro-reach right and anti-reach left). White open circles (○) indicate activity significantly greater than zero (one-sample t-test, $p<0.05$). Error bars are SEM across subjects.

movement direction selectivity in a brain area without needing to correct for multiple comparisons across all time points. As there were 2 t-tests, we performed a Bonferroni correction for 2 comparisons ($\alpha = 0.05$ / 2 comparisons = 0.025 corrected for $p < 0.05$). Our occipital, parietal, and frontal areas are divided into three columns for easier comparison, with ‘early’ to ‘late’ areas organized top to bottom. Again, several trends emerge from this time-course analysis. First, whereas reach general activation followed three peaks of event-related responses (Figure 4), directional selectivity showed only two peaks: the first a visual peak aligned with target presentation, and the second a more prolonged movement peak that in most cases appears to arise late in the planning phase, dropping off just at execution. Second, although visual peaks are more predominant in the occipital areas as one would expect, the motor peak was widespread. In particular, occipital areas SOG and LG show a surprisingly robust ‘movement direction coding’ during the planning phase (we will propose an alternative explanation for this in the discussion). In summary, it appears that movement direction selectivity engages the entire occipital-parietal-frontal reach network.

Although no areas in the right hemisphere met our localizer criteria, we performed a similar analysis on right SOG, mIPS, SPOC, and PMd by flipping the Talariach ‘x’ coordinate and creating a 5mm sphere ROI. These values were similar to right hemisphere coordinates for these areas reported by other papers (Vesia et al., 2010, Monaco et al., 2011, Gallivan et al., 2011, Chen et al., 2015). While right mIPS, SPOC, and PMd did not show much selectivity, right SOG showed a trend to prefer visual target direction early in the task, similar to left SOG. These right hemisphere data do not meet current statistical standards for reporting fMRI data, but we have included these data as a supplementary figure (Supplementary Figure 8).

Transition of Visual-to-Movement Direction Coding through Time in the Anti-Reach Task: If one subtracts contrast #4 (visual direction tuning) from contrast #5 (motor direction tuning), this essentially reduces to a contrast between the left and right anti-reach conditions during movement planning [anti-reach left target – anti-reach right target]. Note that here, direction is defined in terms of stimulus location, so a negative value would indicate contralateral visual direction selectivity, whereas a positive value would indicate contralateral movement direction selectivity (in the anti-reach task). We henceforth refer to this integrated measure as our 'visuo-movement' selectivity parameter. Figure 7 plots this parameter through time for 8 areas in the left hemisphere that have been selected to best represent the occipital-parietal-frontal reach network, ordered to correspond roughly to 'early' (V1) through 'late' (mM1) areas in the visuomotor transformation for reach. We performed paired t-tests between the visually and movement selective data at the time of peak visual (the minimum mean value) and peak movement (the maximum mean value) selectivity to indicate significantly higher visual or movement selectivity, respectively. We limited our comparisons to these two points in time to indicate the presence of significantly higher visual or movement direction selectivity in a brain area without needing to correct for multiple comparisons across all time points. As there were 2 t-tests, we performed a Bonferroni correction for 2 comparisons ($\alpha = 0.05 / 2$ comparisons $= 0.025$ corrected for $p < 0.05$).

As one might predict, only significantly higher visual selectivity was observed in V1, and only significantly higher movement selectivity was observed in mM1. SPOC

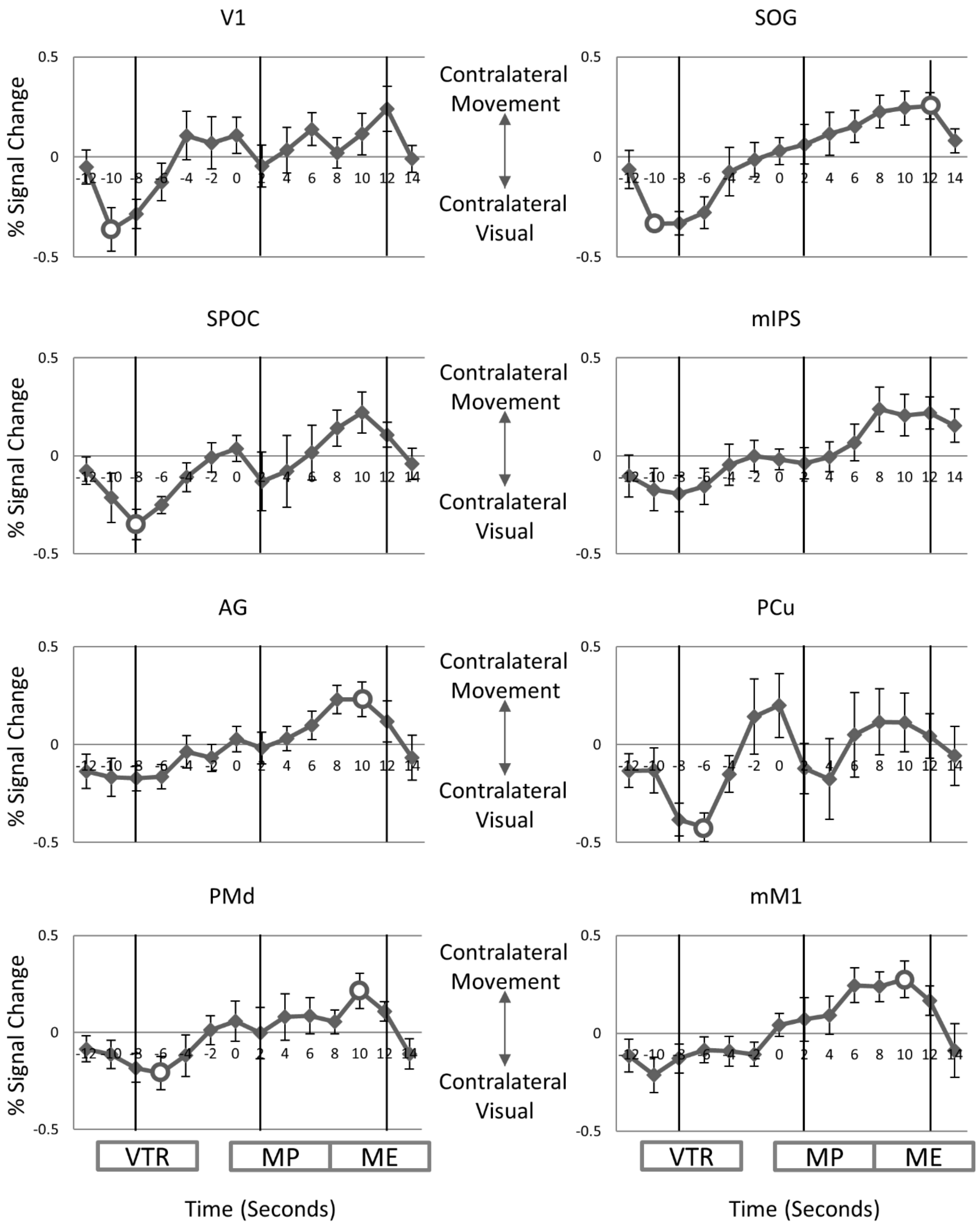
V1
SOG
SPOC
mIPS
AG
PCu
PMd
mM1
% Signal Change
0.5
0
-0.5
-12 -10 -8 -6 -4 -2 0 2 4 6 8 10 12 14
Contralateral Movement
Contralateral Visual
VTR
MP
ME
Time (Seconds)

Figure 7. Visuo-movement direction selectivity plotted through time for left V1, SOG, SPOC, mIPS, AG, aIPS, PMd, and M1. This was calculated by subtracting the visual selective time course data from the movement direction selective time course data displayed in Figure 5. Thus, a negative % signal change indicates visual selectivity and a positive score indicates movement direction selectivity. On the x axis, time is in seconds and 0 indicates the start of the movement planning phase. The three black vertical lines indicate the times of peak activity noted in Figure 3 for the visual target representation (VTR), movement planning (MP), and movement execution (ME) phases, and grey vertical lines indicate their onset. Open circles (○) indicate significantly greater coding for that coordinate system as revealed by a paired t-test ($p<0.05$). Error bars are SEM across subjects.

and PCu also showed significantly higher visual selectivity, while AG also showed significantly higher movement selectivity. SOG and PMd showed both significantly higher visual and movement selectively. Also, as one would expect in the anti-reach task, the switch from visual coding to movement coding occurs around the time of the pro/anti instruction (although we could not establish this statistically because of the size of variance relative to the small visuomotor scores at this cross-over point). What is more remarkable, is the strong resemblance between these curves obtained from very different brain areas, ranging from some that have been categorized as strictly visual (V1) through various visuomotor areas to mM1. The next section further quantifies these observations.

Temporal correlation of direction selectivity between cortical areas

To quantify some of the qualitative observations made above, we performed temporal correlations of visual, movement, and visuo-movement directional selectivity between the regions identified in Figure 5. To do this, we used the % BOLD signal change time series data from 12 seconds before the onset of movement planning (target presentation) to 12 seconds after (peak activity for motor execution as seen in Figure 3). We then correlated between sites (r) by matching their BOLD signal changes for each scan in this time range. Note that the main contribution to these correlations likely came from the target coding phase and late planning phase for the visual and movement parameters respectively (Figure 6), whereas the visuo-movement parameter was modulated throughout the entire sequence (Figure 7).

Figure 8A shows the visual direction selectivity correlations between each brain area. The entries in this matrix have been ordered (top to bottom and left to right) based on the strength of correlation with V1, using the functional region from contrast 5. V1 was selected as the most obvious reference region for visual input to the system. The resulting correlation matrix shows a progressive drop in correlation down and to the left (as expected) progressing generally from more sensory regions like LG to more motor regions such as mM1. This can also be visualized as progression from darker red to lighter pink in the color scheme we have used for the matrix cells. These correlations were often significant (as indicated by bolded numbers) with a $p < 0.05$ with Bonferroni corrections for 10 comparisons [$\alpha = 0.05 / 10$ comparisons $= 0.005$ corrected for $p < 0.05$].

Figure 8D graphically represents the same data as Figure 8A as a network of correlations between our various regions of interest. The width of each line is scaled by the r^2 value for the two regions that it joins, with significant correlations highlighted in yellow ($p < 0.05$, non-significant correlations are shown in orange). This figure also helps to visualize ‘hub’ areas in the visual domain, sprouting thick yellow lines (high correlations with yellow indicating significant correlations) toward numerous other areas, as opposed to thin orange lines (low correlations with orange indicating non-significant correlations). In the visual domain (Figure 8D), one observes an extensive network of significant correlations including V1, SOG, mIPS, M1/S1, and PMd (i.e. these areas have many thick yellow lines), but largely excluding mM1 and PCu (i.e., these areas have mainly thin orange lines). Overall, SOG had the highest mean correlation (0.83) to all other areas in the visual domain.

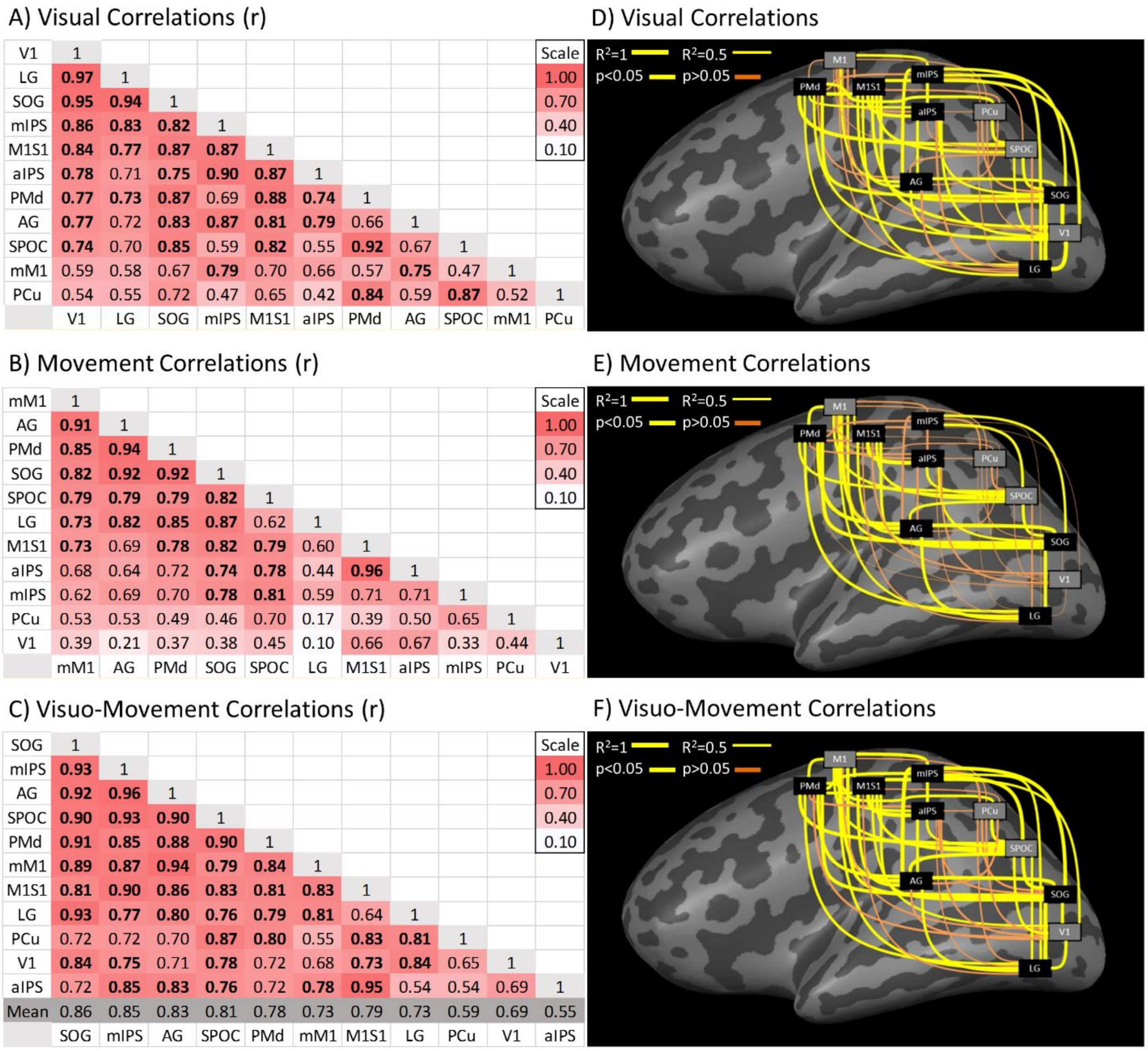

A) Visual Correlations (r)

V1	1										
LG	**0.97**	1									
SOG	**0.95**	**0.94**	1								
mIPS	**0.86**	**0.83**	**0.82**	1							
M1S1	**0.84**	**0.77**	**0.87**	**0.87**	1						
aIPS	**0.78**	0.71	**0.75**	**0.90**	**0.87**	1					
PMd	**0.77**	**0.73**	**0.87**	0.69	**0.88**	**0.74**	1				
AG	**0.77**	0.72	**0.83**	**0.87**	**0.81**	**0.79**	0.66	1			
SPOC	**0.74**	0.70	**0.85**	0.59	**0.82**	0.55	**0.92**	0.67	1		
mM1	0.59	0.58	0.67	**0.79**	0.70	0.66	0.57	**0.75**	0.47	1	
PCu	0.54	0.55	0.72	0.47	0.65	0.42	**0.84**	0.59	**0.87**	0.52	1
	V1	LG	SOG	mIPS	M1S1	aIPS	PMd	AG	SPOC	mM1	PCu

Scale
1.00
0.70
0.40
0.10

B) Movement Correlations (r)

mM1	1										
AG	**0.91**	1									
PMd	**0.85**	**0.94**	1								
SOG	**0.82**	**0.92**	**0.92**	1							
SPOC	**0.79**	**0.79**	**0.79**	**0.82**	1						
LG	**0.73**	**0.82**	**0.85**	**0.87**	0.62	1					
M1S1	**0.73**	0.69	**0.78**	**0.82**	**0.79**	0.60	1				
aIPS	0.68	0.64	0.72	**0.74**	**0.78**	0.44	**0.96**	1			
mIPS	0.62	0.69	0.70	**0.78**	**0.81**	0.59	0.71	0.71	1		
PCu	0.53	0.53	0.49	0.46	0.70	0.17	0.39	0.50	0.65	1	
V1	0.39	0.21	0.37	0.38	0.45	0.10	0.66	0.67	0.33	0.44	1
	mM1	AG	PMd	SOG	SPOC	LG	M1S1	aIPS	mIPS	PCu	V1

Scale
1.00
0.70
0.40
0.10

C) Visuo-Movement Correlations (r)

SOG	1										
mIPS	**0.93**	1									
AG	**0.92**	**0.96**	1								
SPOC	**0.90**	**0.93**	**0.90**	1							
PMd	**0.91**	**0.85**	**0.88**	**0.90**	1						
mM1	**0.89**	**0.87**	**0.94**	**0.79**	**0.84**	1					
M1S1	**0.81**	**0.90**	**0.86**	**0.83**	**0.81**	**0.83**	1				
LG	**0.93**	**0.77**	**0.80**	**0.76**	**0.79**	**0.81**	0.64	1			
PCu	0.72	0.72	0.70	**0.87**	**0.80**	0.55	**0.83**	**0.81**	1		
V1	**0.84**	**0.75**	0.71	**0.78**	0.72	0.68	**0.73**	**0.84**	0.65	1	
aIPS	0.72	**0.85**	**0.83**	**0.76**	0.72	**0.78**	**0.95**	0.54	0.54	0.69	1
Mean	0.86	0.85	0.83	0.81	0.78	0.73	0.79	0.73	0.59	0.69	0.55
	SOG	mIPS	AG	SPOC	PMd	mM1	M1S1	LG	PCu	V1	aIPS

Scale
1.00
0.70
0.40
0.10

D) Visual Correlations

E) Movement Correlations

F) Visuo-Movement Correlations

Figure 8. Correlations through time between regions derived from visual, movement, and visuo-movement spatial parameters. A-C) Matrices showing correlations (r) through time between all areas for each spatial domain tested (redundant entries in upper-right half are omitted). A continuous color scale is used to indicate the strength of correlation (r), i.e., with white close to 0.1 and red close to 1.0, and significant correlations (p<0.05, Bonferroni corrected) are bolded. Site correlations were derived by comparing data points from each point in time derived for the 10 movement-selective areas in the left

hemisphere correlated for visual selectivity from target presentation (-12 seconds) to peak motor execution activation (+12 seconds), time-locked to the onset of movement planning. A) Visual Correlations. The order of areas is based on strength of correlation with V1. B) Movement Correlations. The order of areas is based on strength of correlation with mM1 (the motor output from the system). C) The time courses for the 10 motor-selective areas correlated for visuo-movement selectivity. The order of areas is based on strength of the mean correlation with the other areas (shown in lower row). D-F: Graphical representations of the strength of correlation between left hemisphere brain areas for visual (D), movement (E), and visuo-movement (F) correlations corresponding to data from A, B, and C, respectively. The thickness of the line indicates the r^2 value, with a thin line being close to 0 and a thick line close to 1. For these plots we used r^2 to increase the difference between highly correlated and less correlated areas. These data are superimposed on a left hemisphere ‘inflated brain’ from a typical subject where light gray signifies gyri and dark gray signifies sulci. See table 1 for site abbreviations. Brain areas in black boxes are superficial and those in grey boxes appear on the medial side of the inflated brain.

Figure 8B similarly shows the movement direction selectivity correlations between each brain area. Here, mM1 was chosen as the most obvious reference motor region, such that the matrix entries are ordered based on the strength of correlation with mM1 (the functional region from contrast 5 was used). This resulted in an ordering of sites nearly opposite to Figure 8A, except for a few regions (notably PCu) shifted to the right (meaning its correlations rank remained low) or left (e.g., SOG, meaning that it retained its relatively high rank in both representations). Again, this convention caused higher correlations to cluster in the upper-left of the matrix, many of these significant (bold) with a $p < 0.05$, Bonferroni corrected as in Figure 8A. For movement direction selectivity (arising mainly during the late planning phase; Figure 8E) a network of significant correlations arose between the regions spanning SOG to mM1, including AG, SPOC, M1/S1, and PMd, but excluding the very thin ‘connections’ to the early visual areas V1 and LG, as well as parietal areas aIPS, mIPS and PCu. Perhaps surprisingly, SOG once again had the (marginally) highest overall mean correlation (0.75) to all other regions in the movement domain. AG also had a mean correlation of 0.75, and these regions appear (along with SPOC) as prominent ‘hubs’ in Figure 8E.

Figure 8C provides a similar plot, but in this case using the visuo-movement parameter from Figure 7. In this case there is no obvious reference region or order, so we ordered the chart from highest to lowest mean correlation across all sites (lower row in dark grey), such that SOG ended up in the upper-left cell with (once again) the highest mean correlation to other areas (0.86). Although these plotting conventions tended to place higher correlations to the upper-left of the matrix, the overall distribution of high and significant correlations was broader in this domain (Figure 8C), extending further down and to the right than the individual visual and movement domains (Figure 8 A,B). In addition to SOG, mIPS, AG, and SPOC showed mean correlations above 8.0, with SPOC being noteworthy for being the only site that was significantly correlated to all other areas ($p < 0.05$ with Bonferroni corrected as in Figure 8A). These four areas emerge as major correlation 'hubs' in Figure 8F, as nearly all of the correlations are robust and significant (with PCu remaining the main exception). These analyses suggest that, despite overall biases toward visual or movement function between different sites, the entire occipital-parietal-frontal reach network is involved in the visuomotor transformation for a memory-guided reach task.

When these values were calculated between all possible pairings of our identified regions of interest, we obtained overall r values of 0.739±0.13 for visual, 0.652±0.20 for movement, and 0.799±0.10 for visuo-movement (mean ± SD) selectivity indices. To test if they were significantly higher than zero, we performed three one-sample t-tests on the mean r scores for each brain area, comparing zero to visual (t(10)=37.129, $p<0.001$), motor (t(10)=18.771, $p<0.001$), and visuomotor (t(10)=45.755, $p<0.001$) selectivity frames, all of which were significant. To test for differences between selectivity frames and to investigate differences between brain regions, we performed an ANOVA on the r values with selectivity frame (visual, movement, and visuo-movement) and the 11 brain areas as fixed factors. The ANOVA was significant (F(32,1)=5.689, $p<0.001$) and showed significant main effects for selectivity frame ($p<0.001$) and brain area ($p<0.001$), as well as a significant interaction between selectivity frame and brain area ($p<0.005$). Bonferroni post-hoc tests on selectivity frames revealed that visual, movement, and visuo-movement selectivity were all significantly different from each other. Bonferroni post-hoc tests on brain areas revealed that the precuneus and V1 showed significantly lower correlations than several other brain areas (for PCu: AG, aIPS, mM1, mIPS, PMd, M1/S1, SOG, and SPOC; for V1: AG, mIPS, PMd, M1/S1, SOG, and SPOC). Thus, both retrospective target direction and prospective reach direction were important for describing correlations between these networks at different phases, and a visuo-movement parameter that captured both of these provided the best overall description.

2.5 Discussion

In this study, we used an event-related fMRI design to investigate several key questions. To summarize, the first was to differentiate which cortical areas are involved in spatial target representation, reach movement planning, and reach movement execution. This analysis revealed selective, bilateral PMd and right pIPS activation during the target representation phase, whereas an entire occipital-parietal-frontal reaching network was activated during the motor planning and execution phases. The second question we aimed to answer was, during motor planning, which brain areas are directionally selective in visual or motor coordinates? During our planning phase, the left cuneus showed significant contralateral visual selectivity, but the majority of directionally selective occipital, parietal and frontal activation was tuned for contralateral reach direction. Observing the time courses of these directional parameters across all three phases of our task, we observed that most areas showed visual selectivity following target presentation and most areas showed movement selectivity late in the planning phase, but all reach-related areas showed a progressive visuomotor transition when these measures were collapsed into a single visuo-movement parameter. Likewise, when we correlated these parameters through time between different areas, we found overlapping but distinct visual and motor networks, but that all of the areas activated in occipital, parietal, and frontal cortex were correlated in terms of the visuo-movement index. In the following sections we will discuss each of these findings in more detail.

General activation during visual target memory, reach planning, and reach execution.

Many previous fMRI studies have implicated superior occipital-parietal-frontal cortex in visually guided reaching (Astafiev et al., 2003, Connolly et al., 2003; Medendorp et al., 2003, 2005; Prado et al., 2005; Fernandez-Ruiz et al., 2007; Beurze et al., 2009; Cavina-Pratesi et al., 2010; Fabbri et al., 2012; Konen et al., 2013; Chen et al., 2014). However, to our knowledge none of these clearly separated the three phases of target representation, movement planning, and movement execution through time. To do this within the spatiotemporal limitations of fMRI, we required a paradigm with a series of instructions and delays which likely introduced more cognitive aspects to the task one would see during on-line control, but with this caveat in mind, we were able to trace both general and direction-specific activation through those three phases. Most of our regions of interest showed different degrees of time-locked activation during target representation, planning, and execution (Figure 4), depending on whether the region was more visual (e.g., SOG) or motor (e.g., PMd), but here we will restrict our discussion to significant clusters of activation during these three phases (Figure 3).

Our analysis of the target representation phase (Figure 3A) revealed limited activation in bilateral PMd and right pIPS, perhaps related to spatial working memory (Courtney et al., 1996; Srimal and Curtis, 2008) or activity related to preparatory set (Culham et al., 2006, Chen et al., 2014). Chen et al. (2014) found a broader range of occipital-parietal-frontal activation during the target memory phase of their paradigm. Our target memory phase was followed by target planning and then execution, whereas their target memory phase was followed immediately by motor execution. This may have precipitated earlier preparatory activity in their paradigm and thus explain the difference. Activation in the parietal cortex is consistent with the uncertainty condition found in Gertz and Fiehler (2015), though their parietal activation was in the left hemisphere and ours was in the right. This difference could be due to the additional delay we added before the pro / anti instruction or the way we defined regions of interest (we derived coordinates from peak voxels in our own data whereas they used published coordinates).

Note that in our paradigm, subjects could not anticipate the required movement plan or derive it from the visual stimulus until the pro / anti instruction was given at the start of the second delay. During this movement planning phase (Figure 3B), we observed widespread activation in the classic parieto-frontal reach network, including SPOC, mIPS, SMA, PMd, and M1 (Culham et al, 2006; Gallivan and Culham, 2015). Comparing this widespread planning activation to the limited activation that was observed in the target representation phase suggests that previous studies that combined these two phases (Medendorp et al., 2003, Fernandez-Ruiz et al., 2007) were mainly reporting activity related to visuomotor transformations and/or movement planning, as opposed to target memory. We also observed considerable activation of occipital cortex, including LG, IOG and SOG, during the second delay, a phenomenon known as ‘occipital reactivation’ (Singhal et al., 2013), which we will discuss further in subsequent sections. In all these lobes, lateral cortex activation was greater in the left hemisphere contralateral to the hand, consistent with previous studies (Connolly et al., 2003; Fernandez-Ruiz, 2007; Bernier et al., 2012; Gertz and Fiehler, 2015). Finally, all of these regions of activation became even more extensive (relative to controls) in the movement execution phase (Figure 3C), also extending into prefrontal (e.g., IFG) and inferior parietal (e.g., SMG) areas that might be associated with cognitive aspects of the task, such as guidance of the movement based on spatial memory (Gallivan et al., 2015). In general, through our three phases we observed a general spread and ramping up of activation relative to controls throughout occipital-parietal-frontal cortex, presumably as different constraints were added to the task (target memory, rule based visuomotor transformation, movement planning, and actual execution) while retaining past information.

Directional Selectivity during Movement Planning

A second goal of our study was to look at cortical direction selectivity during movement planning, and determine which areas are selective for visual target direction and movement direction. Note that our paradigm was not designed to explicitly separate cognitive events such as attention vs. intention (Colby and Goldberg, 1999; Andersen and Buneo, 2002), but can only disambiguate directional selectivity relative to our objective measures (visual target direction and movement direction). Clearly attention must play a role in our task: subjects likely attended to remembered target direction in the first memory delay (Rizzolatti et al., 1987), and motor goal direction in the second planning delay, switching attention to the opposite hemifield during the ‘anti’ trials (Rolfs et al., 2013). The latter must especially play a role in the switching of directional tuning from stimulus to motor goal that we observed in occipital cortex (see below for details). On the other hand, massive recruitment of the parieto-frontal reach network that we observed in the late planning and early execution phase of our task (much of which proved to be movement direction selective) is most likely related to the intention to move (Andersen and Buneo, 2002; Cisek and Kalaska, 2010).

In the following, more detailed discussion, we will only consider regions that showed significant clusters of activation. One of the main aims of our visual and movement direction selective contrasts was to localize established reach-related regions for a more detailed temporal analysis on their time course data. We further restricted this analysis to the second delay (movement planning) because 1) this gave much more activation in general than the first delay, 2) the first delay could only yield visual directional selectivity, 3), selective combinations of our pro- and anti-reach data could isolate visual vs. motor selectivity during the second delay, and 4) the movement execution phase was biased by somato-motor activation related to the arm movement itself.

Contralateral Direction Tuning and Handedness. Although we found scattered, non-specific clusters of activation of ipsilateral tuning (for either target or movement, primarily in the right hemisphere) in general, we found a fairly widespread tendency toward contralateral direction tuning within the occipital-parietal-frontal reach system in the left hemisphere. This does not necessarily mean that these areas only code one direction of target or movement (indeed most areas showed responses for both directions; Supplementary Figures 6-8). Instead, it means that there was more activation for contralateral than ipsilateral movement. This generally agrees with previous investigations of occipital, parietal, and prefrontal activity based on fMRI (Medendorp et al. 2003; 2005; Filimon, 2010; Vesia and Crawford, 2012; Gertz and Fiehler, 2015), MEG (Van Der Werf et al., 2010), TMS (Vesia et al. 2010), patients (Khan et al., 2007) and primate neurophysiology (Gail and Andersen, 2006; Gail et al., 2009; Westendorff et al., 2010). Contralateral movement tuning is more surprising in S1 and M1 (because they are associated with moving the contralateral hand in both directions), but this is easily explained. In our set-up, the right hand started from the left side, so it moved more for rightward targets, thus predicting more activation for contralateral targets.

Further, this contralateral tuning was always in the left hemisphere, contralateral to the right hand used in the study. This is consistent with several previous fMRI studies (Connolly et al., 2003; Fernandez-Ruiz et al., 2007; Bernier et al., 2012; Gertz and Fiehler, 2015). This asymmetry could also relate to the statics of fMRI, i.e., the way that several neural signals might need to combine to produce significant effects at the level of the BOLD signal. Here, this likely involves interactions between hand lateralization and visual hemifield lateralization (Perenin and Vighetto, 1988; Rossetti et al., 2003, Medendorp et al., 2005b; Beurze et al., 2007; Blangero et al., 2007, Gallivan et al., 2011; Vesia and Crawford, 2012). In particular, greater activation is expected in the cortex contralateral to the hand (Medendorp et al. 2005; Snyder, 2000), and as mentioned above, this effect would be magnified in motor areas in our experiment because the right hand moves more to the right than it does for left targets. In more visual areas, there may also an influence of handedness on attention (Perry et al., 2015).

<u>Visual directional selectivity</u>. The visual directionally selective contrast in our task found that only the left cuneus showed significant activation for visually contralateral targets regardless of the motor requirement. This implies that there is a region in occipital cortex that is specifically concerned with retaining the visual direction of the original stimulus, regardless of whether subjects are planning a movement in that direction or in the opposite direction. Makino et al. (2004) previously found that the

cuneus can be activated by both visual search and memory search, and suggest that it may be responsible for attentional shifts in short and long term memory. These search and attentional functions may be aided by a visual representation of an object in space, regardless of and independent from the motor requirement of a task. Nonetheless, the extent of visual lateralized activation that we observed here, restricted to cuneus, was rather modest compared to the visually-tuned BOLD response observed throughout occipital and parietal cortex during reversing prism adaptation (Fernandez-Ruiz et al., 2007). We will return to this apparent contradiction in a later sub-section.

Movement direction selectivity. During movement planning, we observed relatively widespread movement-tuned direction selectivity in the left parieto-frontal cortex, including mIPS, SPOC, AG, aIPS, PMd, and M1/S1. This generally agrees with previous reach (and saccade) investigations that have used the pro/anti task combined with fMRI (Medendorp et al., 2005), MEG (Van Der Werf et al., 2008, 2010), and primate neurophysiology (Gail and Andersen, 2006; Gail et al., 2009; Westendorff et al., 2010). Consistent with this, PMd neurons are active during the delay period preceding an instructed movement, as well as tuned for the direction and distance of reaches with either hand (Weinrich and Wise, 1982; Caminiti et al., 1991; Messier and Kalaska, 2000; Cisek et al., 2003). It is perhaps more surprising that we found several occipital areas linked to movement direction during the planning phase, including SOG. Likewise, Chen et al. (2014) found directionally selective occipital activation during their movement execution phase. One does not generally associate occipital cortex with movement planning, but note that in the pro / anti paradigm, subjects may use a strategy of imagining a target that is either contiguous with, or opposite to the original visual stimulus. These findings suggest that occipital cortex plays a more important role in action planning than is often assumed (Pasternak and Greenlee, 2005; Gutteling et al., 2015).

Reconciling Studies of Spatial Tuning for Reach Planning. The Fernandez-Ruiz et al. (2007) prism reversal study showed visual tuning in most of the same occipital-parietal regions that showed movement tuning in the pro- / anti-reach task (see also Gertz and Fiehlher, 2015). This appears to be a contradiction, but Ferandez-Ruiz et al. (2007) offered an explanation based on discriminating the parameter being represented (i.e., visual target, vs. movement goal, vs. movement direction) and the coordinate frame used to represent this (i.e., retinal coordinates vs. body-fixed coordinates). According to this notion, areas such as mIPS do not encode visual target direction (that contradicts the current study) or movement direction (which contradicts the prism-reversal study). Instead, they may encode the direction of the imagined goal in retinal coordinates (which would be linked to retinal input during prism reversal, but reversed relative to retinal input in the anti-reach task). This model fits most of our occipital-parietal regions, with exception of cuneus (which appears to encode visual stimulus direction in both tasks; see above) and AG, which appears to encode extrinsic movement direction in both tasks, perhaps in somatosensory coordinates (Fernandez-Ruiz et al., 2007; Vesia et al., 2006, 2010; Vesia and Crawford, 2012).

A complication to this scheme is that Kuang et al. (2016) recorded action potentials from intraparietal cortex in monkeys trained on both the prism reversal task and the pro- / anti-reach task, and found that some neurons did encode the goal in visual coordinates, but most encoded movement direction. They reconciled this finding with fMRI results by noting that local field potentials –which may drive the BOLD response – agreed better with the visual goal prediction. Alternatively, the massive amount of training required for monkeys to do such tasks may have altered synaptic organization, whereas the human subjects received minimal training. However, these are matters of degree, not fundamental differences. Either way, it appears that the occipital-parietal-frontal reach planning system can simultaneously encode three spatial variables: visual stimulus direction, the goal in visual coordinates, and extrinsic movement direction.

Visual, Movement, and Visuo-movement Selectivity Through the Entire Task

Some of the most interesting findings in this experiment derived from plotting the time courses of visual and movement selectivity (Figure 6) for all of our regions of interest. A number of neurophysiological studies have followed the time course of directional tuning during a pro / anti task (e.g., Zhang and Barash, 2000; Gail and Andersen, 2006; Gail et al., 2009). However, to our knowledge, we are the first to extract these variables from pro- / anti-reach data in the human brain and examine their time course through separate target representation, planning, and reach execution phases. Although fMRI suffers by comparison in spatiotemporal resolution, it compensates by allowing one to compare these responses across the entire brain. In short, although some areas showed primarily visual direction tuning following presentation of the target and some primarily showed movement direction tuning late in the planning phase, most of our regions of interest showed both of these responses. We shall consider these ‘lobe-by-lobe’, and then consider the network.

Occipital cortex. Not surprisingly V1 and cuneus primarily showed visually selective activation, as numerous previous studies have shown human V1 to code visual stimulus responses (Engel et al., 1997; Singh et al., 2000), and perhaps even visual memory responses (Pratte and Tong, 2014; Malik et al., 2015). As mentioned above, the finding that only left occipital areas showed direction selectivity was surprising, and might relate to attentional enhancement related feedback from the contralateral hand and working in that hands preferred areas of space (Gallivan et al. 2011; Perry et al., 2015) Further, SOG and LG showed both visual and 'motor' selectivity. It is possible that these structures initially responded to the visual stimulus, but after the pro/anti instruction were involved in imagining a virtual target that could be flipped opposite to the actual stimulus in the case of anti-reach trials (Rolfs et al., 2013). This could explain the phenomenon of occipital reactivation during reaches, and could involve re-entrant feedback from motor systems (Singhal et al., 2013).

Parietal cortex. To different degrees, all of our parietal structures showed dual spatial selectivity, but SPOC and AG stood out as 'hub' areas that showed both visual and movement selective activation. Consistent with our results, recent studies have implicated SPOC as a visually-guided reaching area (Culham et al., 2006; Filimon et al., 2009; Vesia et al., 2010; Gallivan and Culham, 2015). Previous studies on AG, however, have implicated it as coding the motor output of a task (Fernandez-Ruiz et al., 2007; Vesia et al., 2010), making the visually selective activation unexpected. However, this might indicate transformation of visual signals into somatosensory signals, as suggested by its general role in left-right space discrimination (Hirnstein et al., 2011). The precuneus was found to be visually selective during the target representation phase. This activation could be related to visuo-spatial imagery (Cavanna and Trimble, 2006), although it did not show the anti-reach reversal we observed for SOG. It is also unclear why both PCu and SPOC show slight reversals from motor to visual planning around the time motor planning begins. These reversals did not reach significance, but if they represent a real result, we speculate this may be due to a visual re-activation once the movement is known.

mIPS only showed directionally selective motor activation. This is consistent with the suggestion in Fernandez-Ruiz et al. (2007), discussed above, that such areas would show movement tuning in an anti-reach task. However, the lack of an early visual response is surprising given that it has been linked to both reach and saccade planning, attention, and visual working memory (Curtis et al., 2004; Srimal and Curtis, 2008; Curtis and Connolly, 2008; Jerde et al., 2012). Medendorp et al. (2005) found that for saccades, retinotopic IPS (similar to mIPS) coded the visual location of a target before the pro/anti instruction and the motor direction afterwards. It is important to note, however, that these areas were selected by different methods (an independent localizer versus peak voxel regions of interest) and that activation for saccades may differ from the reach planning network.

<u>Frontal cortex</u>. Left PMd showed visually selective activation during target representation and motor selectivity during movement execution. Previous research has found left PMd activation for right arm reaching (Medendorp et al., 2005; Bernier et al., 2012; Gertz and Fiehler, 2015) and implicated the region in transforming visuospatial information into motor codes (Medendorp et al., 2005; Beurze et al., 2007), which supports our motor-selective finding. There is also evidence from multivariate

fMRI techniques for target selective coding in PMd (Gallivan et al., 2011; Fabbri et al., 2014), which may help explain the visually-selective encoding we noted during the target representation phase. Finally, a recent neurophysiological study suggests that frontal eye fields progressively transition from a target to movement code, even when planning pro-saccades (Sajad et al., 2016).

Visuomotor Selectivity in *all* Areas. One of our more striking findings was that when we described our occipital-parietal-frontal regions with the use of a visuo-movement parameter (derived from the anti-reach data) and plotted these data through the entire time course of our task (Figure 7), every single area, from V1 to M1, looked remarkably similar (with the exception of a mid-task ‘bump’ in some areas like precuneus, around the time of the pro/anti instruction). This appears to illustrate a very simple but profound message: despite the many functional differences between these areas (like those described above and by many other authors), an entire occipital-parietal-frontal network is engaged in the transformation of visual stimuli into motor acts; Not only at different serial stages of processing, but through the entire duration of the task (for example, see the occipital reactivation in our SOG data). In this sense, even though visuomotor transformations can be observed within single structures and even single neurons (e.g., Sajad et al., 2015, 2016; Sadeh et al., 2015), almost the entire cortex is engaged in the entirety of such transformations. This is further supported at the motor output level by recent evidence of upper limb muscles initially encoding the location of the visual stimulus rather than the movement goal for anti-reaching in humans (Gu et al., 2016).

Spatiotemporal Correlations for Visual, Movement, and Visuo-movement Selectivity

We were able to quantitatively summarize our measures of early visual tuning and late movement tuning, and organize these into spatiotemporally correlated modules by correlating these measures through time between left hemisphere regions of interest (Figure 8 A-C), and using these correlations to construct a network of spatiotemporally correlated modules (Figure 7 D-F). This resulted in two widely distributed, overlapping networks: the first strongly correlated to visual input from V1 (Figures 8 A,D), and the second strongly correlated with motor output from M1 (Figures 8 B,E). However, it was the visuo-movement parameter that yielded the best overall correlations between areas (Figures 8 C,F). The full set of sensory, motor, and sensorimotor correlations for all areas are illustrated graphically in Figures 8 D, E, and F. Although correlation does not imply causation (for example, some of these correlations may have been due to common inputs, including attentional processes), the structure of these networks appear to agree well with the known anatomy of the dorsal visual stream system and reach systems (Vesia et al., 2012; Gallivan et al., 2015). Further, it suggests that almost the entire network is concerned with transforming retrospective visual direction into prospective movement direction (Curtis, 2006).

Of these areas, SOG stood out as having the highest mean correlations against all other areas in all three domains: visual, movement, and visuo-movement. This is perhaps surprising for an occipital area, and might be related to a key role for SOG in encoding the potential or actual egocentric goal, independent of initial stimulus (Gallivan et al., 2011; Chen et al., 2014), or occipital cortex receiving visuospatial attention or motor signals from parietal cortex (Lauritzen et al., 2009; Singhal et al., 2013; Perry et al., 2015). SPOC and mIPS also showed high correlations in the visuo-movement domain, with SPOC being noteworthy as the only shared region that significantly correlated with all other areas in the visuo-movement. This seems consistent with SPOC having a prominent role in representation of target location for reach (Vesia et al., 2010; Vesia and Crawford, 2012). However, several other areas (LG, SOG, M1/S1, PMd, and AG) significantly correlated to both V1 in the visual domain and mM1 in the motor domain, so this transformational role is not unique to one area. Nor was it trivially required, because PCu showed relatively weakest correlations in all of the spatial domains that we tested. This may be task specific, because PCu has been implicated in other allocentric functions (Uchimura et al., 2015).

Although dorsal parietal cortex often gets the most attention in the sensorimotor literature, AG –an inferior parietal area— also showed significant visual correlation with V1, movement correlation with mM1, and visuo-movement correlations with most areas (except V1 and PCu), although its overall visual correlations were less than its movement correlations. Together with its multiple roles in coding motion in external space (Fernandez-Ruiz et al., 2007; Vesia and Crawford, 2012), discrimination of left space from right (Hirnstein et al., 2011), controlling multiple effectors (Vesia et al., 2010), and in agency (Farrer et al., 2008), this might suggest that AG plays a central role in monitoring the awareness of one’s actions within external space. In comparison, our current data suggest that other sensory areas like cuneus and SOG may be more concerned with monitoring events and goals in visual space. This again is consistent with the notion that the brain simultaneously monitors space in multiple frames. Overall, these data suggest that the brain uses a broadly distributed, common visuomotor code for memory guided reach, and thus the need for so many network nodes likely arises from other cognitive demands.

Chapter Three: Cortical Mechanisms for Reaches Versus Saccades: Progression of Effector-Specificity Through Target Memory to Movement Planning and Execution

AUTHORS: David C. Cappadocia, Simona Monaco, Ying Chen, and J. Douglas Crawford

(A manuscript in preparation for submission)

3.1 Abstract

Effector-specific cortical mechanisms can be difficult to establish using fMRI, in part because low time resolution might temporally conflate different signals related to target representation, motor planning, and motor execution. Here, we used an event-related fMRI protocol and a cue-separation paradigm to temporally separate these three major sensorimotor stages for saccades vs. reaches. In each trial, subjects (N=12) 1) briefly viewed a target 4-7º left or right of midline fixation on a touchscreen, followed by an 8 second delay (effector-independent *target memory* phase), 2) were instructed by an auditory cue to perform a reach or a saccade, followed by a second delay of 8 seconds (effector-specific *planning* phase), and finally 3) were prompted to move by reaching-to-touch or performing a saccade towards the remembered target (effector-specific *execution* phase). Our analysis of saccade and reach activation (vs. a non-spatial control task) revealed modest effector-agnostic target memory activity (left AG, bilateral mIPS) followed by independent effector parietofrontal sites and time courses during the motor components of the task, specifically: more medial (pIPS, mIPS, M1, and PMd) activity during both *reach planning* and *execution*, and more lateral (mIPS, AG, and FEF) activity only during *saccade execution*. These motor activations were bilateral, with a left (contralateral) preference for reach. A conjunction analysis revealed that left mIPS and right AG, PCu, SPOC, FEF/PMv and LOTC showed activation for both saccades and reaches. Overall, effector-preference contrasts (reach vs. saccade) revealed significantly more parietofrontal activation for reaches than saccades during both planning and execution, with the exception of FEF. Cross-correlation of reach, saccade, and reach-saccade activation through time revealed correlated activation both

within and across effectors in each hemisphere, but with a tendency toward higher correlations in the right hemisphere, especially *between* the eye and hand. These results demonstrate substantially independent but temporally correlated cortical networks for human eye, hand, and eye-hand control, that follow explicit spatiotemporal rules for effector-specific timing, medial-lateral distribution, and hemispheric lateralization.

3.2 Introduction

Human beings rely on the input of sensory information to guide actions and effectively interact with their environment. Two of the most frequent goal-directed actions that use visual information are visually guided saccades and reaches (e.g., a car driver moving their eyes from the road to their rear-view mirror or their right hand from the steering wheel to the radio). In monkeys, very specific signals have been localized for saccades versus reaches in frontal and parietal cortex (Buneo and Andersen, 2002; Synder et al., 2000). In contrast, reach and saccade signals have been very difficult to dissociate in human functional magnetic resonance imaging (fMRI) studies of parietal cortex (Vesia and Crawford 2012). Indeed, several studies have suggested highly distributed reach regions (Filimon et al., 2007; 2009) with large amounts of overlap with saccade activity during planning and execution (Medendorp et al., 2003; Beurze et al., 2007, 2009). These distributed responses have resulted in considerable controversy regarding the localization and degree and of effector specificity in human cortex.

To briefly summarize fMRI evidence for saccade-reach effector specificity in posterior parietal cortex (PPC), a cluster of activation in the midposterior intraparietal sulcus (mIPS) has been linked to saccade planning (Astafiev et al., 2003; Merriam et al., 2003; Schluppeck et al., 2005; Tosoni et al., 2008), eye movements and attention (Corbetta et al., 1998; Astafiev et al., 2003), eye movements and visual working memory (Curtis et al, 2004; Curtis and Connelly, 2008; Srimal and Curtis, 2008) and all three of these processes (Jerde et al., 2012). In reach, human mIPS has been linked to reach planning (DeSouza et al., 2000; Medendorp et al., 2003, 2005; Prado et al., 2005; Beurze et al., 2007, 2009, 2010; Fernandez-Ruiz, 2007; Tosoni et al., 2008; Filimon et al., 2009; Chen et al., 2014; Cappadocia et al., 2017), as have other parietal regions including the superior parietal occipital cortex (SPOC) (Astafiev et al., 2003; Connolly et al., 2003; Prado et al., 2005; Fernandez-Ruiz et al., 2007; Tosoni et al., 2008; Beurze et al., 2009; Gallivan et al., 2009, 2011; Bernier and Grafton, 2010; Cavina-Pratesi et al., 2010; Monaco et al., 2011; Chen et al., 2014; Cappadocia et al., 2017) and the angular gyrus (AG) (Fernandez-Ruiz et al., 2007; Chen et al., 2014; Cappadocia et al., 2017). In frontal cortex, several studies have examined saccade related activation in the human frontal eye fields (FEF) (Astafiev et al., 2003; Beurze et al., 2009; Amiez and Petrides, 2009; Gallivan et al, 2011; Herwig et al, 2014), and reach related activation in the human dorsal premotor cortex (PMd) (Connolly et al, 2007; Curtis et al, 2008; Gallivan et al, 2011, 2015; Bestman et al., 2012).

Despite this progress, several questions remain unresolved. Many of the fMRI studies cited above reported considerable overlap between saccade and reach activity, either due to actual sharing of control, sharing of common inputs required for both saccades and reach, or simply due to the spatial resolution limits of fMRI (Connolly et al, 2007; Curtis et al, 2008; Beurze et al., 2009; Gallivan et al, 2011). Specific questions include the extent to which reach and saccade signals are segregated medially versus laterally relative to the intraparietal sulcus (Culham et al., 2006; Gallivan et al., 2011). Also, there is emerging evidence that reach activation is lateralized to the hemisphere contralateral to the hand as early as parietal and even occipital cortex (Fernandez-Ruiz et al., 2007; Cappadocia et al., 2017). Since the two eyes are normally yoked one would not expect to see the same type of mass contralateral lateralization during saccades, but the degree of general lateralization, if any, for saccades in humans remains unclear (Chen et al. 2016).

One factor that has not been fully considered in this debate is how the low *temporal* resolution of fMRI might interact with multiple neural signals to conflate the spatial resolution of effector-independent, effector-dependent (reach or saccade related activation), and effector-specific (activation specific to reach or saccade and not the other) signals. Specifically, studies that do not separate target and memory responses from motor planning could yield ‘planning’ activation that is actually a combination of these three types of activation. Conversely, studies that do not separate planning from execution might confuse spatial specificity with effector independence if the temporal distribution of activation through these phases is different for saccade and reach. In short, these paradigms might tend to conflate different signals and thus underestimate the spatial specificity of motor effector signals (Cappadocia et al., 2017).

The current study exploited a recently developed cue-separation paradigm (Cappadocia et al., 2017) to examine the temporal progression of neural correlates of both independent and preferential planning and execution for reach and saccades. This study uses an event-related fMRI paradigm that explicitly separates visually-guided reaches and saccades into three phases in time (effector agnostic visual target representation, independent effector movement planning, and independent effector movement execution), by introducing an effector instruction between visual target memory and planning phases, and a ‘go signal’ between planning and execution times. We then analyzed the concomitant BOLD activation in cortex to investigate how independent and preferential effector-specific planning and execution signals are temporally and spatially distributed through the cortical networks for action in the human, and the degree to which these signals are correlated through time within and across the reach and saccade networks. We find that, when visuospatial activation is disentangled from motor activation, the cortical networks for human reach and saccade control show substantially different distributions in both the spatial and temporal domains.

3.3 Methods

Participants

Twelve right-handed subjects (3 males, 9 females aged 20-36) were recruited from the York University community. We chose this number of subjects based on precedents set in similar studies of visuomotor control in healthy subjects (Cavina-Pratesi et al., 2007, Gallivan et al., 2011). The resulting dataset was sufficient to yield statistically significant results that survived corrections for multiple comparisons (see Results). All subjects had normal or corrected-to-normal vision and none of the subjects had any known neurological deficits. The York University Human Participants Review Sub-committee approved all techniques used in this study and all participants gave their informed consent prior to the experiment.

Experimental stimuli and apparatus

The experimental stimuli and apparatus were the same as the setup used in Chen et al. (2014) and Cappadocia et al. (2017). Visual stimuli consisted of optic fibers embedded into a custom-built board with adjustable tilt. The board was mounted atop a platform whose height was also adjustable (Figure 9A). The platform was attached to the MRI scanner bed and placed over the abdomen of the subject. The height of the platform and tilt of the board were adjusted for each participant to ensure comfortable reaching movements. A translucent touchscreen (Keytec, 170 mm X 126 mm) was affixed on the board to record reach endpoints. An eye-tracking system (iView X) was

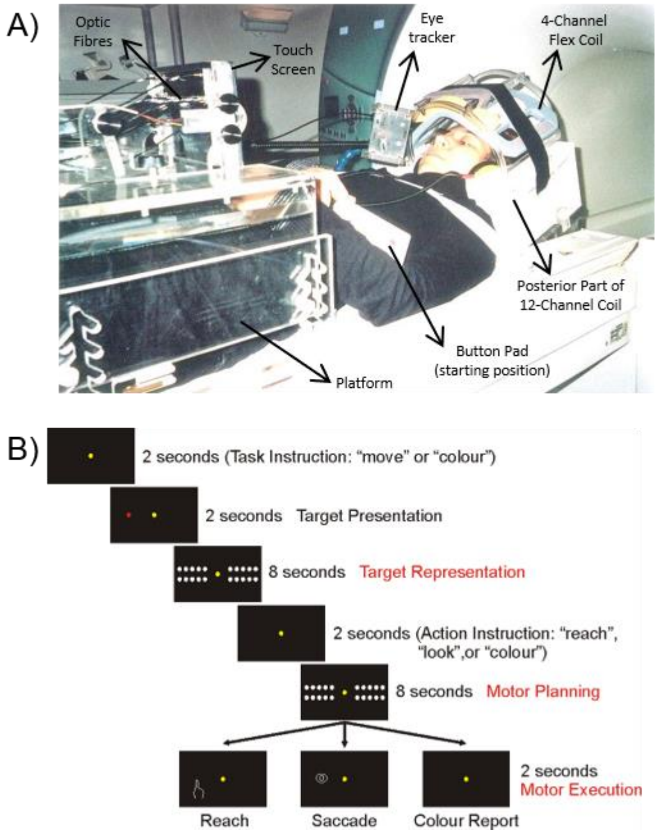

Figure 9. Experimental setup and paradigm. **A*)*** Photograph of The experimental setup.

B) Illustration of the experimental paradigm. The display of visual targets is the same for all three tasks (Reach, Saccade, and Color Report). The key difference between the two action tasks is the auditory effector command, informing the effector to be used. As the target presentation and effector instruction are separated by an 8 second delay, this allows the task to disentangle target representation from movement planning and execution. In the Color Report task, target color (red or green) rather than location is remembered and reported.

used in conjunction with the MRI-compatible Avotec Silent Vision system (RE-5701) to record movements of the right eye during the experiment.

The head of the participant was slightly tilted (~20º) to allow direct viewing of the stimuli presented on the board (Figure 9A). The board was approximately perpendicular to gaze and ~60 cm from the eyes. The upper arm was strapped to the scanner bed to limit motion artifacts during reach trials. Reaches were thus performed by movements of the right forearm and hand. A button pad was placed on the left side of the participants' abdomen and served as both the starting point for each trial and as the response for the color report control task (see experimental paradigm and timing). Participants wore headphones to hear auditory instructions and cues. During each trial, subjects were in complete darkness apart from the visual stimuli, which were not bright enough to illuminate the workspace. The hand was never visible to the subject, even during reaching.

There were 3 types of visual stimuli presented by different colors: the fixation point in yellow, targets in green or red, and masks in white. All stimuli were presented horizontally on the touchscreen and had the same diameter of 3 mm as the optic fibres. There was one central fixation location. Eight horizontal peripheral targets (4 on each side of the touchscreen) were used (Figure 9B), and twenty "mask" LEDs were located above and below the target line (ten on each side with five above and five below the targets). The visual mask was used during the delay periods to control for visual afterimages. The distance between the eyes of the subject and the center of the touchscreen was ~60 cm. The target LEDs were located approximately 4°, 5°, 6° or 7° to the left or right of the fixation LED.

Experimental paradigm and timing

We used an event-related design, with each trial lasting 38 seconds (including an inter-trial interval of 12 seconds). The paradigm included 3 tasks: reach, saccade, and color report as a control (Figure 9B). Each trial began with the presentation of the yellow fixation LED (this was displayed for 24 seconds before the first trial in each run). Concurrently, subjects were given the auditory instruction “move” or “color” to indicate the type of task they had to perform at the end of that trial. The important distinction between these two instructions is that while remembering the spatial location of the target LED (the visual target) was required for the movement trials, this information could be ignored for the color report trials. After 2 seconds, a green or red target LED was illuminated for 2 seconds, followed by an 8 second delay period (the effector-agnostic ‘visual target representation’ phase) during which the fixation LED and mask LEDs were illuminated. At the end of the delay, subjects were given one of 3 auditory instructions. For movement trials: “reach” (indicating a reach trial) or “look” (indicating a saccade trial). For color report trials the instruction “color” was repeated. This took 2 seconds. The independent effector instruction being given in the middle of the trial prevented subjects from forming their movement plan during the first delay period. The auditory instruction was followed by another 8 second delay period (the ‘movement planning’ phase) during which the fixation LED and mask LEDs were illuminated. After the mask LEDs were turned off, subjects heard a beep that served as a ‘go’ signal for subjects to move their arm or eye to the remembered location of the target in movement trials, or press the button once if the target LED was green or twice if it was red for the color report trials (or vice versa, this was be counterbalanced across subjects). This is referred to as the ‘movement execution’ phase. After touching the touchscreen or fixating the target location for 2 seconds, subjects heard a beep that instructed them to return their arm or eye to the starting position. The following trial started 12 seconds later.

Each functional run consisted of 12 trials presented in a random order (4 for each of the three tasks; 50% of targets presented in each visual hemifield for each task) and lasted about 8 minutes. For analysis, target locations were collapsed together as “left” or “right”. Subjects participated in 8 functional runs in one session. They were trained to perform the required tasks 1-2 days before imaging and practiced all tasks within the MRI scanner before scanning to ensure that they were comfortable with the task.

Behavioral recordings

Following the fMRI experiments, the eye position and reach endpoints were inspected. Eye movement errors were defined as trials where subjects were unable to maintain visual fixation from target presentation until touching the touchscreen, or when the eye moved to the direction opposite of the instructed saccade goal. Reaching errors were defined as reaches to the direction opposite to the instructed reach goal.

Imaging parameters

The experiment was conducted at the York MRI Facility at the Sherman Health Sciences Centre at York University with a 3-T whole-body MRI system (Siemens Magnetom TIM Trio). The posterior half of a 12-channel head coil (6 channels) was placed at the back of the head, with a 4-channel flex coil over the anterior part of the head (Figure 9B). The head was tilted ~20º to allow for direct viewing of the stimuli during experimental trials.

Functional data was acquired using an EPI (echo-planar imaging) sequence (repetition time [TR] = 2000 ms; echo time [TE] = 30 ms; flip angle [FA] = 90º; field of view [FOV] = 192 mm X 192 mm, matrix size = 64 X 64 leading to an in-slice resolution of 3 mm X 3 mm; slice thickness = 3.5 mm, no gap; 36 transverse slices angled at ~25º covering the whole brain). Slices were collected in ascending and interleaved order. During each experimental session, a T1–weighted anatomical reference volume was acquired using an MPRAGE sequence (TR = 1900 ms; TE = 2.52 ms; inversion time TI = 900 ms; FA = 90º; FOV = 256 mm X 256 mm X 192 mm, voxel size = 1 X 1 X 1 mm^3).

Preprocessing

All data was analyzed using BrainVoyager QX 2.2 (Brain Innovation). The first 2 volumes of each scan were discarded to avoid T1 saturation effects. For each run, slice scan time correction (cubic spline), temporal filtering (removing frequencies <2 cycles/run) and 3D motion correction (trilinear/sinc) were performed. The 3D motion correction was performed by aligning each volume of one run to the volume of the functional scan that was closest in time to the anatomical scan. 3 runs showing abrupt head movement of 1 mm or 1° were discarded. Functional runs were coregistered to the anatomical image. Functional data was then transformed into Talairach space using the spatial transformation parameters from each individual subject's anatomical scan. The voxel size of the native functional images was 3x3x3 and was not resampled to a different voxel size during the preprocessing steps. Functional data was spatially smoothed using a FWHM of 8 mm.

Data analysis

For each participant, we used a general linear model with 33 predictors. Two predictors were used for the initial auditory instruction (move or color); four predictors were used for visual target presentation (left or right X move or color trial); four predictors were used for visual target representation (left or right X move or color trial); three predictors were used for the 2nd auditory instruction (reach, saccade, or color trial); six predictors were used for motor preparation (left or right X reach, saccade, or color trial); six predictors were used for motor execution (left or right X reach, saccade, or color trial). In addition, six motion correction parameters and predictors for behavioral errors and inter-trial intervals were added as confound errors. Each predictor was derived from a rectangular wave function convolved with a standard hemodynamic response function using BrainVoyager QX's default double-gamma hemodynamic response function.

Voxelwise analysis

Contrasts were performed on β weights using an RFX (random effects) GLM with a percentage signal change transformation. This GLM was used to investigate the first two main questions for this study. To investigate the brain areas involved in effector-independent visual target representation and effector-dependent reach and saccade movement planning and movement execution, we performed five contrasts to find brain areas that showed higher activity for movement trials (reach and saccade) than the control (color) trials during each phase. We also performed two additional contrasts to test if brain areas showed effector-specific activation for reaches or saccades during movement planning and execution.

Activation maps for group voxelwise results were overlaid on the inflated brain of one representative subject. To correct for multiple comparisons, cluster threshold corrections (Forman et al., 1995) were performed for each contrast using BrainVoyager QX's cluster-level statistical threshold estimator plug-in (1000 iterations). Areas that did not survive were excluded from further analysis. A Bonferroni correction was applied to the t value for each contrast to account for the two types of contrasts performed in the experiment: 1) movement trials > control trials (reach > control; saccade > control), and 2) effector specificity contrasts (reach > saccade). These two types of contrasts were planned a priori, with contrasts 1-5 being movement > control trials at three different time periods (1 effector independent and 2 effector-dependent) and contrasts 6 & 7 investigating effector-specificity during the planning and execution phases. ($\alpha = 0.05 / 2$ comparisons = 0.025 corrected for $p < 0.05$).

3.4 Results

To examine reach and saccade planning, we looked at general, non-directional movement activation; combining left and right movements for reach, saccade, and the colour control task. Figure 10 plots the effector-agnostic activation during the visual target representation phase, with the corresponding Talairach coordinates shown in Table 7. Figure 11 plots the independent effector activation for both reaches and saccades (vs the control task) during the planning and execution phases, with the corresponding Talairach coordinates shown in Tables 8 and 9. Brain areas were labeled by comparing the Talairach coordinates from the peak voxel within a cluster and comparing it to known sites of activation in the visuomotor system. It is important to note that at this point certain effector-specific overlapping functional areas have been labeled based on the effector used in the task (e.g., frontal eye fields vs. dorsal premotor cortex in frontal cortex). These data are described in more detail in the following sections. For a complete list of abbreviations for regions of interest (ROI) discussed in this study, see table 6.

Effector-agnostic activation during the Target representation phase.

Note that in our paradigm subjects could not predict which effector they would use in the first Target Representation delay, so one might expect activation related to target memory, general motor preparation, or motor preparation required for both effectors. Contrast 1 [Target Representation Move > Target Representation Color] investigated which brain areas showed higher activation for visuospatial coding required to plan a target-directed movement (either reach or saccade) than activation related to

Table 6. List of ROI brain area abbreviations

Area	Abbreviation
Occipital	
Primary Visual Cortex	V1
Lingual Gyrus	LG
Superior Occipital Gyrus	SOG
Inferior Occipital Gyrus	IOG
Parietal	
Superior Parietal Occipital Cortex	SPOC
Posterior Intraparietal Sulcus	pIPS
Midposterior Intraparietal Sulcus	mIPS
Anterior Intraparietal Sulcus	aIPS
Angular Gyrus	AG
Supramarginal Gyrus	SMG
Precuneus	PCu
Frontal	
Primary Moror Cortex	M1
Dorsal Premotor Cortex	PMd
Ventral Premotor Cortex	PMv
Brodmann Area 4	BA4
Brodmann Area 24	BA24
Frontal Eye Field	FEF

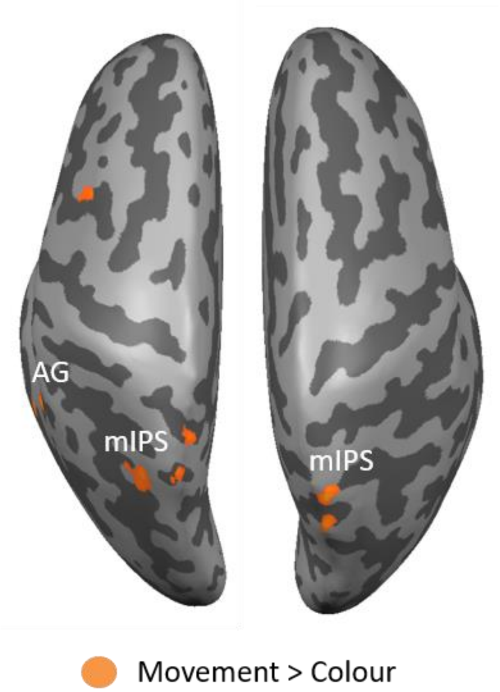

Figure 10. Effector-agnostic target representation phase (before the effector is known). Voxelwise statistical maps obtained from the RFX GLM for the contrast Movement (Reach+Saccade) > Color report. Event-related group activation maps for target representation are displayed on the ‘inflated brain’ of one representative subject, where light gray represents gyri and dark gray represents sulci. The leftward inflated brain represents the left hemisphere, and the rightward brain represents the right hemisphere. Highlighted areas show significantly higher activation than control data with a $p<0.05$ with Bonferroni and cluster threshold corrections. These areas include the left and right mIPS and Left AG.

Table 7. Talairach coordinates and number of voxels for ROIs from the effector-agnostic target representation phase

Area	Mean X	Mean Y	Mean Z	Voxels
Left mIPS	-30.5	-58.99	47.1	366
Left AG	-49.76	-47.12	12.59	464
Right mIPS	20.82	-61.59	50.39	617

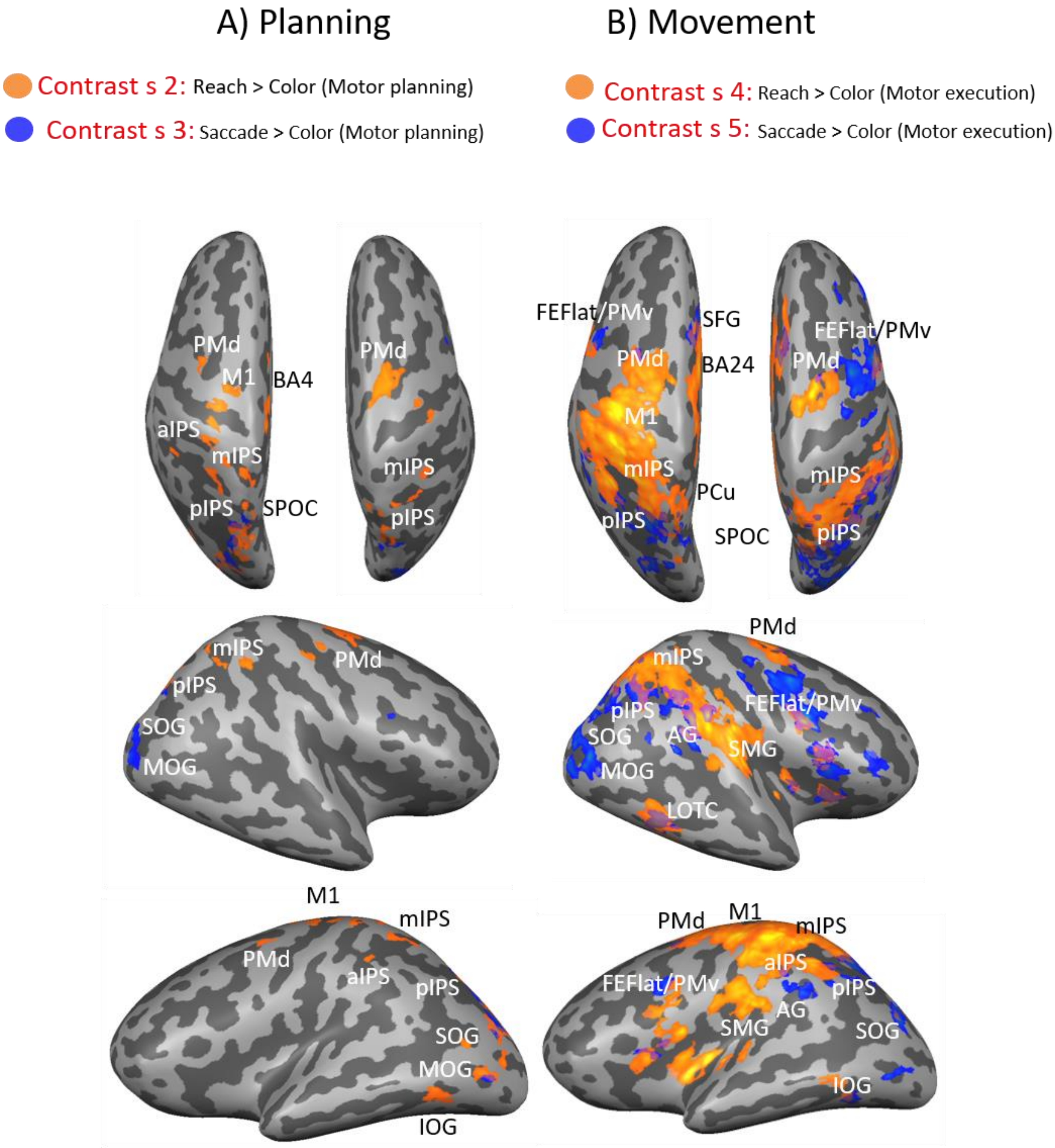

Figure 11. Independent Effector movement planning and execution (once the effector is known). A) Voxelwise statistical maps obtained from the RFX GLM for the contrasts Reach > Color report (orange) and Saccade > Colour report (blue). Event-related group activation maps are displayed on the inflated brain of one representative subject for movement planning. Highlighted areas show significantly higher activation than control

data with a $p<0.05$ with Bonferroni and cluster threshold corrections. These areas include for reach bilateral PMd, mIPS, pIPS, and SOG. Significant activation was also observed in left M1, SPOC, and IOG. For Saccades, significant activation was observed in bilateral pIPS and SOG. B) Voxelwise statistical maps obtained from the RFX GLM for the contrasts Reach > Color report (orange) and Saccade > Colour report (blue). Event-related group activation maps are displayed on the inflated brain of one representative subject for movement execution. Highlighted areas show significantly higher activation than control data with a $p<0.05$ with Bonferroni and cluster threshold corrections. These areas include for reach bilateral PMd, PMv, mIPS, SMG, IOG, SMA and IFG. Significant activation was also observed in left M1. For Saccades, activation was observed in bilateral FEF, mIPS, pIPS, SPOC, AG, and SOG. (See Table 1 for site abbreviations)

Table 8. Talairach coordinates and number of voxels for ROIs from the independent effector movement planning phase

Area	Mean X	Mean Y	Mean Z	Voxels
Reach Areas				
Left PMd	-26.73	-6.3	57.55	422
Left M1	-23.2	-29.79	63.76	370
Left BA4	-7.03	-22.43	44.92	672
Left aIPS	-13.84	-43.84	61.19	342
Left mIPS	-18.85	-48.09	52.67	688
Left pIPS	-23.33	-73.21	44.08	350
Left SPOC	-14.45	-72.06	41.09	519
Left SOG	-20.43	-78.7	26.72	846
Left MOG	-33.25	-70.6	10.3	443
Left IOG	-41.42	-67.91	-4.36	237
Right PMd	21.76	-11.53	58.03	710
Right mIPS	21.44	-57.75	52.86	338
Right pIPS	12.3	-72.25	46.49	257
Saccade Areas				
Left pIPS	-17.04	-69.09	48.84	616
Left SOG	-24.67	-84.38	19.38	355
Left MOG	-32.89	-81.34	3.02	221
Right pIPS	21.44	-68.48	36.94	441
Right MOG	31.1	-76.62	9.19	294
Right SOG	21.36	-81.64	22.22	318

Table 9. Talairach coordinates and number of voxels for ROIs from the independent effector movement execution phase

Area	Mean X	Mean Y	Mean Z	Voxels
Reach Areas				
SFG	2.5	6.5	47.5	1000
BA24	-4.52	-4.47	41.54	992
Left PMd	-27.97	-8.91	59.03	835
Left PMv	-54.45	3.28	28.38	683
Left M1	-37.5	-30.5	46.5	1000
Left SMG	-55.44	-29.25	18.67	882
Left aIPS	-29.64	-41.49	49.61	970
Left mIPS	-22.54	-56.46	54.53	991
Left AG	-54.43	-37.2	30.08	501
Left SPOC	-11.88	-68.25	53.12	782
Left Pcu	-6.67	-62.16	51.54	906
Right PMd	22.67	-11.39	57.33	907
Right PMv	49.3	3.71	29.47	946
Right SMG	54.47	-24.47	18.54	992
Right mIPS	18.83	-56.8	55.59	857
Right SPOC	4.58	-62.61	46.63	861
Right AG	52.56	-35.4	29.55	976
Right Pcu	3.9	-55.01	50.9	668
Right LOTC	50.46	-48.21	-9.88	811
Saccade Areas				
SFG	1.69	6.7	48.64	930
Left FEF	-46.37	-3.83	32.34	573
Left mIPS	-23.47	-62.53	50.17	723
Left pIPS	-11.18	-69.9	46.98	567
Left AG	-58.27	-41.91	30.85	656
Left PCu	-8.55	-61.5	48.97	386
Left SOG	-25.27	-82.56	26.49	790
Left IOG	-48.35	-64.54	-10.61	515
Right FEF	46.44	4.59	29.58	977
Right mIPS	22.76	-58.71	53.32	557
Right SPOC/pIPS	10.64	-71.64	44.29	896
Right AG	52.69	-34.95	34.91	865
Right PCu	4.57	-53.34	45.82	475
Right SOG	25.96	-74.62	22.52	888
Right MOG	29.23	-79.85	5.08	443
Right LOTC	51.23	-52.95	-9.72	756

representing the color of the target (the requirement of the control task). In this phase, only the target location was known (as the effector was only specified by an auditory instruction after this delay period), and any activation revealed by this contrast may be related to any aspect of target coding (not limited to spatial location) or early effector-independent movement preparation. Figure 10 shows the activation map for this contrast superimposed on inflated cortical surfaces viewed from above. The indicated areas survived a cluster threshold correction of 15 voxels. This contrast revealed modest bilateral activation near the midposterior intraparietal sulcus (mIPS), and modest unilateral activation in the left angular gyrus (AG). At first glance it might seem odd that only areas associated with movement control (Gallivan and Culham, 2015) were activated, but recall that the control task also involves memory of a non-spatial, non-motor target type. Thus, this subtraction shows areas with memory-epoch activity *specific to spatial location or early effector-independent motor preparation for saccade, reach, or both*.

Independent Effector activation versus Color Control During Planning and Execution.

Following the target representation phase, subjects were provided with an effector cue (Figure 9), allowing us to test the influence of this cue on BOLD activation during motor planning. To do this, we started with two independent, independent effector contrasts: <u>Movement planning phase:</u> Contrast 2 [Movement Planning Reach > Movement Planning Color] and Contrast 3 [Movement Planning Saccade > Movement Planning Color] investigated which brain areas showed higher activation for movement planning for reach and saccade, respectively, than activation related to representing the color of the target (the requirement of the control task). Activation during this phase could be related to planning a specific movement and/or general motor preparation in anticipation of an upcoming reach (for Contrast 2) or saccade (for Contrast 3). The activation map for these contrasts are shown on an inflated cortical surface viewed from above and the lateral view (Figure 11a), with orange activation representing reach activation and blue activation representing saccade activation. The marked areas survived a cluster threshold correction of 26 voxels for Contrast 2 (reach), and 27 voxels for Contrast 3 (saccade). For reach, Contrast 2 revealed modest bilateral activation near the intersection of the precentral and superior frontal sulci, consistent with the location of dorsal premotor cortex (PMd) (Monaco et al. 2011), midposterior intraparietal sulcus (mIPS), and posterior intraparietal sulcus (pIPS). Activation was also found in the left hemisphere in primary motor cortex (M1), Brodmann Area 4 (BA4), superior parietal occipital cortex (SPOC), superior occipital gyrus (SOG), middle occipital gyrus (MOG), and inferior occipital gyrus (IOG). For a complete list of abbreviations for regions of interest (ROI) discussed in this study, see table 6. For Saccade, Contrast 3 revealed modest bilateral activation for posterior intraparietal sulcus (pIPS) and superior occipital gyrus (SOG). A conjunction analysis was also performed to investigate any ROIs involved in both processes, however no regions were found to be significantly active for both effectors.

Movement execution phase: Contrast 4 [Movement Execution Reach > Movement Execution Color] and Contrast 5 [Movement Execution Saccade > Movement Execution Color] investigated which brain areas showed higher activation related to executing a reach or saccade, respectively, than activation related to indicating the color of the target with a button press (the requirement of the control task). The activation map for these contrasts are shown on an inflated cortical surface (Figure 11B). The marked areas survived a cluster threshold correction of 43 voxels for Contrast 4 (reach), and 29 voxels for Contrast 5 (saccade). For reach, Contrast 4 revealed widespread activation in bilateral mIPS, pIPS, SPOC, AG, PMd, PMv, Brodmann Area 24 (BA24), superior frontal gyrus (SFG), supramarginal gyrus (SMG), and AG. Activation was also found in the left hemisphere in precuneus (PCu), aIPS, M1, SOG, and IOG, and in the right hemisphere in lateral occipital temporal cortex (LOTC). For saccades, Contrast 5 revealed activation in bilateral lateral frontal eye fields (FEF), mIPS, pIPS, SPOC, AG, and SOG, as well as right LOTC. A conjunction analysis on contrasts 4 and 5 was done to investigate any ROIs involved in both processes, and the results can be found in Figure 12. Left mIPS and right AG, PCu, SPOC, LOTC, and FEF/PMv were found to be significantly active for both effectors.

Independent Effector Time Series Analysis

To provide a more detailed understanding of the temporal progression of BOLD signals during our task, we examined time series data derived from the saccade and reach regions of interest identified in the movement execution phases in Figure 11.

Figure 13 illustrates the time course data of the reach and color conditions for 12 brain areas from Contrast 4, chosen because they have been linked to visuomotor reach planning, including: left and right mIPS, left and right SPOC, left and right AG, left and right SMG, left and right PMd, left M1, and left SOG. Figure 14 illustrates the time

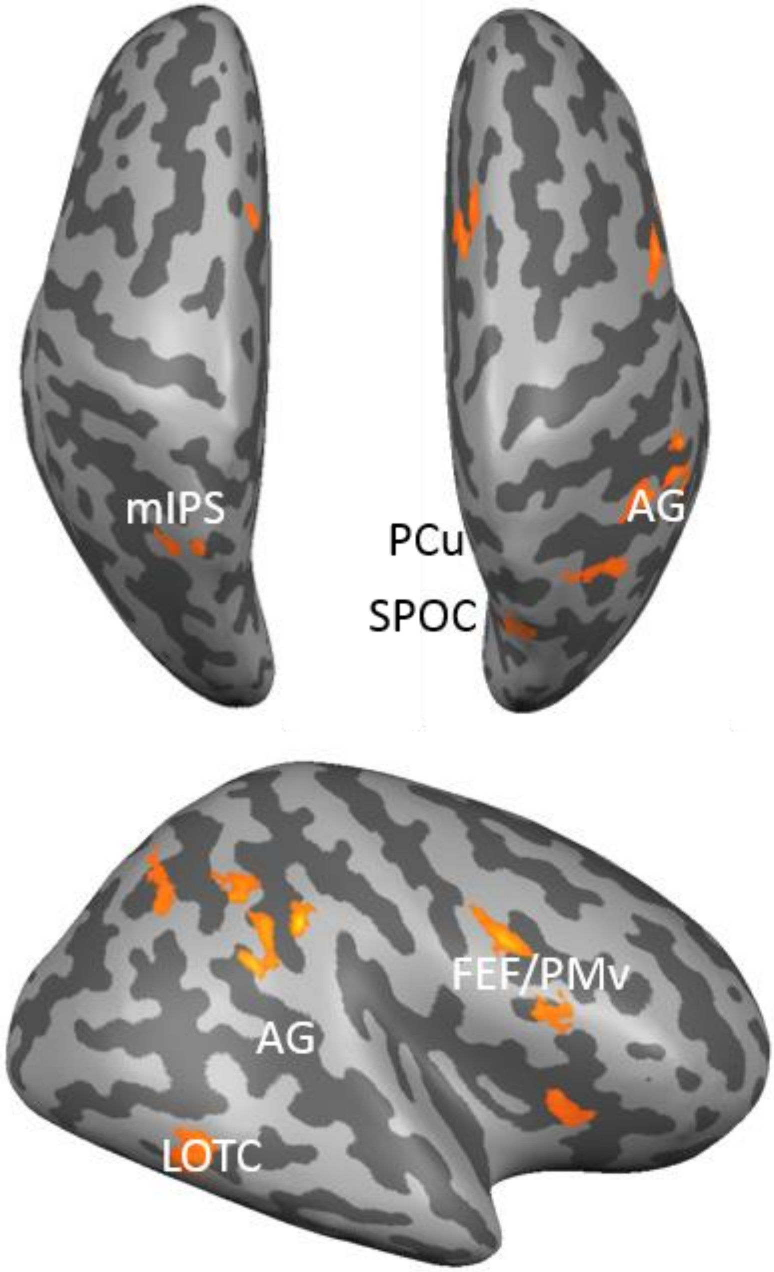

Figure 12. A conjunction analysis on contrasts 4 and 5 (reach>colour and saccade>colour during movement execution. Event-related group activation maps are displayed on the inflated brain of one representative subject for movement planning. Highlighted areas show significantly higher activation than control data with a $p<0.05$

with Bonferroni and cluster threshold corrections. Left mIPS and right AG, PCu, SPOC, LOTC, and FEF/PMv were found to be significantly active for both effectors.

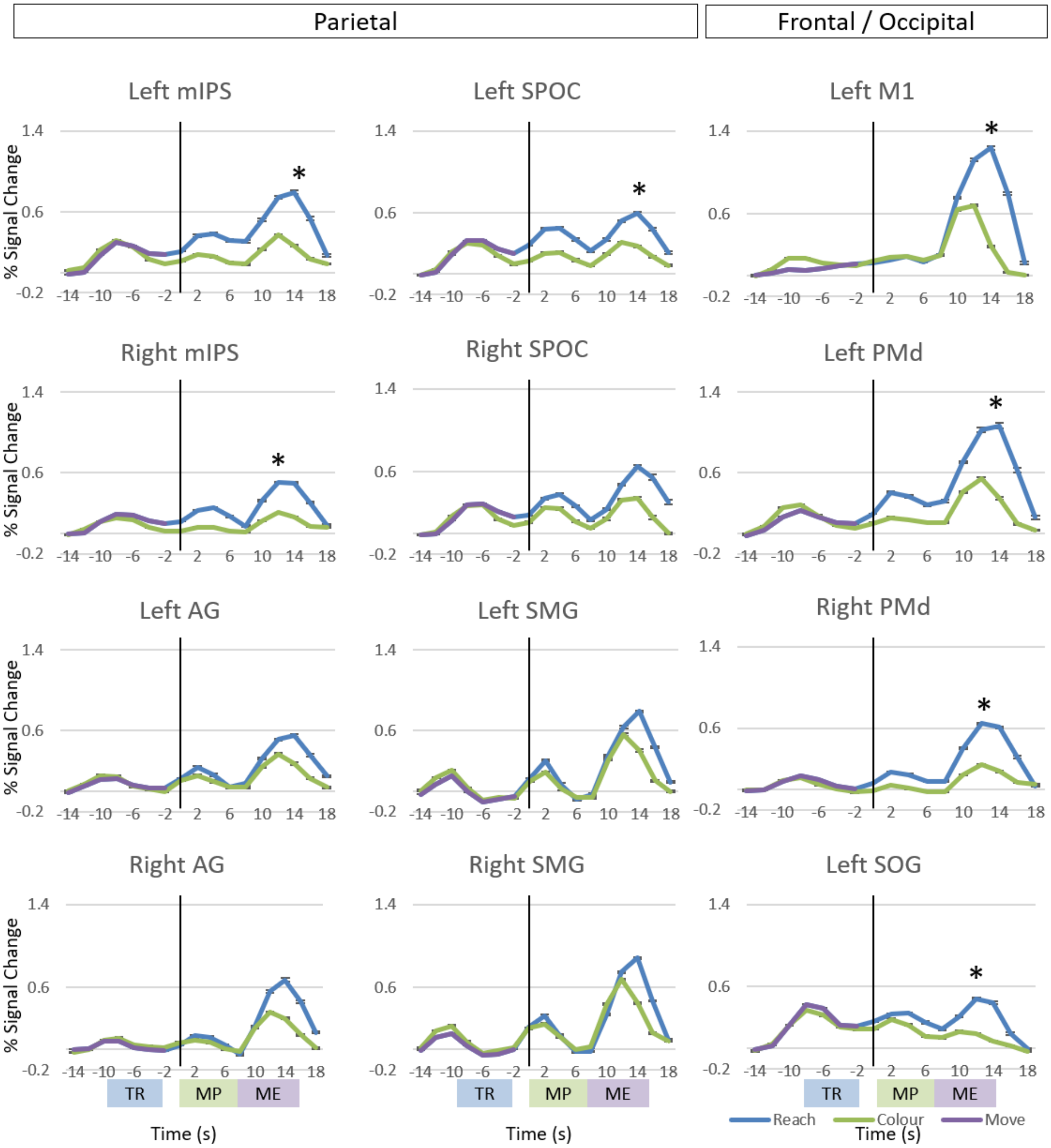

Figure 13. Time courses for brain areas of interest (bilateral mIPS, SPOC, AG, SMG, and PMd; left M1 and SOG) that were active from the Reach > Color contrast during the movement execution phase. The blue line indicates activity (% signal change) from reach trials and the green line indicates activity from color report trials. The purple line

indicates activation in reach trials before the effector was known (general pre-movement activation). Error bars are SEM across subjects. The x axis displays time in seconds and is time locked to the movement planning phase. The vertical black line indicates the onset of the movement planning (MP) phase, while the Target Representation (TR), movement planning, and Movement Execution (ME) phases are identified along the x axis (from left to right). An asterisk (*) indicates a significant difference between the reach and colour activation at the time peak reach activation.

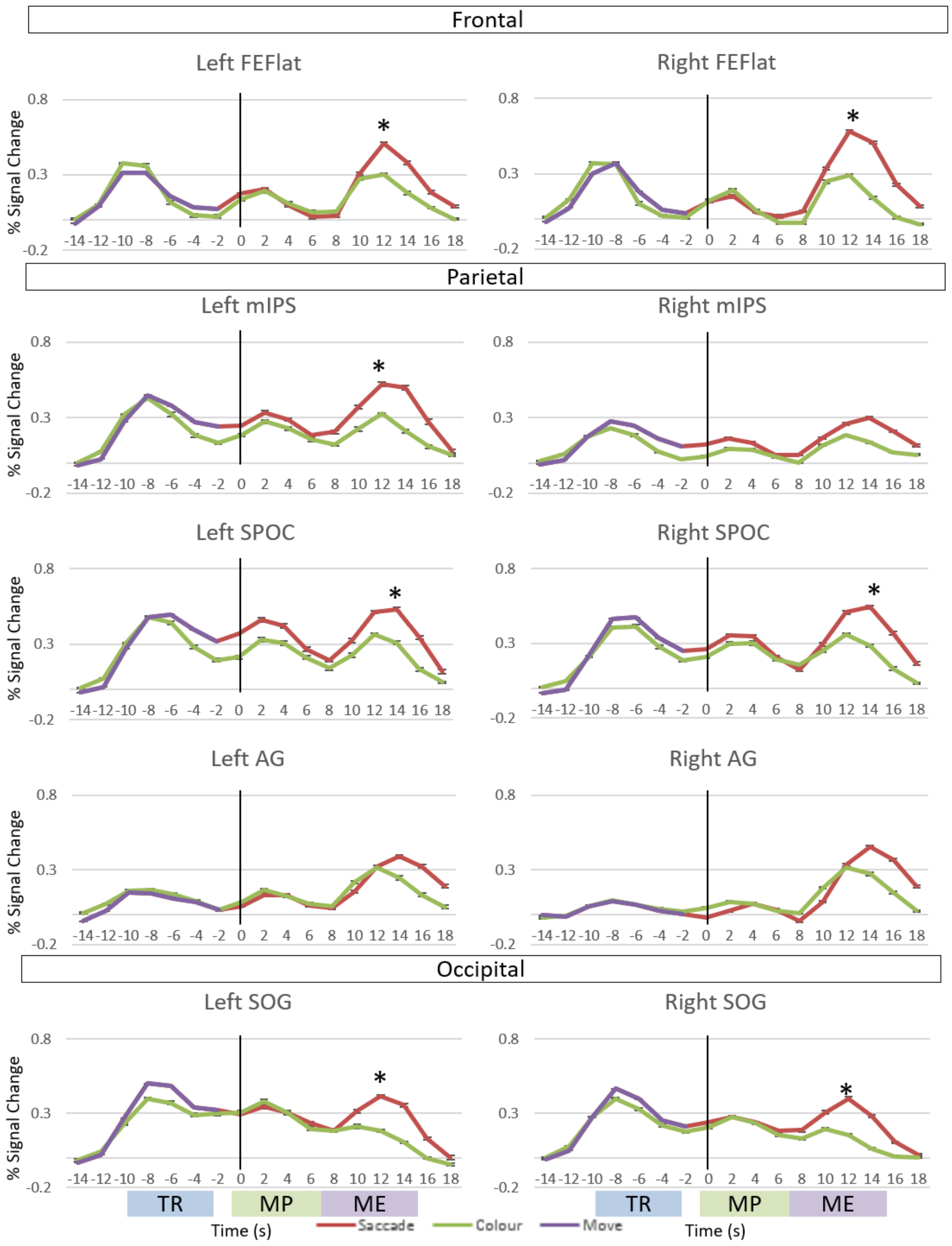
Frontal
Left FEFlat
Right FEFlat
Parietal
Left mIPS
Right mIPS
Left SPOC
Right SPOC
Left AG
Right AG
Occipital
Left SOG
Right SOG
% Signal Change
0.8
0.3
-0.2
-14 -12 -10 -8 -6 -4 -2 0 2 4 6 8 10 12 14 16 18
*
TR
MP
ME
Time (s)
Saccade
Colour
Move

Figure 14. Time courses for brain areas of interest (bilateral FEF, mIPS, SPOC, AG, and SOG) that were active from the Saccade > Color contrast during the movement execution phase. The red line indicates activity (% signal change) from saccade trials and the green line indicates activity from color report trials. The purple line indicates activation in reach trials before the effector was known (general pre-movement activation). Error bars are SEM across subjects. The x axis displays time in seconds and is time locked to the movement planning phase. The vertical black line indicates the onset of the movement planning (MP) phase, while the Target Representation (TR), movement planning, and Movement Execution (ME) phases are identified along the x axis (from left to right). An asterisk (*) indicates a significant difference between the reach and colour activation at the time peak saccade activation.

courses data of the saccade and color conditions for 10 brain areas from Contrast 5, chosen because they have been linked to visuomotor saccade planning, including: left and right FEF, left and right mIPS, left and right SPOC, left and right AG, and left and right SOG.

Looking at these time courses, several patterns emerge that help to understand the previous observations and provide reference events for further analysis. First, all regions of interests show three peaks of activation, aligned closely with target representation, movement planning, and movement execution phases. Second, the relative heights of these peaks were dependent on the known functional role of each area, with SOG (in occipital cortex) showing a relatively larger target peak (than ‘planning’ and ‘execution’), SPOC showing roughly equal target, planning, and execution peaks, and mIPS, PMd, AG, FEF, and M1 showing predominant movement execution peaks. Third, the degree of movement task-specificity (gap between task vs. control lines) generally increased both in time from visual target representation to movement execution and in cortical space from occipital cortex to parietal cortex to frontal cortex. Thus, the entire occipital-parietal-frontal axis was activated during target coding, planning, and execution, but the task-specificity of these responses increased along the antero-frontal axis and in the temporal transition from target, planning, and execution responses.

To quantify independent effector activation in the time courses in figures 13 and 14, we performed paired two tailed t-tests between the reach and colour (figure 13) and saccade and colour (figure 14) data at the time of peak independent effector activation (the maximum % signal change value once the effector has been specified for the trial) to indicate significant reach or saccade activation, respectively. We limited our comparisons to this time point to indicate the presence of independent effector activation without needing to correct for multiple comparisons across all time points.

As one might predict, the peak activation for all reach and saccade areas following the specification of the effector to be used in the trial occurred during motor execution. For reach (figure 13), the peak activation during reach execution was significantly higher than the colour activation at the same time point in bilateral mIPS, bilateral PMd, left SPOC, left M1, and left SOG. For saccades (figure 14), the peak activation during saccade execution was significantly higher than the colour activation at the same time point in bilateral FEF, bilateral SPOC, bilateral SOG, and left mIPS. For both reach and saccade, we observed significant differences between the experimental and control conditions during motor execution in areas that have been linked to reach and saccade planning. It is worth noting, however, that the overall shapes of the curves for all these brain areas were similar (including those that did not reach significance), indicating a degree of planning and execution activation across frontal, parietal, and occipital areas for both reach and saccade. To better understand how this activation differs for reaches and saccades, the next section examines effector-specific activation during planning and execution.

Effector-Preference Direct Contrasts: Reach vs. Saccade Activation for Planning and Execution.

While our first set of contrasts on the movement planning and execution phases assessed independent effector activation, we also performed effector-preference contrasts to directly compare reach and saccade activation. Figure 15 plots the effector-preference activation during the planning and execution phases, with the corresponding Talairach coordinates shown in Tables 10 and 11, respectfully.

Effector-preference activation during the movement planning phase: Contrast 6 [Movement Planning Reach > Movement Planning Saccade] investigated which brain areas showed higher activation for movement planning for reaches than for saccades. The activation map for this contrast is shown on an inflated cortical surface viewed from above and the lateral view (Figure 15a), with orange activation representing reach activation and blue activation representing saccade activation. The marked areas survived a cluster threshold correction of 32 voxels. During movement planning, no saccade areas survived cluster threshold corrections. Several reach-specific areas were identified, including bilateral mIPS, S1, M1, PMd, and BA24, as well as left SMG and MOG.

Effector-preference activation during the movement execution phase: Contrast 7 [Movement Execution Reach > Movement Execution Saccade] investigated which brain areas showed higher activation for movement execution for reaches than for saccades. The activation map for this contrast is shown on an inflated cortical surface viewed from above and the lateral view (Figure 15b), with orange activation representing reach activation and blue activation representing saccade activation. The marked areas survived a cluster threshold correction of 38 voxels. Several reach-specific areas were identified, including bilateral mIPS and SMG, as well as left PMd, M1, S1, and BA24. The only saccade-specific area found was right FEF.

● Reach > Saccade ● Saccade > Reach

A) Contrast 6: Reach>Saccade during Movement Planning

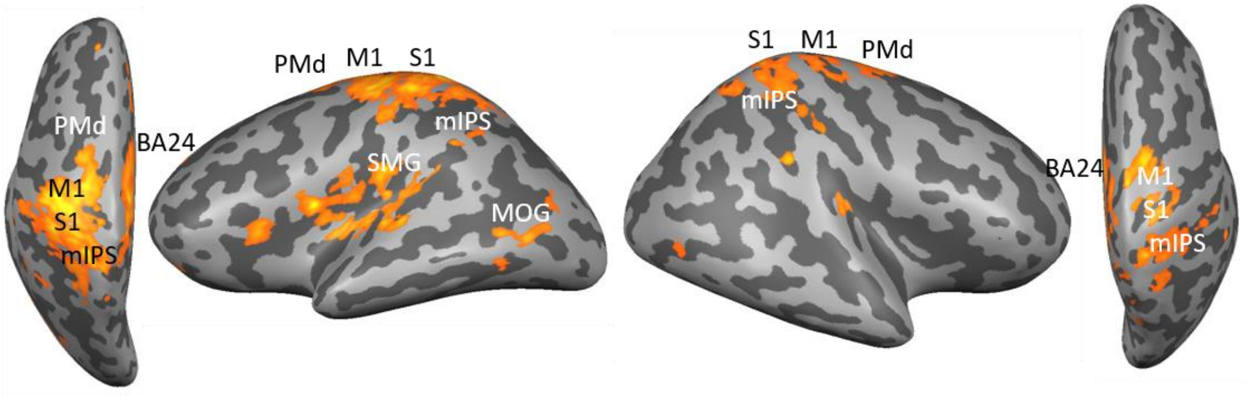

B) Contrast 7: Reach>Saccade during Movement Execution

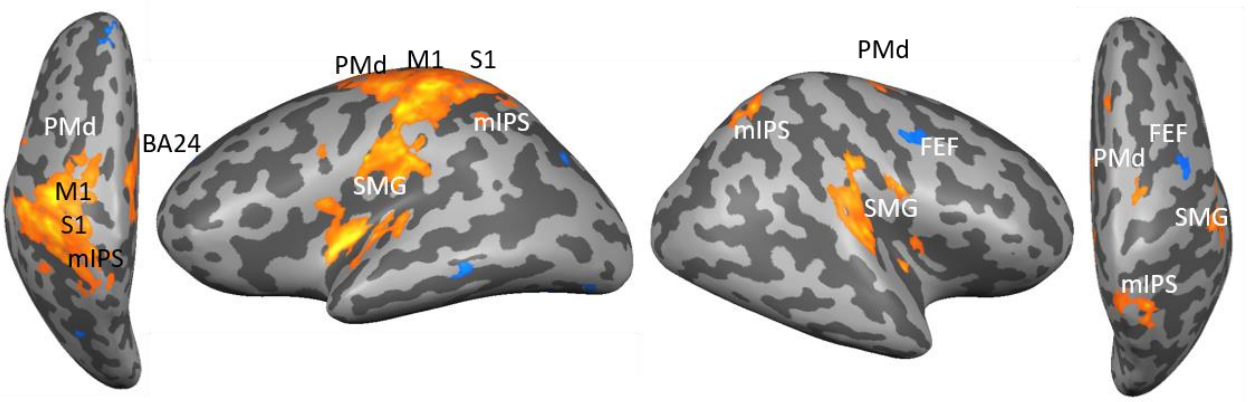

Figure 15. Effector-preference movement planning and execution. A) Voxelwise statistical maps obtained from the RFX GLM for the contrasts Reach > Saccade. Event-related group activation maps are displayed on the inflated brain of one representative subject for movement planning. Highlighted areas show significantly higher reach activation than saccade data with a p<0.05 with Bonferroni and cluster threshold corrections. These areas include for reach bilateral PMd, mIPS, S1, and BA24, as well as left MOG and SMG. B) Voxelwise statistical maps obtained from the RFX GLM for

the contrasts Reach > Saccade. Event-related group activation maps are displayed on the inflated brain of one representative subject for movement execution. Highlighted areas show significantly higher activation than control data with a $p<0.05$ with Bonferroni and cluster threshold corrections. These areas include for reach bilateral PMd, mIPS and SMG, as well as left BA24, M1, and S1. For Saccades, significantly higher activation was observed in right FEF.

Time series data: To better understand the evolution of activation for these effector-preference brain areas at the time of movement execution, we examined their time series. We selected 8 ROIs from Contrast 7, including left and right PMd, left and right mIPS, left and right SMG, left M1, and left FEF (the only saccade-preference area). To quantify effector-preference activation differences in the time courses, we performed two tailed paired t-tests between the reach and saccade data at the time of peak effector-specific activation (the maximum % signal change value once the effector has been specified for the trial) to indicate significant reach-preference or saccade-preference activation. We limited our comparisons to this time point to indicate the presence of effector-preference activation without needing to correct for multiple comparisons across all time points. Looking at these time courses, one can start to see separation between saccade and reach planning during the movement planning phase. For the reach-specific areas, the increased activation observed in reach trials over saccade trials becomes quite pronounced during the motor execution phase, with all 7 areas showing significantly higher activation for reach than saccade trials. For right FEF, the activation appeared to be similar with the peak saccade activation not being significantly different than the reach activation at the same time point.

Temporal correlation of effector preference between cortical areas

To quantify some of the qualitative observations made above, we performed temporal correlations of reach activation, saccade activation, and reach-saccade effector specificity activation between the regions identified in the movement execution effector-preference contrasts (from Figure 11B), which can be found in Figure 16. To do this, we used the % BOLD signal change time series data from the time when the effector-specific command is given (time 0) to 14 seconds after (to be inclusive of movement planning and movement execution phases). We then correlated between sites (r) by matching their BOLD signal changes for each scan in this time range.

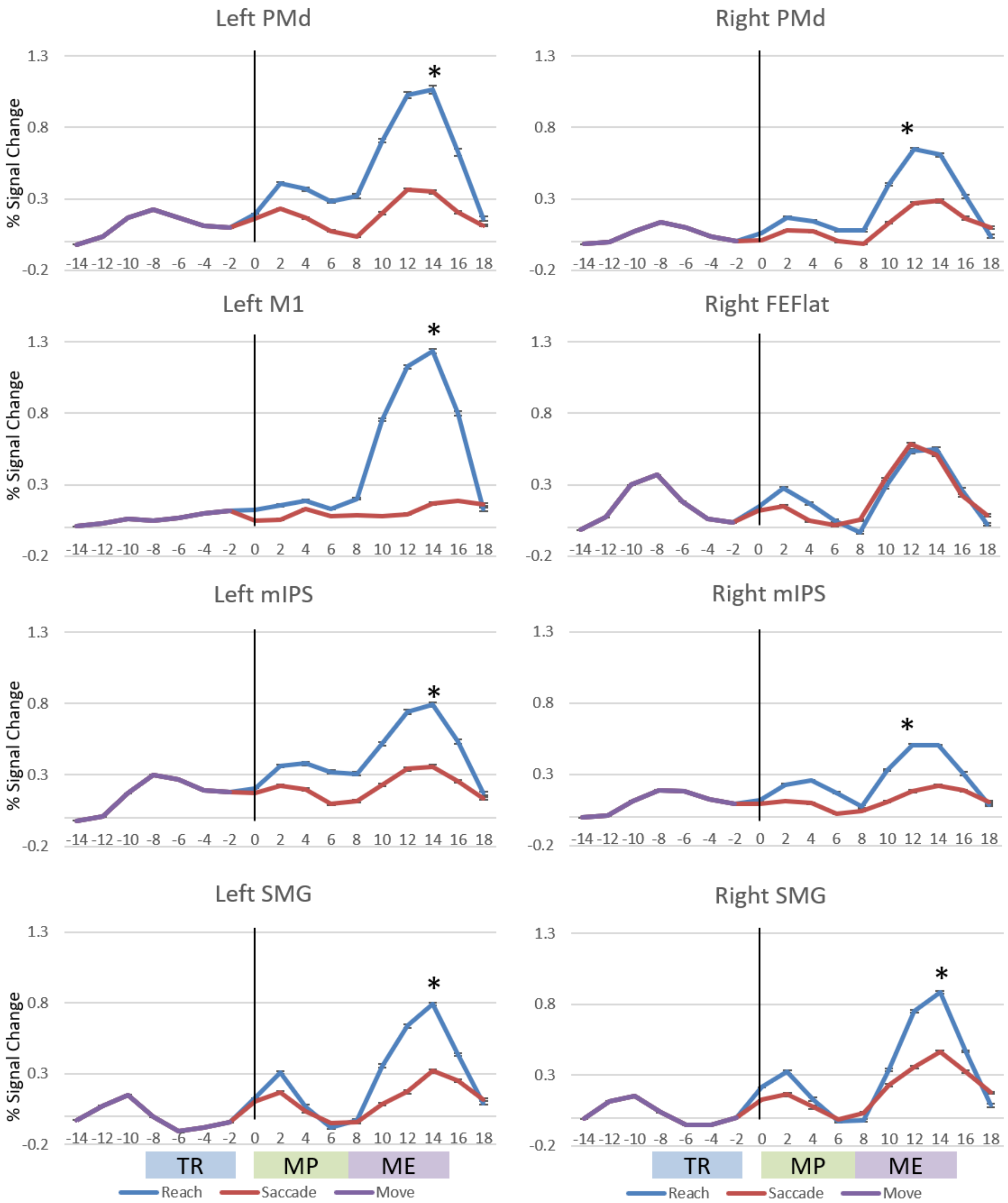

Figure 16. Time courses for brain areas of interest (bilateral PMd, mIPS, SMG; left M1; right FEF) that were active from the Reach > Saccade contrast during the movement execution phase. The blue line indicates activity (% signal change) from reach trials

and the red line indicates activity from saccade trials. Error bars are SEM across subjects. The x axis displays time in seconds and is time locked to the movement planning phase. The vertical black line indicates the onset of the movement planning (MP) phase, while the Target Representation (TR), movement planning, and Movement Execution (ME) phases are identified along the x axis (from left to right). An asterisk (*) indicates a significant difference between the reach and colour activation at the time peak reach activation.

Given the hemispheric differences in reach planning found in our previous study (Cappadocia et al., 2017), we performed separate analyses for the left and right hemispheres.

Figure 17A shows the *saccade* effector preference correlations between each brain area for the right hemisphere and the left hemisphere. The brain areas have been ordered from posterior to anterior, and the variable shown is the r score. The resulting correlation matrix shows high r scores across the board, with notably high scores (indicated by a darker shade of red) for parietal brain regions (mIPS, PCu, AG). This was especially the case for mIPS, which consistently showed high ($r > 0.9$) correlations with all other saccade areas. These correlations were often significant (as indicated by bolded numbers) with a $p < 0.05$ with Bonferroni corrections for 6 comparisons [$\alpha = 0.05 / 6\text{-}1$ comparisons $= 0.01$ corrected for $p < 0.05$].

Figure 17B graphically represents the same data as Figure 17A as a ‘network’ of correlations between our various regions of interest. The width of each line is scaled by the r^2 value for the two regions that it joins, with significant correlations highlighted in yellow ($p < 0.05$), non-significant correlations are shown in orange ($p \geq 0.05$). This figure also helps to visualize ‘hub’ areas in the visual domain, sprouting thick yellow lines (high correlations with yellow indicating significant correlations) toward numerous other areas, as opposed to thin orange lines (low correlations with orange indicating non-significant correlations). For saccades, one observes an extensive network of significant correlations in both hemispheres. Of note, FEF has non-significant correlations in both the left and right hemispheres to PCu and SPOC, and mIPS and AG appear as key hubs, with significant correlations to almost all regions.

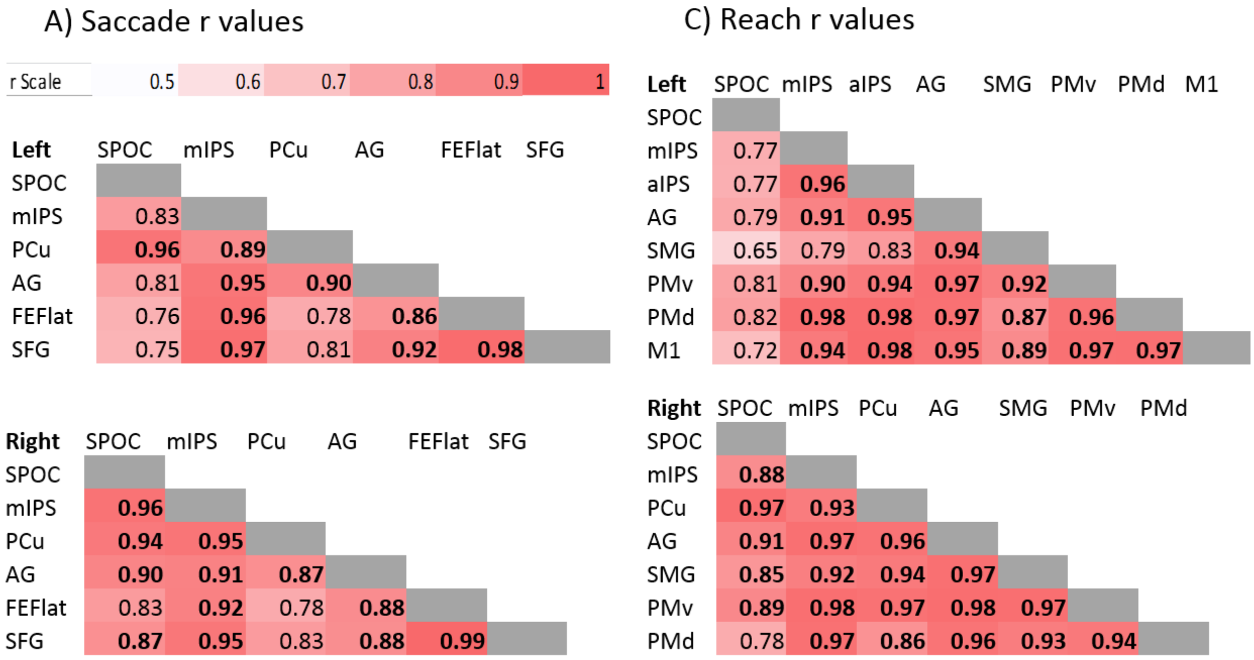

A) Saccade r values

r Scale	0.5	0.6	0.7	0.8	0.9	1

Left	SPOC	mIPS	PCu	AG	FEFlat	SFG
SPOC						
mIPS	0.83					
PCu	**0.96**	**0.89**				
AG	0.81	**0.95**	**0.90**			
FEFlat	0.76	**0.96**	0.78	**0.86**		
SFG	0.75	**0.97**	0.81	**0.92**	**0.98**	

Right	SPOC	mIPS	PCu	AG	FEFlat	SFG
SPOC						
mIPS	**0.96**					
PCu	**0.94**	**0.95**				
AG	**0.90**	**0.91**	**0.87**			
FEFlat	0.83	**0.92**	0.78	**0.88**		
SFG	**0.87**	**0.95**	0.83	**0.88**	**0.99**	

C) Reach r values

Left	SPOC	mIPS	aIPS	AG	SMG	PMv	PMd	M1
SPOC								
mIPS	0.77							
aIPS	0.77	**0.96**						
AG	0.79	**0.91**	**0.95**					
SMG	0.65	0.79	0.83	**0.94**				
PMv	0.81	**0.90**	**0.94**	**0.97**	**0.92**			
PMd	0.82	**0.98**	**0.98**	**0.97**	**0.87**	**0.96**		
M1	0.72	**0.94**	**0.98**	**0.95**	**0.89**	**0.97**	**0.97**	

Right	SPOC	mIPS	PCu	AG	SMG	PMv	PMd
SPOC							
mIPS	**0.88**						
PCu	**0.97**	**0.93**					
AG	**0.91**	**0.97**	**0.96**				
SMG	**0.85**	**0.92**	**0.94**	**0.97**			
PMv	**0.89**	**0.98**	**0.97**	**0.98**	**0.97**		
PMd	0.78	**0.97**	**0.86**	**0.96**	**0.93**	**0.94**	

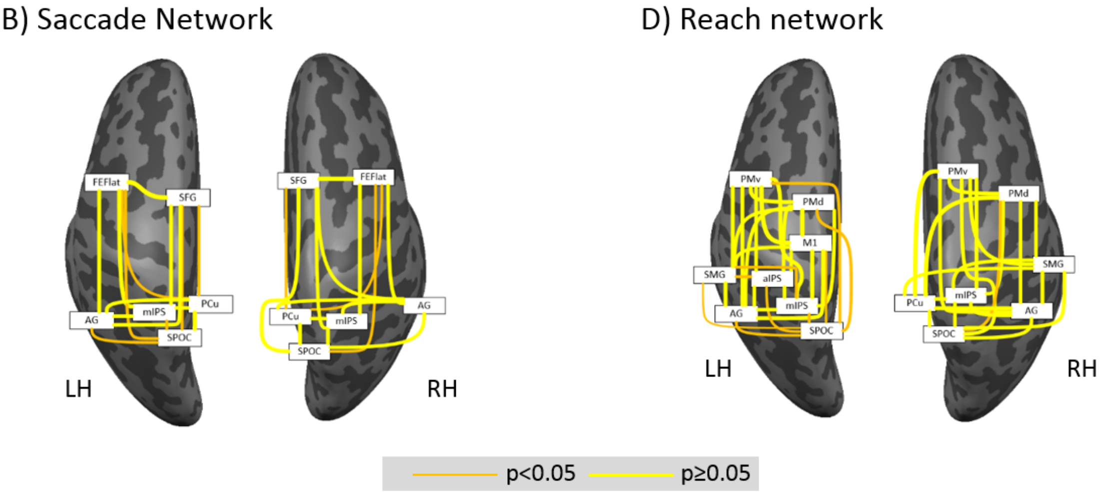

B) Saccade Network

D) Reach network

Figure 17. Correlations through time between regions derived from the saccade > colour report movement execution contrast. A) SACCADE: Matrices showing correlations (r) through time between all areas for each spatial domain tested (redundant entries in upper-right half are omitted) within each hemisphere. A continuous color scale is used to indicate the strength of correlation (r), i.e., with white close to 0.5 and red close to 1.0, and significant correlations (p<0.05, Bonferroni

corrected) are bolded. B) Graphical representations of the strength of correlation between left and right hemisphere brain areas for saccades. The thickness of the line indicates the r^2 value, with a thin line being close to 0 and a thick line close to 1. For these plots we used r^2 to increase the difference between highly correlated and less correlated areas. These data are superimposed on left and right hemisphere ‘inflated brains’ from a typical subject where light gray signifies gyri and dark gray signifies sulci. C) REACH: Matrices showing correlations (r) through time between all areas for each spatial domain tested (redundant entries in upper-right half are omitted) within each hemisphere (same conventions as A). D) Graphical representations of the strength of correlation between left and right hemisphere brain areas for reach (same conventions as B).

Figure 17C similarly shows the effector preference *reach* correlations between each brain area. Again, areas were ordered from posterior to anterior. Most of our reach areas showed high ($r > 0.9$) and statistically significant correlations with all of the other areas (the exception being SMG, which was not significantly correlated with aIPS or mIPS). Another notable exception was left SPOC, which did not have significant correlations with any other areas in the left hemisphere. Similarly, in the right hemisphere, almost all areas had high and significantly correlated activation, with the one exception being the pairing of PMd and SPOC. These highly correlated networks can be viewed graphically in figure 17D, which demonstrates a much more extensive and densely correlated 'network' compared to the saccade 'network' illustrated in figure 16B.

Figure 18A shows the correlations *betwee*n reach and saccade ROIs within each hemisphere. This analysis was performed to assess the similarity in activation across effectors in each hemisphere. Again, areas were ordered from posterior to anterior, this time with saccade regions listed horizontally and reach regions listed vertically. Even at first glance, once can observe a stark difference between the hemispheres, where almost all right hemisphere brain areas (37/42) show statistically significant correlations, compared to the left hemisphere where only 15/48 regions (31%) are significantly correlated. In the left hemisphere, AG appears as a clear hub for both effectors, showing significant correlations with 7/8 reach areas and 3/6 saccade areas. Notable, left FEF did not have any significant correlations with any of the reach areas. These highly correlated networks can be viewed graphically in figure 18B, using the same methodology used for 17B.

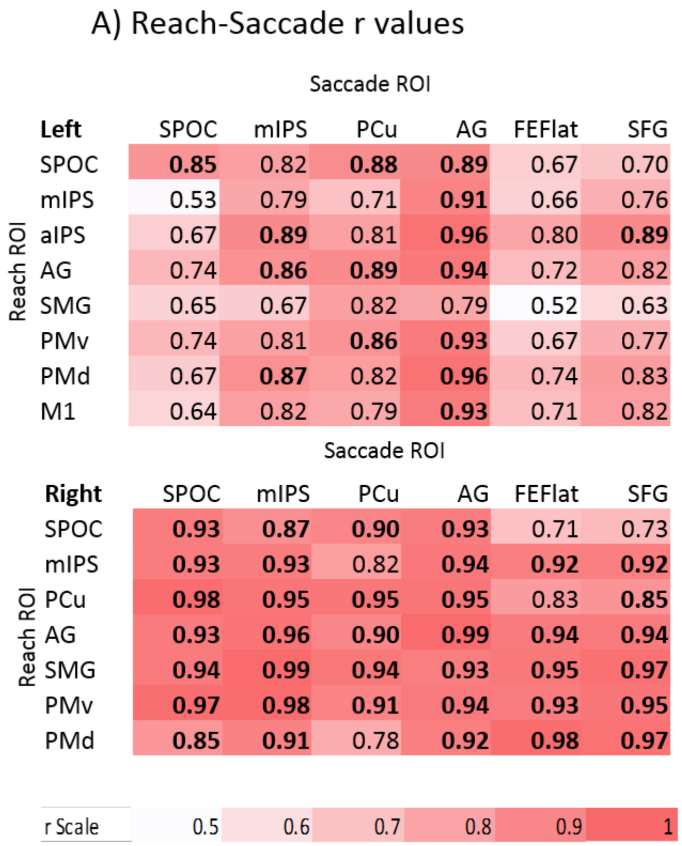

A) Reach-Saccade r values

Saccade ROI

Reach ROI	Left	SPOC	mIPS	PCu	AG	FEFlat	SFG
	SPOC	**0.85**	0.82	**0.88**	**0.89**	0.67	0.70
	mIPS	0.53	0.79	0.71	**0.91**	0.66	0.76
	aIPS	0.67	**0.89**	0.81	**0.96**	0.80	**0.89**
	AG	0.74	**0.86**	**0.89**	**0.94**	0.72	0.82
	SMG	0.65	0.67	0.82	0.79	0.52	0.63
	PMv	0.74	0.81	**0.86**	**0.93**	0.67	0.77
	PMd	0.67	**0.87**	0.82	**0.96**	0.74	0.83
	M1	0.64	0.82	0.79	**0.93**	0.71	0.82

Saccade ROI

Reach ROI	Right	SPOC	mIPS	PCu	AG	FEFlat	SFG
	SPOC	**0.93**	**0.87**	**0.90**	**0.93**	0.71	0.73
	mIPS	**0.93**	**0.93**	0.82	**0.94**	**0.92**	**0.92**
	PCu	**0.98**	**0.95**	**0.95**	**0.95**	0.83	**0.85**
	AG	**0.93**	**0.96**	**0.90**	**0.99**	**0.94**	**0.94**
	SMG	**0.94**	**0.99**	**0.94**	**0.93**	**0.95**	**0.97**
	PMv	**0.97**	**0.98**	**0.91**	**0.94**	**0.93**	**0.95**
	PMd	**0.85**	**0.91**	0.78	**0.92**	**0.98**	**0.97**

r Scale	0.5	0.6	0.7	0.8	0.9	1

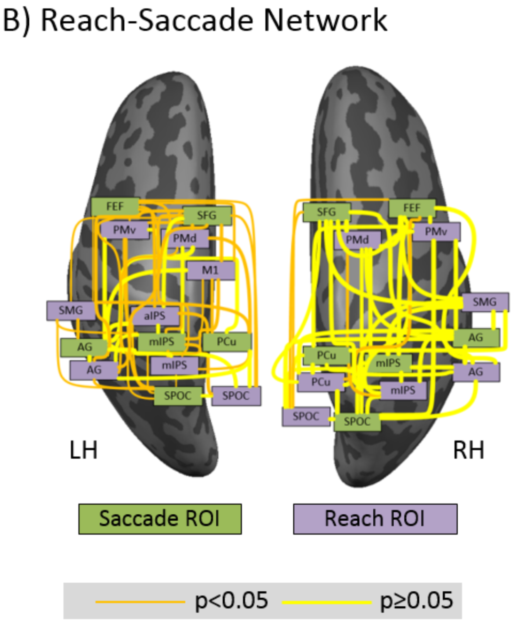

B) Reach-Saccade Network

Figure 18. Correlations through time between regions derived from comparing the saccade > colour report ROIs to reach > colour report ROIs during the movement execution contrast. A) Matrices showing correlations (r) through time between all areas for each spatial domain tested within each hemisphere. A continuous color scale is used to indicate the strength of correlation (r), i.e., with white close to 0.5 and red close to 1.0, and significant correlations ($p<0.05$, Bonferroni corrected) are bolded. Reach areas are listed vertically and saccade areas are listed horizontally. B) Graphical representations of the strength of correlation between left and right hemisphere brain

areas. The thickness of the line indicates the r^2 value, with a thin line being close to 0 and a thick line close to 1. For these plots we used r^2 to increase the difference between highly correlated and less correlated areas. These data are superimposed on left and right hemisphere ‘inflated brains’ from a typical subject where light gray signifies gyri and dark gray signifies sulci.

3.5 Discussion

In this study, we used an event-related fMRI design to investigate several key questions. To summarize, the first was to identify which regions are differentially activated for effector-agnostic visual target representation, as well as independent effector reach and saccade movement planning and movement execution. This analysis revealed selective, bilateral mIPS and left AG activation during the effector-independent target representation phase. In the independent effector planning phase, the entire occipital-parietal-frontal reaching network was activated, while only bilateral pIPS and SOG activation was observed for saccades. For the independent effector movement execution phase, broad activation of occipital-parietal-frontal reach and saccade networks was observed. Taken together, this suggests earlier independent effector planning for reaches than saccades, with the saccade network becoming fully engaged around the time of movement execution. The second question we aimed to answer was how saccade and reach differ from each other during the planning and execution phases. To do this, we directly contrasted saccade and reach activation during these time periods and found that for both planning and execution, the effector-preference activation corresponding to reaches was much stronger than the activation corresponding to saccades. During the planning phase, no region showed greater activation for saccades than reaches, and only right FEF showed greater activation for saccades than reaches during execution. The third question we aimed to answer was how effector-specific movement planning and execution are temporally and spatially distributed through the brain. We found that for the within-effector analysis, the time courses for ROIs during the effector-preference planning and execution phases were very highly correlated across parietal and frontal brain regions for both reach and saccade. When comparing activation across effectors, there were much stronger correlations in the right hemispheres (ipsilateral to the arm use to reach) than the contralateral left hemisphere, where AG was the only area strongly correlated across effectors. This suggests left AG may serve a similar role in right-handed reach planning and saccades, the activation seen in other areas is more heavily modulated depending on the effector to be used.

General activation during visual target memory, reach planning, and reach execution.

Many previous fMRI studies have implicated a widespread number of areas in occipital, parietal, and frontal cortex in visually guided reaching (Astafiev et al., 2003, Connolly et al., 2003; Medendorp et al., 2003, 2005; Prado et al., 2005; Fernandez-Ruiz et al., 2007; Beurze et al., 2009; Cavina-Pratesi et al., 2010; Fabbri et al., 2012; Konen et al., 2013; Chen et al., 2014) and saccades (Astafiev et al., 2003; Beurze et al., 2009; Connolly et al, 2007; Curtis et al, 2008; Gallivan et al, 2011, 2015; Bestman et al., 2012; Herwig et al, 2014). However, to our knowledge none of these studies clearly separated the three phases of effector-agnostic target representation, independent effector movement planning, and independent effector movement execution through time. To do this within the spatiotemporal limitations of fMRI, we required a paradigm with a series of instructions and delays which likely introduced more cognitive aspects to the task than one would see during on-line control, but with this caveat in mind, we were able to trace both general and direction-specific activation through those three phases. Most of our regions of interest showed different degrees of time-locked activation during target representation, planning, and execution (Figures 13 and 14), depending on whether the region was more visual (e.g., SOG) or motor (e.g., PMd/M1), but here we will restrict our discussion to significant clusters of activation during these three phases (Figures 10 and 11).

Our analysis of the effector-agnostic target representation phase (Figure 10) revealed limited activation in bilateral mIPS and left AG, perhaps related to spatial working memory (Courtney et al., 1996; Srimal and Curtis, 2008) or activity related to preparatory set (Culham et al., 2006, Chen et al., 2014). Cappadocia et al. (2017) found that bilateral PMd and right pIPS are involved in the target memory phase for reach planning, and activation in the parietal cortex is consistent with the uncertainty condition found in Gertz and Fiehler (2015), where parietal activation was also in the left hemisphere.

During this movement planning phase (Figure 11A), we observed widespread activation in the medial parieto-frontal reach network for reaches, including SPOC, mIPS, PMd, and left M1 (Culham et al, 2006; Gallivan and Culham, 2015; Cappadocia et al., 2017). This was consistent to the activation previously observed in Cappadocia et al. (2017), and further suggests that previous studies that combined target representation and movement planning (Medendorp et al., 2003, Fernandez-Ruiz et al., 2007; Culham et al, 2011) were mainly reporting activity related to visuomotor transformations and/or movement planning, as opposed to target memory. The activation we observed for saccades builds on the importance of separating out the target representation and planning phases, as we were able to observe bilateral pIPS activation in the saccade motor network. Previous research has shown the parietal saccade-related areas to be involved in both eye movements and attention (Corbetta et al., 1998; Astafiev et al., 2003), eye movements and visual working memory (Curtis et al, 2004; Curtis and Connelly, 2008; Srimal and Curtis, 2008) and all three processes (Jerde et al., 2012), and it is very possible that the activation we observed incorporates both early motor planning for saccades, as well as a memory component.

We also observed activation of occipital cortex, including LG, IOG and SOG, during the movement planning phase for both reaches and saccades. A phenomenon known as 'occipital reactivation' (Singhal et al., 2013), which involves re-entrant feedback from motor systems and has been previously observed for reaches (Singhal et al., 2013; Cappadocia et al., 2017), could explain this activation. For reaches, lateral cortex activation was greater in the left hemisphere contralateral to the hand, consistent with previous studies (Connolly et al., 2003; Fernandez-Ruiz, 2007; Bernier et al., 2012; Gertz and Fiehler, 2015; Cappadocia et al., 2017).

During motor execution, all medial reach-related regions of activation noted in the planning phase became even more extensive (relative to controls) (Figure 11B), also extending into prefrontal (e.g., SFG) and inferior parietal (e.g., SMG) areas that might be associated with cognitive aspects of the task, such as guidance of the movement based on spatial memory (Gallivan et al., 2015, Cappadocia et al., 2017). For saccade trials, the more lateral parieto-frontal saccade network became much more engaged at the time of execution, including bilateral activation of the FEF, mIPS, and AG. This activation is consistent with saccade-related activity observed in other studies (Astafiev et al., 2003; Beurze et al., 2009; Connolly et al, 2007; Curtis et al, 2008; Gallivan et al, 2011, 2015; Bestman et al., 2012; Herwig et al, 2014), and suggests that the saccade system becomes more heavily engaged much closer to the time of execution than the reach network. Given the nature and frequency of saccades, which are preformed 3-5 times per second (Rayner et al., 1998), this finding is not surprising.

The conjunction analysis identifying areas involved in both reach and saccade execution (figure 12) revealed left mIPS and right AG, PCu, SPOC, LOTC, and FEF/PMv as active for both reaches and saccades (compared to the colour control task). The inclusion of both parietal and frontal motor areas in planning for both effectors is consistent with previous studies, and may explain some of the difficulties in observing effector-preferential activation (Connolly et al, 2007; Curtis et al, 2008; Beurze et al., 2009; Gallivan et al, 2011). The increased overlap in the right hemisphere can likely be explained by the overall increase in activation observed for the saccade>colour analysis, and may not necessarily be reflective of true increased overlap in the right hemisphere. This could be due to the motor requirements of the control task (which required the subject to press a button once or twice with their right hand indicating if the target was red or green) increasing the baseline control activation in the left hemisphere and thus limiting the number of saccade regions that could be identified by the contrast.

The later activation of the saccade network compared to the reach network is further supported when examining the time courses for saccade and reach execution ROIs in figures 13 and 14. In both sets of time courses, most of the ROIs show significantly higher activation when compared to the control condition, with left SOG, left mIPS, and left SPOC showing significantly higher activation during execution for both effectors. As mIPS and SPOC have been implicated in both reach and saccade planning (Culham et al., 2006; Gallivan et al., 2011, Cappadocia et al., 2017) it is not surprising that these areas show significant execution-related activation for both effectors. Although we did not run statistics on this, one can also observe that for reach, bilateral mIPS, SPOC, and PMd all show activation above the control condition during the planning phase, while only left SPOC shows this for saccades. This observationally supports our finding that the saccade network becomes engaged later than the reach network during the execution phase.

Effector Preference during Movement Planning and Execution

A second goal of our study was to look at cortical effector preference during movement planning and execution. To do this, we contrasted reach and saccade task activation during both movement planning and execution. During the planning phase, we found only effector-preference activation for reach. This is consistent with previous studies that have seen fMRI activation related to reaches produce broader and more spread out BOLD activation than that seen for saccades (DeSouza et al. 2000; Astafiev et al., 2003; Beurze et al., 2007; Gallivan et al., 2011). A similar trend was observed during the motor execution phase, with right FEF appearing as the sole saccade effector-selective ROI. This explanation is further supported by the time course analysis shown in figure 16, where preferential activation can be observed for reaching during the movement planning phase, and even more so during execution. In fact, bilateral PMd, bilateral mIPS, bilateral SMG, and left M1 all showed significantly higher % signal change during execution, even though for all areas but left M1, there was clear activation observed for saccades as well. The complete lack of saccade-related areas in the left hemisphere during the planning phase (figure 15A) may be due to contralateral direction tuning and handedness for reaches that has been observed in other studies: fMRI (Medendorp et al. 2003; 2005; Filimon, 2010; Vesia and Crawford, 2012; Gertz and Fiehler, 2015; Cappadocia et al., 2017), MEG (Van Der Werf et al., 2010), TMS (Vesia et al. 2010), patients (Khan et al., 2007) and primate neurophysiology (Gail and Andersen, 2006; Gail et al., 2009; Westendorff et al., 2010). This asymmetry could also relate to the statics of fMRI, i.e., the way that several neural signals might need to combine to produce significant effects at the level of the BOLD signal. It is also possible that we observed reach-preferential planning due to the increased complexity required for reaches (more degrees of freedom, complex movement dynamics, and the need for hand position information; see Blohm et al., 2007, 2008), thus requiring more planning before the initiation of a movement. It is also possible that there was some implicit saccade planning in the reach task, as eye and arm movements are normally coupled (Flanagan and Johansson, 2003).

Shared inputs within and between effector-preference networks

To understand saccade and reach planning at a network level, we cross-correlated saccade activation for ROIs observed during reach and saccade motor execution within and across effectors. We found that within each effector, the time courses for ROIs during the planning and execution phases were very highly correlated across parietal and frontal brain regions. For reaches (Figure 17C/D), there were significant correlations between almost all pairs of areas in the right hemisphere (SPOC, mIPS, PCu, AG, SMG, PMv, and PMd), with the one exception being the pairing of

SPOC and PMd. In the left hemisphere, significant correlations were found between mIPS, aIPS, AG, SMG, PMv, PMd, and M1 (with the two exceptions being SMG-mIPS and SMG-aIPS). Left SPOC, however, did not significantly correlate with any of the other areas in the left hemisphere. Recent studies have implicated SPOC as a visually-guided reaching area (Culham et al., 2006; Filimon et al., 2009; Vesia et al., 2010; Gallivan and Culham, 2015, Cappadocia et al., 2017), and our previous study showed that for reach, SPOC was identified as a 'hub' areas, showing both visual and movement selective activation (Cappadocia et al., 2017). Its important to note that our previous study was examining visual and motor selectivity, and on the visual selectivity index (which is similar to trials in this study), SPOC was only significantly correlated to 5/10 reach-related areas in the left hemisphere.

For saccades (Figure 17A/B), in both the left and right hemisphere mIPS and AG appear as 'hubs' that are highly correlated with the activation seen in several other areas. mIPS specifically was significantly correlated with all areas in the right hemisphere and 4/5 other areas in the left hemisphere (the exception being SPOC). Given the strong research linking mIPS to saccade planning (Astafiev et al., 2003; Beurze et al., 2009; Connolly et al, 2007; Curtis et al, 2008; Gallivan et al, 2011, 2015; Bestman et al., 2012; Herwig et al, 2014), it is not surprizing that mIPS was observed to be a highly correlated 'hub'. AG was previously found to be visually selective for reach planning (Cappadocia et al., 2017) and is involved in left/right spatial discrimination (Hirnstein et al., 2011). It has also been implicated as a saccade planning region in previous TMS tasks (Vesia et al., 2010). Previous TMS studies targeting P3/P4 [which is around the angular gyrus (Ryan et al., 2006)] have found various saccade effects

(Elkington et al., 1992; Oyachi and Ohtsuka, 1995; Muri et al., 1996; Kapoula et al., 2005), and it has been suggested that AG is a human homologue of monkey LIP (Koyama et al., 2004), which support its inclusion as a ‘hub’.

Comparing across effectors (Figure 18), there were much stronger correlations in the right hemisphere than in the left. As mentioned earlier in this discussion, this could be due to the high degree of contralateral activation seen for reaches when compared with ipsilateral activation. This generally agrees with previous investigations of occipital, parietal, and prefrontal activity based on fMRI (Medendorp et al. 2003; 2005; Filimon, 2010; Vesia and Crawford, 2012; Gertz and Fiehler, 2015; Cappadocia et al., 2017), MEG (Van Der Werf et al., 2010), TMS (Vesia et al. 2010), patients (Khan et al., 2007) and primate neurophysiology (Gail and Andersen, 2006; Gail et al., 2009; Westendorff et al., 2010). Bilaterally, AG was found to be a ‘hub’ area, showing high correlations across effectors. This is consistent with previous TMS studies to the nearby P3/P4 sights, which have shown that TMS to AG disrupts the integration of saccade information for reach planning (Van Donkelaar et al., 2000). AG has also shown to code motor coordinates, perhaps in somatosensory coordinates (Fernandez-Ruiz et al., 2007; Vesia et al., 2006, 2010; Vesia and Crawford, 2012), signaling it may integrate visual information to produce a motor output common to both effectors. Within the left hemisphere, SPOC, FEF, and SFG from the saccade contrast all showed minimal significant correlations to reach areas (SPOC was only correlated to the reach-SPOC and SFG was only correlated to aIPS). This suggests that these areas are more effector-specific, with recent primate neurophysiology evidence implicating FEF as transitioning from a more general visual code to a saccade movement code (Sajad et al., 2016). While this has not been assessed for effector specificity, the role of the FEF in saccade target selection and production is consistent with its output being more effector-specific (Andersen et al. 1985; Bruce et al., 1985; Schall and Hanes, 1993; Schall et al., 1995; Tehovnik et al., 2000).

Implications for independent effector control and eye-hand coordination.

Consistent with previous studies, there was considerable overlap observed for both reaches and saccades around the time of movement execution (Connolly et al, 2007; Curtis et al, 2008; Beurze et al., 2009; Gallivan et al, 2011). When the timeseries were analyzed between reaches and saccades, an interesting pattern emerged between the hemispheres. As observed in figure 18, almost all right hemisphere brain areas (37/42) show statistically significant correlations, compared to the left hemisphere where only 15/48 regions (31%) are significantly correlated. As all subjects were right handed and reached with their dominant right arm, this could be related to increased reach activation in the left hemisphere (Medendorp et al. 2003; 2005; Filimon, 2010; Vesia and Crawford, 2012; Gertz and Fiehler, 2015; Cappadocia et al., 2017). However, the strong overlap in brain areas revealed in the effector-dependent contrasts combined with the strong correlations observed between reach and saccade areas at execution suggests that for independent or coordinated movements using the eye and hand, a similar network is activated.

Conclusion

This study shows that when separating visually guided reaches and saccades into distinct target memory, movement planning, and movement execution phases, the evolution of these processes over time reveal increased activation. During effector-agnostic target memory, only modest activation in left AG and bilateral mIPS was observed. For reaches, the occipital-parietal-frontal reach network was engaged medially during both reach *planning and execution*. For saccades, more lateral (mIPS, AG, and FEF) activity was observed only during saccade *execution*. These motor activations were bilateral, with a left (contralateral) preference for reach. With the exception of right FEF, effector-preference contrasts revealed significantly more parietofrontal activation for reaches than saccades during both planning and execution. Cross-correlation of reach, saccade, and reach-saccade activation through time revealed spatiotemporally correlated activation both within and across effectors in each hemisphere, but with a tendency toward higher correlations in the right hemisphere. These results demonstrate cortical networks for eye, hand, and eye-hand control that are widely distributed, but with effector-specific rules for timing, medial-lateral localization, and hemispheric lateralization.

Chapter Four: General Discussion

General Conclusions and Future Directions

Using two similarly designed event-related, cue-separation fMRI experiments, this dissertation examined the following key aspects of the visuomovement system: (1) The brain areas involved in visual target representation, motor planning, and motor execution for visually-guided reaching, (2) the evolution of visual and movement directional coding over time for visually-guided reaching, (3) brain areas involved in visual target representation, motor planning, and motor execution for visually-guided saccades, and (4) effector specificity in movement planning and execution for saccades and reaches. Overall, it was found that the fronto-parietal visuomotor system for reach was active for both movement planning and execution, with the saccade system showing increased activation around the time of execution. For reaches, a visuo-movement parameter that factors in both the visual input and motor output of the system shows the highest temporal correlations between brain areas.

4.1 The brain areas involved in visual target representation, motor planning, and motor execution for visually-guided reaching

In general, it was found that for both saccades and reaches, the activation observed during the visual target representation phase was limited to mild activation in frontal and parietal cortex. The key regions that were engaged included PMd, mIPS, and AG. All three of these regions have been linked to movement planning (Gallivan et al., 2011; 2015, Chen et al., 2015, Feihler et al., 2015), making their inclusion unsurprising. Our results, however, suggest that this mild activation may serve as either a precursor to more specific movement planning, or be related to attention spatial working memory

(Courtney et al., 1996; Srimal and Curtis, 2008) or activity related to preparatory set (Culham et al., 2006, Chen et al., 2014).

During movement planning, across both tasks we noted significant activation, for reach in occipital, parietal and frontal regions that have been linked to reach planning, which is consistent with previous studies (Astafiev et al., 2003, Connolly et al., 2003; Medendorp et al., 2003, 2005; Prado et al., 2005; Fernandez-Ruiz et al., 2007; Beurze et al., 2009; Cavina-Pratesi et al., 2010; Fabbri et al., 2012; Konen et al., 2013; Chen et al., 2014; Bernier et al., 2017). Since our studies were the first to separate reach planning into three distinct phases, we can conclude that this activation was due to planning and not the initial encoding of visual information or working memory alone. One significant difference between the two experiments during this phase is that in the 1st experiment, subjects could not anticipate the required movement plan or derive it from the visual stimulus until the pro / anti instruction was given at the start of the second delay, while in the second experiment, subjects did know the location of the movement goal, but were agnostic to the effector. Since the activation observed during the movement planning phase in both experiments was remarkably similar, this suggests that the majority of general, spatial, effector independent planning that occurs prior to this phase is minimal.

During motor execution, we observed wide recruitment of the occipital, parietal and frontal regions linked to reach planning for reach trials and saccade planning for saccade trials. This was an expected outcome given the fact that a movement was occurring. One interesting finding from experiment 2 was the high correlations across reach areas in both the left and right hemispheres, except for left SPOC. While SPOC was significantly active during reach execution, its lower correlations with other areas suggests its activation through planning and execution is different from other areas. Looking at the time course for the region, left SPOC shows an activation peak during motor planning that is much less pronounced than in other regions, suggesting this lower correlation value may be due to earlier involvement in movement planning. Applying TMS to this region during the planning phase and comparing it to TMS on more execution-specific regions (e.g. AG) may help differentiate these regions and their impact on movement planning and execution.

Given the activation observed in this task, an interesting future investigation could apply TMS to the parietal and frontal regions identified during the movement planning and execution phases to causally investigate their impact on reach and saccade planning and execution. For example, across both tasks SMG was observed during motor execution, but not planning, and its impact on reach planning in humans is not well understood [e.g., it could be involved in guidance of the movement based on spatial memory (Gallivan et al., 2015)]. Fully understanding its role in delayed reach planning could provide valuable insights on the contributions of inferior parietal lobe on reaches. Along a related vein, the angular gyrus was found to be involved in movement execution for both saccades and reaches, but not planning. Given previous studies that have suggested it encodes extrinsic movement direction, perhaps in somatosensory coordinates (Fernandez-Ruiz et al. 2007; Vesia et al. 2006, 2010; Vesia and Crawford 2012), applying TMS before and after a movement plan can be formed could yield significant insights on the region’s role in reach planning.

4.2 Evolution of visual and movement directional coding over time for visually-guided reaching

The evolution of visual and movement directional coding over time for visually-guided reaching was the second key research question. When comparing visual, movement, and visuo-movement directional selectivity, the visuo-movement selectivity showed the highest correlations over time. The visuo-movement parameter used in experiment 1 was found to show the highest correlations across multiple brain regions, suggesting that despite the many functional differences between these areas (like those described above and by many other authors), an entire occipital-parietal-frontal network is engaged in the transformation of visual stimuli into motor acts; Not only at different serial stages of processing, but through the entire duration of the task. A recent investigation by Bernier et al. (2017) revealed an intermediate stage of sensorimotor transformations in bilateral parietal cortex (when a target location was not specified) which potentially strengthens our finding in Chapter 2 that SPOC and AG serve as 'hubs' in visuomotor transformations. Our findings show that visuomotor transformations can be observed within single structures and even single neurons (e.g., Sajad et al. 2015, 2016, Sadeh et al. 2015), almost the entire cortex is engaged in the entirety of such transformations. An interesting future direction that would build on this work would be to examine how this phenomenon evolved for saccades (so a pro/anti saccade paradigm using the same event-related design), with a hypothesis that the directional selectivity would follow a similar pattern. It would also be interesting to test this using multiple limbs, as all of the results in our experiment were based on an analysis of the left hemisphere (contralateral to the right limb which was used for reached). It would be interesting to understand if there is any limb-specificity at play related to hand dominance, which is present in humans but not monkeys. Given the role of AG and SPOC as hubs in the correlational analysis, as well as their general role in visuomotor transformations, one could hypothesize that they are the location where visuomotor transformations occur, as they have evidence for both visual and motor signals. This is also consistent with MEG studies, which have found directional selectivity in PPC in the gamma frequency (Van Der Wref et al., 2010). Adding a dynamical systems perspective, the visuo-movement activation observed in this study may bridge the gap between inputs and outputs, placing a focus on the evolution of signals within the brain leading to goal-directed movements (Shenoy et al., 2013).

4.3 Brain areas involved in visual target representation, motor planning, and motor execution for visually-guided saccades

For saccade movement planning, we observed minimal activation during the movement planning phase, which was a departure from the activation observed for reaches. Given the high complexity and reference frame transformations involved with planning multi-joint arm movements (Blohm and Crawford, 2007; Blohm et al., 2008), as well as the fact that limb movements are much more likely to be delayed than eye movements in real life, this may explain the recruitment of the reach network for planning at an earlier phase. Compared to arm movements, we also observed less hemispheric specificity (activation for right handed reaching was much higher I the left hemisphere, while activation for saccades was similar across hemispheres). Understanding the key regions involved in saccade planning (specifically pIPS and SOG) could reveal insights on their role in saccade planning, and a TMS experiment could test the impact of TMS during planning on a region like pIPS vs TMS to a more motor region in parietal cortex (e.g., AG) during movement planning and execution to tease apart the causal role of these regions.

When analyzing the overlap in the conjunction analysis, left mIPS and right AG, PCu, SPOC, LOTC, and FEF/PMv were active for both reaches and saccades (compared to the colour control task). The inclusion of both parietal and frontal motor areas in planning for both effectors is consistent with previous studies, and may explain some of the difficulties in observing effector-specific activation (Connolly et al, 2007; Curtis et al, 2008; Beurze et al., 2009; Gallivan et al, 2011). The increased overlap in the right hemisphere can likely be explained by the overall increase in activation observed for the saccade>colour analysis, and may not necessarily be reflective of true increased overlap in the right hemisphere. This could be due to the motor requirements of the control task (which required the subject to press a button once or twice with their right hand indicating if the target was red or green) increasing the baseline control activation in the left hemisphere and thus limiting the number of saccade regions that could be identified by the contrast.

4.4 Effector specificity in movement planning and execution for saccades and reaches

Examining effector specificity in experiment 2 revealed significantly more BOLD activation for reaches than saccades during both planning and execution in the effector-dependent contrasts. This is similar to activation patterns seen in other studies (DeSouza et al., 2000; Medendorp et al., 2003; Connolly et al., 2003; Beurze et al., 2007, 2009), and highlights both the difficulty previous studies have had in differentiating saccades and reaches, as well as the larger BOLD activation observed for reaches than saccades. Another novel observation is the fact that the reach network showed widespread activation for both planning and execution, while the saccade network only showed limited activation during planning before displaying broader activation at the time of execution. Given that people perform 3-5 saccades per second (Rayner et al., 1998), compared to reaches which occur much less frequently, the increased activation observed for reach planning when compared to saccades is consistent with how the effectors are used.

In our study, only the right FEF showed significantly higher BOLD activation for saccades than reaches, and this may be due to the fact that reaches in general showed less activation in the right hemisphere (as it was the hemisphere ipsilateral to the right arm used for reaching). Looking at the correlations between reach and saccade regions from motor planning, these hemispheric differences are further highlighted by the high amount of correlations across effectors observed in the right hemisphere (ipsilateral to the reach effector) and the low amount of correlations observed in the left (contralateral) hemisphere. To further understand effector specificity given the large hemispheric differences observed for reach, a study involving both right and left arm reaches could reveal key insights on the role of brain regions (as it would control for contralateral/ipsilateral effector).

4.5 Implications for Cognitive Neuroscience and Sensorimotor Control

Chapter 2 revealed the broad networks that are involved in both visual and motor direction tuning & sensorimotor transformations for reach. Understanding these processes is important for the field, as people constantly rely in visual input to produce meaningful actions in the environment. The studies presented in this dissertation add valuable spatiotemporal information to our understanding of action and perception that could be applied to other fields. For example, the study of memory has investigated the temporal aspects of working memory for features and objects (Luck and Vogel, 1997; Vogel et al., 2001; Olson and Jiang, 2002; Alvarez and Cavanagh, 2004; Bays and Husain, 2008). Ultimately, when a person interacts with the world, they do not plan and perform a saccade or a reach in the absence of other cognitive processes, and incorporating our findings to the study of these other cognitive processes may help us understand the larger picture of how the brain works. For example, how would this activation differ if reaches to multiple targets had to be planned, thus increasing the attentional, memory, and motor requirements of the task? Would the activation observed in the target representation phase increase and mirror the activation in the movement planning/execution phases, or would the activation follow a similar pattern? Understanding the intersection of these fields within neuroscience would help advance our understanding of how the brain functions in the real world, where multiple processes must be integrated seamlessly in healthy adults.

Chapter 3 increases our understanding of how the brain is able to plan and execute both saccades and reaches. While this chapter examined these processes independently, adding to the body of research can motivate future studies examining coordinated eye and hand movements to understand these processes with more real-world validity, as eye and arm movements are often performed together. For example, a future study that added a “both” condition where subjects had to reach and saccade to remembered location of the target would allow for the comparison or effector independent and coordinated movements, which would be more similar to how people interact with the environment in the real world.

4.6 Potential applications of this research

While this dissertation is fundamental discovery science, the findings of this work have the potential to be applied to both patients and technological innovations.

Patients with Alzheimer's disease (AD) and mild cognitive impairment (MCI) show deficits in tasks involving both fine and complex motor function, as well as deficits in gross motor function (Kluger et al., 1997). In an analysis of movement with and without visual feedback, it was found that Alzheimer's patients rely more on online external cues to guide movement than controls, indicating impairment in visuomotor integration, with a positive correlation observed between motor errors and cognitive decline (Ghilardi et al., 1999, 2000). In more recent studies using non-standard mapping, both AD and MCI patients showed impairments in transforming visual input into motor output when compared to controls (Tippett et al., 2006, 2007, 2012; Salek et al., 2011). The brain regions that have been linked to non-standard mapping include primary motor cortex, medial motor areas, lateral premotor cortex, and the superior parietal lobule (Gorbet et al., 2004). These regions significantly overlap with the ROIs identified in both chapter 2 and 3, and a greater understanding of the contributions of these regions to both motor planning and execution for reach, as well as visuomotor transformations (explored in chapter 2), could potentially aide in the development of assessment tools or the design of cognitive strategies to aide help patients account for deficits. For example, given the reliance AD patients have on online cues, this may imply that the regions involved in planning (e.g., pIPM, mIPS, PMd) are more impacted than the execution regions in the visuomotor pathway (e.g., AG, SMG, M1), however more study would be needed to understand a possible connection.

For innovation, several neurophysiology labs are currently working on animal models for neural prosthetics (E.g., Revechkis et al., 2015), with the goal of decoding cortex and allowing patients to use an artificial limb based on these signals. Both experiments in this dissertation expand on our understanding of the spatiotemporal aspects of movement planning in the human. This necessitates an understanding of the role of cortical regions in the human brain. As the use of invasive recording technologies in the human are limited, using fMRI to understand the spatiotemporal contributions of these regions, and combining these results with other techniques (MEG, EEG, TMS) can begin to provide the requisite information that would be needed to potentially test more invasive techniques (E.g., recording from neurons) in humans, a likely precursor for clinical trials.

These studies also offer an interesting methodology to study the temporal evolution of the fMRI BOLD signal. In both studies, the event-related time course data (% signal change) was correlated across visuospatial parameters (visual, movement, and visuomovement) and effectors (reach, saccade, and reach-saccade) to understand similarities in this evolution over time across ROIs. This methodology allowed us to identify ‘hubs’, which we interpret to be regions that receive similar inputs, produce similar outputs, or both, and are likely central to the parameter or effector being studied. This methodology could be applied to other research questions where a signal is likely to evolve over time based on an event-related design to identify key hubs in other motor or cognitive neuroscience fields (E.g., the study of visual working memory for features or objects).

4.7 Final conclusions

In conclusion, this dissertation examined the cortical activation through target representation, movement planning, and movement execution for both reaches and saccades, and found that for both effectors, activation generally increased from limited parietal and frontal areas during the target memory phase to broad occipital-parietal-frontal activation at the time of execution. For saccades, the activation was much more modest during the effector-dependent movement planning phase than what was observed in the reach trials. Comparing between effectors, activation during both planning and execution was significantly higher for reach in the effector-specific contrasts in Chapter 3. Cross-correlation of reach, saccade, and reach-saccade activation through time revealed spatiotemporally correlated activation both within and across effectors in each hemisphere, but with a tendency toward higher correlations in the right hemisphere.

In addition to assessing the evolution of cortical activation for visually guided saccades and reaches, Chapter 2 of this dissertation also examined visual and directional coding for visually guided reaching. By using a pro/anti task where the instruction was provided in the middle of the trial, visually selective activation, movement selective activation, and a visuo-movement parameter could be assessed to determine which showed the highest correlations among reach ROIs. Although all schemas displayed high correlations between cortical areas, in the end the visuo-movement parameter showed the highest correlations as it accounts for both the directional selectivity of the input and the output of the system.

These results demonstrate that for both reaches and saccades, widely distributed cortical networks are involved in movement planning and execution, with effector-specific rules for timing, and visual and movement selective activation. They also demonstrate that a visuo-movement parameter selective to both visual input and motor output best describes the directional tuning for reach.

References

Abrams RA, Davoli CC, Du F, Knapp WH, Paull D. 2008. Altered vision near the hands. Cognition. 107:1035–1047.

Ajemian, R., Bullock, D., & Grossberg, S. (2000). Kinematic coordinates in which motor cortical cells encode movement direction. Journal of Neurophysiology, 84(5), 2191-2203.

Andersen, R. A., Bracewell, R. M., Barash, S., Gnadt, J. W., & Fogassi, L. (1990). Eye position effects on visual, memory, and saccade-related activity in areas lip and 7a of macaque. Journal of Neuroscience, 10(4), 1176-1196.

Andersen, R. A., Brotchie, P. R., & Mazzoni, P. (1992). Evidence for the lateral intraparietal area as the parietal eye field. Current Opinion in Neurobiology, 2(6), 840-6. doi: 10.1016/0959-4388(92)90143-9

Andersen, R. A., & Buneo, C. A. (2002). Intentional maps in posterior parietal cortex. Annual Review of Neuroscience, 25, 189-220. doi: 10.1146/annurev.neuro.25.112701.142922

Andersen, R. A., Essick, G. K., & Siegel, R. M. (1985). Encoding of spatial location by posterior parietal neurons. Science, 230(4724), 456-458.

Andersen, R. A., Snyder, L. H., Bradley, D. C., & Xing, J. (1997). Multimodal representation of space in the posterior parietal cortex and its use in planning movements. Annual Review of Neuroscience, 20, 303-330. doi: 10.1146/annurev.neuro.20.1.303

Andersen, R. A., & Cui, H. (2009). Intention, action planning, and decision making in parietal-frontal circuits. Neuron, 63(5), 568-583. doi: 10.1016/j.neuron.2009.08.028

Astafiev S V, Shulman GL, Stanley CM, Snyder AZ, Van Essen DC, Corbetta M. 2003. Functional organization of human intraparietal and frontal cortex for attending, looking, and pointing. J Neurosci. 23:4689–4699.

Barany DA, Shapiro AD, Lee TG. (2015) Multivariate fMRI Approaches to Flexible Sensorimotor Maps in Parietal Cortex. J. Neurosci. 35(34):11763-11765

Batista, A. P., Buneo, C. A., Snyder, L. H., & Andersen, R. A. (1999). Reach plans in eye-centered coordinates. Science, 285(5425), 257-260. doi: 10.1126/science.285.5425.257

Batista, A. P., Santhanam, G., Yu, B. M., Ryu, S. I., Afshar, A., & Shenoy, K. V. (2007). Reference frames for reach planning in macaque dorsal premotor cortex. Journal of Neurophysiology, 98(2), 966-983. doi: 10.1152/jn.00421.2006

Battaglia-Mayer, A., Ferraina, S., Mitsuda, T., Marconi, B., Genovesio, A., Onorati, P., . . . Caminiti, R. (2000). Early coding of reaching in the parietooccipital cortex. Journal of Neurophysiology, 83(4), 2374-2391.

Baumann, M. A., Fluet, M., & Scherberger, H. (2009). Context-specific grasp movement representation in the macaque anterior intraparietal area. Journal of Neuroscience, 29(20), 6436-6448. doi: 10.1523/JNEUROSCI.5479-08.2009

Berman R, Colby C. 2009. Attention and active vision. Vision Res. 49:1233–1248.

Bernier P-M, Cieslak M, Grafton ST. 2012. Effector selection precedes reach planning in the dorsal parietofrontal cortex. J Neurophysiol. 108:57–68.

Bernier P-M, Grafton ST. 2010. Human posterior parietal cortex flexibly determines reference frames for reaching based on sensory context. Neuron. 68:776–788.

Bernier P-M, Whittingstall K,Grafton ST. 2017. Differential Recruitment of Parietal Cortex during Spatial and Non-spatial Reach Planning. Front Hum Neurosci. 2017 11:249.

Beurze SM, de Lange FP, Toni I, Medendorp WP. 2007. Integration of target and effector information in the human brain during reach planning. J Neurophysiol. 97:188–199.

Beurze SM, de Lange FP, Toni I, Medendorp WP. 2009. Spatial and effector processing in the human parietofrontal network for reaches and saccades. J Neurophysiol. 101:3053–3062.

Beurze SM, Toni I, Pisella L, Medendorp WP. 2010. Reference frames for reach planning in human parietofrontal cortex. J Neurophysiol. 104:1736–1745.

Binkofski, F., Dohle, C., Posse, S., Stephan, K. M., Hefter, H., Seitz, R. J., & Freund, H. J. (1998). Human anterior intraparietal area subserves prehension - A combined lesion and functional MRI activation study. Neurology, 50(5), 1253-1259.

Bisley, J. W., & Goldberg, M. E. (2003). Neuronal activity in the lateral intraparietal area and spatial attention. Science, 299(5603), 81-86. doi: 10.1126/science.1077395

Blangero A, Gaveau V, Luauté J, Rode G, Salemme R, Guinard M, Boisson D, Rossetti Y, Pisella L. 2008. A hand and a field effect in on-line motor control in unilateral optic ataxia. Cortex. 44(5):560-568.

Blohm, G., & Crawford, J. D. (2007). Computations for geometrically accurate visually guided reaching in 3-D space. Journal of Vision, 7(5), 4. doi: 10.1167/7.5.4

Blohm, G., & Crawford, J. D. (2009). Fields of gain in the brain. Neuron, 64(5), 598-600. doi: 10.1016/j.neuron.2009.11.022

Blohm, G., & Crawford, J. D. (2009). Fields of gain in the brain. Neuron, 64(5), 598-600. doi: 10.1016/j.neuron.2009.11.022

Bock, O. (1986). Contribution of retinal versus extraretinal signals towards visual localization in goal-directed movements. Experimental Brain Research, 64(3), 476-482. doi: 10.1007/BF00340484

Buneo, C. A., Jarvis, M. R., Batista, A. P., & Andersen, R. A. (2002). Direct visuomotor transformations for reaching. Nature, 416(6881), 632-636. doi: 10.1038/416632a

Busan, P., Barbera, C., Semenic, M., Monti, F., Pizzolato, G., Pelamatti, G., & Battaglini, P. P. (2009a). Effect of transcranial magnetic stimulation (TMS) on parietal and premotor cortex during planning of reaching movements. Plos One, 4(2), e4621. doi: 10.1371/journal.pone.0004621

Busan, P., Jarmolowska, J., Semenic, M., Monti, F., Pelamatti, G., Pizzolato, G., & Battaglini, P. P. (2009b). Involvement of ipsilateral parieto-occipital cortex in the planning of reaching movements: Evidence by TMS. Neuroscience Letters, 460(2), 112-116. doi: 10.1016/j.neulet.2009.05.028

Busan, P., Monti, F., Semenic, M., Pizzolato, G., & Battaglini, P. P. (2009c). Parieto-occipital cortex and planning of reaching movements: A transcranial magnetic stimulation study. Behavioural Brain Research, 201(1), 112-119. doi: 10.1016/j.bbr.2009.01.040

Calton, J. L., & Taube, J. S. (2009). Where am I and how will I get there from here? A role for posterior parietal cortex in the integration of spatial information and route planning. Neurobiology of Learning and Memory, 91(2), 186-196. doi: 10.1016/j.nlm.2008.09.015

Caminiti R, Johnson PB, Galli C, Ferraina S, Burnod Y. 1991. Making arm movements within different parts of space: the premotor and motor cortical representation of a coordinate system for reaching to visual targets. J Neurosci. 11(5):1182-1197.

Caminiti, R., Johnson, P. B., & Urbano, A. (1990). Making arm movements within different parts of space - dynamic aspects in the primate motor cortex. Journal of Neuroscience, 10(7), 2039-2058.

Cappadocia DC, Monaco S, Chen Y, Blohm G, Crawford JD. 2017. Temporal Evolution of Target Representation, Movement Direction Planning, and Reach Execution in Occipital–Parietal–Frontal Cortex: An fMRI Study. Cerebral Cortex. 27(11):5242–5260.

Cattaneo, Z., Silvanto, J., Pascual-Leone, A., & Battelli, L. (2009). The role of the angular gyrus in the modulation of visuospatial attention by the mental number line. Neuroimage, 44(2), 563-568. doi: 10.1016/j.neuroimage.2008.09.003

Cavanna AE, Trimble MR. 2006. The precuneus: a review of its functional anatomy and behavioural correlates. Brain. 129:564–583.

Cavina-Pratesi, C., Valyear, K. F., Culham, J. C., Kohler, S., Obhi, S. S., Marzi, C. A., & Goodale, M. A. (2006). Dissociating arbitrary stimulus-response mapping from movement planning during preparatory period: Evidence from event-related functional magnetic resonance imaging. Journal of Neuroscience, 26(10), 2704-2713.

Cavina-Pratesi C, Monaco S, Fattori P, Galletti C, McAdam TD, Quinlan DJ, Goodale MA, Culham JC. 2010. Functional magnetic resonance imaging reveals the neural substrates of arm transport and grip formation in reach-to-grasp actions in humans. J Neurosci. 30:10306–10323.

Chang, S. W. C., Papadimitriou, C., & Snyder, L. H. (2009). Using a compound gain field to compute a reach plan. Neuron, 64(5), 744-755. doi: 10.1016/j.neuron.2009.11.005

Chen Y, Monaco S, Byrne P, Yan X, Henriques DYP, Crawford JD. 2014. Allocentric versus egocentric representation of remembered reach targets in human cortex. J Neurosci. 34:12515–12526.

Chapman, C. S., Gallivan, J. P., Culham, J. C., & Goodale, M. A. (2011). Mental blocks: FMRI reveals top-down modulation of early visual cortex when obstacles interfere with grasp planning. Neuropsychologia, 49(7), 1703-1717. doi: 10.1016/j.neuropsychologia.2011.02.048

Chouinard, P. A., Leonard, G., & Paus, T. (2005). Role of the primary motor and dorsal premotor cortices in the anticipation of forces during object lifting. Journal of Neuroscience, 25(9), 2277-2284. doi: 10.1523/JNEUROSCI.4649-04.2005

Chouinard, P. A., Van der Werf, Y. D., Leonard, G., & Paus, T. (2003). Modulating neural networks with transcranial magnetic stimulation applied over the dorsal premotor and primary motor cortices. Journal of Neurophysiology, 90(2), 1071-1083. doi: 10.1152/jn.01105.2002

Chouinard, P. A. & Paus, T. (2010). What we have learned from “perturbing” the human cortical motor system with transcranial magnetic stimulation. Frontiers in Human Neuroscience, 4:173. doi: 10.3389/fnhum.2010.00173

Cisek P, Kalaska JF. 2010. Neural mechanisms for interacting with a world full of action choices. Annu Rev Neurosci. 33:269–298.

Cisek P, Kalaska JF. 2002. Simultaneous encoding of multiple potential reach directions in dorsal premotor cortex. J Neurophysiol. 87:1149–1154.

Cisek P, Kalaska JF. 2005. Neural correlates of reaching decisions in dorsal premotor cortex: specification of multiple direction choices and final selection of action. Neuron. 45:801–814.

Cohen YE, Andersen RA. 2002. A common reference frame for movement plans in the posterior parietal cortex. Nat Rev Neurosci. 3(7):553-62.

Colby, C. L., Duhamel, J. R., & Goldberg, M. E. (1996). Visual, presaccadic, and cognitive activation of single neurons in monkey lateral intraparietal area. Journal of Neurophysiology, 76(5), 2841-2852.

Colby and Goldberg. 1999. Space and attention in parietal cortex. Annual Review of Neuroscience. 22: 319-349.

Connolly JD, Andersen RA, Goodale MA. 2003. FMRI evidence for a “parietal reach region” in the human brain. Exp brain Res. 153:140–145.

Connolly JD, Goodale MA, Cant JS, Munoz DP. 2007. Effector-specific fields for motor preparation in the human frontal cortex. Neuroimage. 34:1209–1219.

Connolly JD, Goodale MA, DeSouza JF, Menon RS, Vilis T. 2000. A comparison of frontoparietal fMRI activation during anti-saccades and anti-pointing. J Neurophysiol. 84:1645–1655.

Corbetta, M., Akbudak, E., Conturo, T. E., Snyder, A. Z., Ollinger, J. M., Drury, H. A., . . . Shulman, G. L. (1998). A common network of functional areas for attention and eye movements. Neuron, 21(4), 761-773.

Courtney SM, Ungerleider LG, Keil K, Haxby J V.1996. Object and spatial visual working memory activate separate neural systems in human cortex. Cereb Cortex. 6:39–49.

Crawford JD, Henriques DY, Medendorp WP. 2011. Three-dimensional transformations for goal-directed action. Annu Rev Neurosci. 34:309-31.

Crawford JD, Medendorp WP, Marotta JJ. 2004. Spatial transformations for eye-hand coordination. J Neurophysiol. 92(1):10-9.

Culham, J. C., Danckert, S. L., DeSouza, J. F. X., Gati, J. S., Menon, R. S., & Goodale, M. A. (2003). Visually guided grasping produces fMRI activation in dorsal but not ventral stream brain areas. Experimental Brain Research, 153(2), 180-189. doi: 10.1007/s00221-003-1591-5

Culham, J. C., & Kanwisher, N. G. (2001). Neuroimaging of cognitive functions in human parietal cortex. Current Opinion in Neurobiology, 11(2), 157-163. doi: 10.1016/S0959-4388(00)00191-4

Culham, J. C., & Valyear, K. F. (2006). Human parietal cortex in action. Current Opinion in Neurobiology, 16(2), 205-212. doi: 10.1016/j.conb.2006.03.005

Culham, J. C., Cavina-Pratesi, C., & Singhal, A. (2006). The role of parietal cortex in visuomotor control: What have we learned from neuroimaging? Neuropsychologia, 44(13), 2668-2684. doi: 10.1016/j.neuropsychologia.2005.11.003 Curtis CE, Connolly JD. 2008. Saccade preparation signals in the human frontal and parietal cortices. J Neurophysiol. 99(1):133-145.

Curtis CE, Rao VY, D'Esposito M. 2004. Maintenance of spatial and motor codes during oculomotor delayed response tasks. J Neurosci. 24(16):3944-3952.

Curtis CE. 2006. Prefrontal and parietal contributions to spatial working memory. Neuroscience 139(1):173-80.

Davare, M., Andres, M., Cosnard, G., Thonnard, J. L., & Olivier, E. (2006). Dissociating the role of ventral and dorsal premotor cortex in precision grasping. Journal of Neuroscience, 26(8), 2260-2268.

Davare, M., Zenon, A., Pourtois, G., Desmurget, M., & Olivier, E. (2012). Role of the medial part of the intraparietal sulcus in implementing movement direction. Cerebral Cortex, 22(6), 1382-1394.

Davare, M., Lemon, R., & Olivier, E. (2008). Selective modulation of interactions between ventral premotor cortex and primary motor cortex during precision grasping in humans. Journal of Physiology-London, 586(11), 2735-2742.

Davare, M., Montague, K., Olivier, E., Rothwell, J. C., & Lemon, R. N. (2009). Ventral premotor to primary motor cortical interactions during object-driven grasp in humans. Cortex, 45(9), 1050-1057.

Davare, M., Kraskov, A., Rothwell, J. C., & Lemon, R. N. (2010). Interactions between areas of the cortical grasping network. Current Oninion in Neurobiology, 21:565-570.

Davare, M., Rothwell, J. C., & Lemon, R. N. (2010). Causal connectivity between the human anterior intraparietal area and premotor cortex during grasp. Current Biology, 20(2), 176-181.

Desmurget, M., Epstein, C. M., Turner, R. S., Prablanc, C., Alexander, G. E., & Grafton, S. T. (1999). Role of the posterior parietal cortex in updating reaching movements to a visual target. Nature Neuroscience, 2(6), 563-567.

Desmurget M, Pélisson D, Rossetti Y, Prablanc C. 1998. From eye to hand: planning goal-directed movements. Neurosci Biobehav Rev. 22(6):761-88.

DeSouza JF, Dukelow SP, Gati JS, Menon RS, Andersen RA, Vilis T. 2000. Eye position signal modulates a human parietal pointing region during memory-guided movements. J Neurosci. 20:5835–5840.

Dessing, J. C., Vesia, M., & Crawford, J. D. (2013). The role of areas MT+/V5 and SPOC in spatial and temporal control of manual interception: An rTMS study. Frontiers in Behavioral Neuroscience, 7, 15.

Elkington, P. T. G., Kerr, G. K., & Stein, J. S. (1992). The effect of electromagnetic stimulation of the posterior parietal cortex on eye-movements. Eye, 6, 510-514.

Engel SA, Glover GH, Wandell BA. 1997. Retinotopic organization in human visual cortex and the spatial precision of functional MRI. Cereb Cortex. 7:181–192.

Eskandar, E. N., & Assad, J. A. (1999). Dissociation of visual, motor and predictive signals in parietal cortex during visual guidance. Nature Neuroscience, 2(1), 88-93.

Fabbri S, Caramazza A, Lingnau A. 2012. Distributed sensitivity for movement amplitude in directionally tuned neuronal populations. J Neurophysiol. 107:1845–1856.

Farrer C, Frey SH, Van Horn JD, Tunik E, Turk D, Inati S, Grafton ST. 2008. The angular gyrus computes action awareness representations. Cereb Cortex. 18(2):254-61.

Fattori, P., Gamberini, M., Kutz, D. F., & Galletti, C. (2001). 'Arm-reaching' neurons in the parietal area V6A of the macaque monkey. European Journal of Neuroscience, 13(12), 2309-2313.

Fattori, P., Breveglieri, R., Marzocchi, N., Filippini, D., Bosco, A., & Galletti, C. (2009). Hand orientation during reach-to-grasp movements modulates neuronal activity in the medial posterior parietal area V6A. Journal of Neuroscience, 29(6), 1928-1936.

Fernandez-Ruiz J, Goltz HC, DeSouza JFX, Vilis T, Crawford JD. 2007. Human parietal “reach region” primarily encodes intrinsic visual direction, not extrinsic movement direction, in a visual motor dissociation task. Cereb Cortex. 17:2283–2292.

Ferraina, S., Battaglia-Mayer, A., Genovesio, A., Marconi, B., Onorati, P., & Caminiti, R. (2001). Early coding of visuomanual coordination during reaching in parietal area PEc. Journal of Neurophysiology, 85(1), 462-467.

Filimon, F. (2010). Human cortical control of hand movements: Parietofrontal networks for reaching, grasping, and pointing. Neuroscientist, 16(4), 388-407.

Filimon, F., Nelson, J. D., Huang, R., & Sereno, M. I. (2009). Multiple parietal reach regions in humans: Cortical representations for visual and proprioceptive feedback during on-line reaching. Journal of Neuroscience, 29(9), 2961-2971.

Flanagan JR, Johansson RS. 2003. Action plans used in action observation. Nature. 424:769–771.

Fogassi, L., Gallese, V., Fadiga, L., Luppino, G., Matelli, M., & Rizzolatti, G. (1996). Coding of peripersonal space in inferior premotor cortex (area F4). Journal of Neurophysiology, 76(1), 141-157.

Gail A, Andersen RA. 2006. Neural dynamics in monkey parietal reach region reflect context-specific sensorimotor transformations. J Neurosci. 26:9376–9384.

Gail A, Klaes C, Westendorff S. 2009. Implementation of spatial transformation rules for goal-directed reaching via gain modulation in monkey parietal and premotor cortex. J Neurosci. 29(30):9490-9499.

Gallese, V., Murata, A., Kaseda, M., Niki, N., & Sakata, H. (1994). Deficit of hand preshaping after muscimol injection in monkey parietal cortex. Neuroreport, 5(12), 1525-1529.

Galletti, C., Kutz, D. F., Gamberini, M., Breveglieri, R., & Fattori, P. (2003). Role of the medial parieto-occipital cortex in the control of reaching and grasping movements. Experimental Brain Research, 153(2), 158-170.

Gallivan JP, Cavina-Pratesi C, Culham JC. 2009. Is that within reach? fMRI reveals that the human superior parieto-occipital cortex encodes objects reachable by the hand. J Neurosci. 29:4381–4391.

Gallivan JP, Culham JC. 2015. Neural coding within human brain areas involved in actions. Curr Opin Neurobiol. 33:141–149.

Gallivan JP, McLean A, Culham JC. 2011. Neuroimaging reveals enhanced activation in a reach-selective brain area for objects located within participants' typical hand workspaces. Neuropsychologia. 49:3710–3721.

Georgopoulos, A. P., Kalaska, J. F., Caminiti, R., & Massey, J. T. (1982). On the relations between the direction of two-dimensional arm movements and cell discharge in primate motor cortex. Journal of Neuroscience, 2(11), 1527-1537.

Gertz H, Fiehler K. 2015. Human posterior parietal cortex encodes the movement goal in a pro-/anti-reach task. J Neurophysiol. 114:170–183.

Ghilardi, M. F., Alberoni, M., Marelli, S., Rossi, M., Franceschi, M., Ghez, C., & Fazio, F. (1999). Impaired movement control in alzheimer's disease. Neuroscience Letters, 260(1), 45-48. doi: 10.1016/S0304-3940(98)00957-4

Ghilardi, M. F., Alberoni, M., Rossi, M., Franceschi, M., Mariani, C., & Fazio, F. (2000). Visual feedback has differential effects on reaching movements in parkinson's and alzheimer's disease. Brain Research, 876(1-2), 112-123. doi: 10.1016/S0006-8993(00)02635-4

Glover, S., Miall, R. C., & Rushworth, M. F. S. (2005). Parietal rTMS disrupts the initiation but not the execution of on-line adjustments to a perturbation of object size. Journal of Cognitive Neuroscience, 17(1), 124-136.

Goodale MA. 2011 Transforming Vision into Action. Vision Res. 51(13):1567-87.

Goodale, M. A., & Milner, A. D. (1992). Separate visual pathways for perception and action. Trends in Neurosciences, 15(1), 20-25.

Goodale, M. A., Milner, A. D., Jakobson, L. S., & Carey, D. P. (1991). A neurological dissociation between perceiving objects and grasping them. Nature, 349(6305), 154-156.

Gorbet, D. J., Staines, W. R., & Sergio, L. E. (2004). Brain mechanisms for preparing increasingly complex sensory to motor transformations. Neuroimage, 23(3), 1100-1111. doi: 10.1016/j.neuroimage.2004.07.043

Gottlieb, J., & Goldberg, M. E. (1999). Activity of neurons in the lateral intraparietal area of the monkey during an antisaccade task. Nature Neuroscience, 2(10), 906-912. doi: 10.1038/13209

Gottlieb, J. P., Kusunoki, M., & Goldberg, M. E. (1998). The representation of visual salience in monkey parietal cortex. Nature, 391(6666), 481-484.

Graziano, M. S. A., Hu, X. T. A., & Gross, C. G. (1997). Visuospatial properties of ventral premotor cortex. Journal of Neurophysiology, 77(5), 2268-2292.

Gu C, Wood DK, Gribble PL, Corneil BD. A trial-by-trial window into sensorimotor transformations in the human motor periphery. J Neurosci. 36(31):8273-8282.

Gutteling TP, Petridou N, Dumoulin SO, Harvey BM, Aarnoutse EJ, Kenemans JL, Neggers SF. 2015. Action preparation shapes processing in early visual cortex. J Neurosci. 35(16):6472-6480.

Haar S, Donchin O, Dinstein I (2015) Dissociating visual and motor directional selectivity using visuomotor adaptation. J Neurosci 35:6813–6821.

Hawkins KM, Sayegh P, Yan X, Crawford JD, Sergio LE. 2013. Neural activity in superior parietal cortex during rule-based visual-motor transformations. J Cogn Neurosci. 25:436–454.

Heed, T., Beurze, S. M., Toni, I., Roder, B., & Medendorp, W. P. (2011). Functional rather than effector-specific organization of human posterior parietal cortex. Journal of Neuroscience, 31(8), 3066-3076.

Henriques DY, Klier EM, Smith MA, Lowy D, Crawford JD. 1998. Gaze-centered remapping of remembered visual space in an open-loop pointing task. J Neurosci. 18:1583–1594.

Hirnstein M, Bayer U, Ellison A, Hausmann M. 2011. TMS over the left angular gyrus impairs the ability to discriminate left from right. Neuropsychologia. 49(1):29-33.

Hocherman, S., & Wise, S. P. (1991). Effects of hand movement path on motor cortical activity in awake, behaving rhesus-monkeys. Experimental Brain Research, 83(2), 285-302.

Humphrey, G. K., Goodale, M. A., Jakobson, L. S., & Servos, P. (1994). The role of surface information in object recognition - studies of a visual form agnosic and normal subjects. Perception, 23(12), 1457-1481.

Jeannerod, M., Arbib, M. A., Rizzolatti, G., & Sakata, H. (1995). Grasping objects - the cortical mechanisms of visuomotor transformation. Trends in Neurosciences, 18(7), 314-320.

Jerde TA, Merriam EP, Riggall AC, Hedges JH, Curtis CE. 2012. Prioritized maps of space in human frontoparietal cortex. 32(48):17382-90.

Johnson, P. B., Ferraina, S., Bianchi, L., & Caminiti, R. (1996). Cortical networks for visual reaching: Physiological and anatomical organization of frontal and parietal lobe arm regions. Cerebral Cortex, 6(2), 102-119.

Kakei, S., Hoffman, D. S., & Strick, P. L. (2001). Direction of action is represented in the ventral premotor cortex. Nature Neuroscience, 4(10), 1020-1025.

Kakei, S., Hoffman, D. S., & Strick, P. L. (2003). Sensorimotor transformations in cortical motor areas. Neuroscience Research, 46(1), 1-10.

Kalaska, J. F. (1996). Parietal cortex area 5 and visuomotor behavior. Canadian Journal of Physiology and Pharmacology, 74(4), 483-498. doi: 10.1139/cjpp-74-4-483

Kalaska, J. F., Scott, S. H., Cisek, P., & Sergio, L. E. (1997). Cortical control of reaching movements. Current Opinion in Neurobiology, 7(6), 849-859.

Kapoula, Z., Yang, Q., Coubard, O., Daunys, G., & Orssaud, C. (2005). Role of the posterior parietal cortex in the initiation of saccades and vergence: Right/left functional asymmetry. Clinical and Basic Oculomotor Research: In Honor of David S.Zee, 1039, 184-197.

Konen CS, Mruczek REB, Montoya JL, Kastner S. 2013. Functional organization of human posterior parietal cortex: grasping- and reaching-related activations relative to topographically organized cortex. J Neurophysiol. 109:2897–2908.

Koyama, M., Hasegawa, I., Osada, T., Adachi, Y., Nakahara, K., & Miyashita, Y. (2004). Functional magnetic resonance imaging of macaque monkeys performing visually guided saccade tasks: Comparison of cortical eye fields with humans. Neuron, 41(5), 795-807.

Kravitz DJ, Saleem KS, Baker CI, Mishkin M. 2011 A new neural framework for visuospatial processing. Nat Rev Neurosci. 12(4):217-230.

Kuang S, Morel P, Gail A. 2016. Planning Movements in Visual and Physical Space in Monkey Posterior Parietal Cortex. Cerebral Cortex. 26(2):731-747.

Kluger, A., Gianutsos, J. G., Golomb, J., Ferris, S. H., George, A. E., Franssen, E., & Reisberg, B. (1997). Patterns of motor impairment in normal aging, mild cognitive decline, and early alzheimer's disease. Journals of Gerontology Series B-Psychological Sciences and Social Sciences, 52(1), P28-P39.

Lauritzen TZ, D’Esposito M, Heeger DJ, Silver MA. 2009. Top–down flow of visual spatial attention signals from parietal to occipital cortex. Journal of Vision 9(13):18.

Lee, J. H., & van Donkelaar, P. (2006). The human dorsal premotor cortex generates on-line error corrections during sensorimotor adaptation. Journal of Neuroscience, 26(12), 3330-3334.

Macaluso E, Frith C, Driver J. 2000. Selective spatial attention in vision and touch: unimodal and multimodal mechanisms revealed by PET. J Neurophysiol. 83:3062–3075.

Mackay, W. A. (1992). Properties of reach-related neuronal-activity in cortical area 7a. Journal of Neurophysiology, 67(5), 1335-1345.

Makino Y, Yokosawa K, Takeda Y, Kumada T. 2004. Visual search and memory search engage extensive overlapping cerebral cortices: an fMRI study. Neuroimage. 23:525–533.

Malfait, N., Valyear, K. F., Culham, J. C., Anton, J., Brown, L. E., & Gribble, P. L. (2010). fMRI activation during observation of others' reach errors. Journal of Cognitive Neuroscience, 22(7), 1493-1503.

Malik P, Dessing JC, Crawford JD. 2015. Role of early visual cortex in trans-saccadic memory of object features. J Vis. 15(11):7.

Medendorp WP, Goltz HC, Crawford JD, Vilis T. 2005. Integration of target and effector information in human posterior parietal cortex for the planning of action. J Neurophysiol. 93:954–962.

Medendorp WP, Goltz HC, Vilis T. 2006. Directional selectivity of BOLD activity in human posterior parietal cortex for memory-guided double-step saccades. J Neurophysiol. 95:1645–1655.

Medendorp WP, Goltz HC, Vilis T, Crawford JD. 2003. Gaze-centered updating of visual space in human parietal cortex. J Neurosci. 23:6209–6214.

Medendorp, W. P., Buchholz, V. N., Van Der Werf, J., & Leone, F. T. M. (2011). Parietofrontal circuits in goal-oriented behaviour. European Journal of Neuroscience, 33(11), 2017-2027.

Merriam, E. P., Genovese, C. R., & Colby, C. L. (2003). Spatial updating in human parietal cortex. Neuron, 39(2), 361-373.

Messier J, Kalaska JF. 2000. Covariation of primate dorsal premotor cell activity with direction and amplitude during a memorized-delay reaching task. J Neurophysiol. 84(1):152-165.

Miller, L., Sun, F., Curtis, C., & D'Esposito, M. (2005). Functional interactions between oculomotor regions during prosaccades and antisaccades. Human Brain Mapping, 26(2), 119-127.

Milner, A. D., Dijkerman, H. C., Pisella, L., McIntosh, R. D., Tilikete, C., Vighetto, A., & Rossetti, Y. (2001). Grasping the past: Delay can improve visuomeotor performance. Current Biology, 11(23), 1896-1901.

Mishkin, M., & Ungerleider, L. G. (1982). Contribution of striate inputs to the visuospatial functions of parieto-preoccipital cortex in monkeys. Behavioural Brain Research, 6(1), 57-77.

Monaco S, Cavina-Pratesi C, Sedda A, Fattori P, Galletti C, Culham JC. 2011. Functional magnetic resonance adaptation reveals the involvement of the dorsomedial stream in hand orientation for grasping. J Neurophysiol. 106:2248–2263.

Moore, T., & Fallah, M. (2001). Control of eye movements and spatial attention. Proceedings of the National Academy of Sciences of the United States of America, 98(3), 1273-1276.

Morris, A. P., Chambers, C. D., & Mattingley, J. B. (2007). Parietal stimulation destabilizes spatial updating across saccadic eye movements. Proceedings of the National Academy of Sciences of the United States of America, 104(21), 9069-9074.

Mountcastle, V. B., Lynch, J. C., Georgopoulos, A., Sakata, H., & Acuna, C. (1975). Posterior parietal association cortex of monkey - command functions for operations within extrapersonal space. Journal of Neurophysiology, 38(4), 871-908.

Murata, A., Gallese, V., Luppino, G., Kaseda, M., & Sakata, H. (2000). Selectivity for the shape, size, and orientation of objects for grasping in neurons of monkey parietal area AIP. Journal of Neurophysiology, 83(5), 2580-2601.

Muri, R. M., Vermersch, A. I., Rivaud, S., Gaymard, B., & PierrotDeseilligny, C. (1996). Effects of single-pulse transcranial magnetic stimulation over the prefrontal and posterior parietal cortices during memory-guided saccades in humans. Journal of Neurophysiology, 76(3), 2102-2106.

Olson CR. 2003. Brain representation of object-centered space in monkeys and humans. Annu Rev Neurosci. 26:331–354.

Oyachi, H., & Ohtsuka, K. (1995). Transcranial magnetic stimulation of the posterior parietal cortex degrades accuracy of memory-guided saccades in humans. Investigative Ophthalmology & Visual Science, 36(7), 1441-1449.

Pare, M., & Wurtz, R. H. (1997). Monkey posterior parietal cortex neurons antidromically activated from superior colliculus. Journal of Neurophysiology, 78(6), 3493-3497.

Pare, M., & Wurtz, R. H. (2001). Progression in neuronal processing for saccadic eye movements from parietal cortex area LIP to superior colliculus. Journal of Neurophysiology, 85(6), 2545-2562.

Pasternak T, Greenlee MW. 2005. Working memory in primate sensory systems. Nat Rev Neurosci. 6:97–107.

Perenin MT, Vighetto A. 1988. Optic ataxia: a specific disruption in visuomotor mechanisms. I. Different aspects of the deficit in reaching for objects. Brain. 111 (Pt 3:643–674.

Perry CJ, Sergio LE, Crawford JD, Fallah M. 2015. Hand placement near the visual stimulus improves orientation selectivity in V2 neurons. 113(7): 2859-2870.

Pesaran, B., Pezaris, J. S., Sahani, M., Mitra, P. P., & Andersen, R. A. (2002). Temporal structure in neuronal activity during working memory in macaque parietal cortex. Nature Neuroscience, 5(8), 805-811.

Pesaran, B., Nelson, M. J., & Andersen, R. A. (2006). Dorsal premotor neurons encode the relative position of the hand, eye, and goal during reach planning. Neuron, 51(1), 125-134.

Petit, L., & Haxby, J. V. (1999). Functional anatomy of pursuit eye movements in humans as revealed by fMRI. Journal of Neurophysiology, 82(1), 463-471.

Picard N, Strick PL. 2001. Imaging the premotor areas. Curr Opin Neurobiol. 11:663–672.

Pisella, L., Sergio, L., Blangero, A., Torchin, H., Vighetto, A., & Rossetti, Y. (2009). Optic ataxia and the function of the dorsal stream: Contributions to perception and action. Neuropsychologia, 47(14), 3033-3044.

Prablanc, C., Echallier, J. F., Komilis, E., & Jeannerod, M. (1979). Optimal response of eye and hand motor systems in pointing at a visual target .1. spatio-temporal characteristics of eye and hand movements and their relationships when varying the amount of visual information. Biological Cybernetics, 35(2), 113-124.

Prado J, Clavagnier S, Otzenberger H, Scheiber C, Kennedy H, Perenin M-T. 2005. Two cortical systems for reaching in central and peripheral vision. Neuron. 48:849–858.

Pratte MS, Tong F. 2014. Spatial specificity of working memory representations in the early visual cortex. J Vis. 14(3):22.

Prime, S. L., M. Vesia, et al. (2008). Transcranial magnetic stimulation over posterior parietal cortex disrupts transsaccadic memory of multiple objects. Journal of Neuroscience 28(27): 6938-6949.

Prime, S. L., M. Vesia, et al. (2010). TMS Over Human Frontal Eye Fields Disrupts Trans-saccadic Memory of Multiple Objects. Cerebral Cortex 20(4): 759-772.

Quinlan, D. J., & Culham, J. C. (2007). fMRI reveals a preference for near viewing in the human parieto-occipital cortex. Neuroimage, 36(1), 167-187.

Rawley JB, Constantinidis C. 2009. Neural correlates of learning and working memory in the primate posterior parietal cortex. Neurobiol Learn Mem. 91:129–138.

Reed CL, Grubb JD, Steele C. 2006. Hands up: attentional prioritization of space near the hand. J Exp Psychol Hum Percept Perform. 32:166–177.

Revechkis B, Aflalo TN, Kellis S, Pouratian N, Andersen RA. Parietal neural prosthetic control of a computer cursor in a graphical-user-interface task. J Neural Eng. 11(6): 066014.

Rice, N. J., Tunik, E., Cross, E. S., & Grafton, S. T. (2007). On-line grasp control is mediated by the contralateral hemisphere. Brain Research, 1175, 76-84.

Rice, N. J., Tunik, E., & Grafton, S. T. (2006). The anterior intraparietal sulcus mediates grasp execution, independent of requirement to update: New insights from transcranial magnetic stimulation. Journal of Neuroscience, 26(31), 8176-8182.

Rizzolatti, G., Fadiga, L., Gallese, V., & Fogassi, L. (1996). Premotor cortex and the recognition of motor actions. Cognitive Brain Research, 3(2), 131-141.

Rizzolatti, G., & Luppino, G. (2001). The cortical motor system. Neuron, 31(6), 889-901.

Rolfs M, Lawrence B, Carrasco, M. 2013. Reach preparation enhances visual performance and appearance. Philosophical Transactions of the Royal Society B: Biological Sciences, 368:20130057.

Rossetti Y, Pisella L, Vighetto A. 2003. Optic ataxia revisited: visually guided action versus immediate visuomotor control. Exp Brain Res. 153(2):171-179.

Ryan, S., Bonilha, L., & Jackson, S. R. (2006). Individual variation in the location of the parietal eye fields: A TMS study. Experimental Brain Research, 173(3), 389-394.

Sabes PN. The planning and control of reaching movements. Curr Opin Neurobiol. 10(6):740-6.

Sadeh M, Sajad A, Wang H, Yan X, Crawford JD. 2015. Spatial transformations between superior colliculus visual and motor response fields during head-unrestrained gaze shifts. Eur J Neurosci. 42(11):2934-51.

Sajad A, Sadeh M, Keith GP, Yan X, Wang H, Crawford JD. 2015. Visual-Motor Transformations Within Frontal Eye Fields During Head-Unrestrained Gaze Shifts in the Monkey. Cereb Cortex. 25(10):3932-52.

Sajad A, Sadeh M, Yan X, Wang H, Crawford JD. 2016. Transition from Target to Gaze Coding in Primate Frontal Eye Field during Memory Delay and Memory–Motor Transformation. e0040-16.2016 1–20.

Salek, Y., Anderson, N. D., & Sergio, L. (2011). Mild cognitive impairment is associated with impaired visual-motor planning when visual stimuli and actions are incongruent. European Neurology, 66(5), 283-293. doi: 10.1159/000331049

Schall, J. D., & Hanes, D. P. (1993). Neural basis of saccade target selection in frontal eye field during visual-search. Nature, 366(6454), 467-469.

Schall, J. D., Hanes, D. P., Thompson, K. G., & King, D. J. (1995a). Saccade target selection in frontal eye field of macaque .1. visual and premovement activation. Journal of Neuroscience, 15(10), 6905-6918.

Schall, J. D., Morel, A., King, D. J., & Bullier, J. (1995b). Topography of visual-cortex connections with frontal eye field in macaque - convergence and segregation of processing streams. Journal of Neuroscience, 15(6), 4464-4487.

Schall, J., Sato, T., Thompson, K., Vaughn, A., & Juan, C. (2004). Effects of search efficiency on surround suppression during visual selection in frontal eye field. Journal of Neurophysiology, 91(6), 2765-2769.

Schenk, T. (2006). An allocentric rather than perceptual deficit in patient DF. Nature Neuroscience 9(11): 1369-1370.

Schluppeck, D., Curtis, C., Glimcher, P., & Heeger, D. (2006). Sustained activity in topographic areas of human posterior parietal cortex during memory-guided saccades. Journal of Neuroscience, 26(19), 5098-5108.

Schluppeck, D., Glimcher, P., & Heeger, D. J. (2005). Topographic organization for delayed saccades in human posterior parietal cortex. Journal of Neurophysiology, 94(2), 1372-1384.

Scott, S. H., & Kalaska, J. F. (1997). Reaching movements with similar hand paths but different arm orientations .1. activity of individual cells in motor cortex. Journal of Neurophysiology, 77(2), 826-852.

Sergio, L. E., Hamel-Paquet, C., & Kalaska, J. F. (2005). Motor cortex neural correlates of output kinematics and kinetics during isometric-force and arm-reaching tasks. Journal of Neurophysiology, 94(4), 2353-2378.

Sergio, L. E., & Kalaska, J. F. (2003). Systematic changes in motor cortex cell activity with arm posture during directional isometric force generation. Journal of Neurophysiology, 89(1), 212-228.

Singh KD, Smith AT, Greenlee MW. 2000. Spatiotemporal frequency and direction sensitivities of human visual areas measured using fMRI. Neuroimage. 12:550–564.

Singhal A, Monaco S, Kaufman LD, Culham JC. 2013. Human fMRI reveals that delayed action re-recruits visual perception. PLoS One. 8(9):e73629.

Smith, E., & Jonides, J. (1998). Neuroimaging analyses of human working memory. Proceedings of the National Academy of Sciences of the United States of America, 95(20), 12061-12068. doi: 10.1073/pnas.95.20.12061

Smyrnis, N., Theleritis, C., Evdokimidis, I., Muri, R. M., & Karandreas, N. (2003). Single-pulse transcranial magnetic stimulation of parietal and prefrontal areas in a memory delay arm pointing task. Journal of Neurophysiology, 89(6), 3344-3350.

Snyder, LH. 2000. Coordinate transformations for eye and arm movements in the brain. Current Opinion in Neurobiology. 10:747–754.

Soechting, J. F., & Flanders, M. (1992). Moving in 3-dimensional space - frames of reference, vectors, and coordinate systems. Annual Review of Neuroscience, 15, 167-191.

Srimal R, Curtis CE. 2008. Persistent neural activity during the maintenance of spatial position in working memory. Neuroimage. 39(1):455-468.

Striemer, C. L., Chouinard, P. A., & Goodale, M. A. (2011). Programs for action in superior parietal cortex: A triple-pulse TMS investigation. Neuropsychologia, 49(9), 2391-2399.

Tehovnik, E. J., Sommer, M. A., Chou, I. H., Slocum, W. M., & Schiller, P. H. (2000). Eye fields in the frontal lobes of primates. Brain Research Reviews, 32(2-3), 413-448.

Thier, P., & Andersen, R. A. (1998). Electrical microstimulation distinguishes distinct saccade-related areas in the posterior parietal cortex. Journal of Neurophysiology, 80(4), 1713-1735.

Thomas, N. W. D., & Pare, M. (2007). Temporal processing of saccade targets in parietal cortex area LIP during visual search. Journal of Neurophysiology, 97(1), 942-947. doi: 10.1152/jn.00413.2006

Thompson, K. G., Bichot, N. P., & Schall, J. D. (1997). Dissociation of visual discrimination from saccade programming in macaque frontal eye field. Journal of Neurophysiology, 77(2), 1046-1050.

Thompson, K. G., Biscoe, K. L., & Sato, T. R. (2005). Neuronal basis of covert spatial attention in the frontal eye field. Journal of Neuroscience, 25(41), 9479-9487. doi: 10.1523/JNEUROSCI.0741-05.2005

Tippett, W. J., Krajewski, A., & Sergio, L. E. (2007). Visuomotor integration is compromised in alzheimer's disease patients reaching for remembered targets. European Neurology, 58(1), 1-11. doi: 10.1159/000102160

Tippett, W. J., & Sergio, L. E. (2006). Visuomotor integration is impaired in early stage alzheimer's disease. Brain Research, 1102, 92-102. doi: 10.1016/j.brainres.2006.04.049

Tippett, W. J., Sergio, L. E., & Black, S. E. (2012). Compromised visually guided motor control in individuals with alzheimer's disease: Can reliable distinctions be observed? Journal of Clinical Neuroscience, 19(5), 655-660. doi:10.1016/j.jocn.2011.09.013

Tosoni A, Galati G, Romani GL, Corbetta M. 2008. Sensory-motor mechanisms in human parietal cortex underlie arbitrary visual decisions. Nat Neurosci. 11:1446–1453.

Trotter, Y., & Celebrini, S. (1999). Gaze direction controls response gain in primary visual-cortex neurons. Nature, 398(6724), 239-242.

Tunik, E., Rice, N. J., Hamilton, A., & Grafton, S. T. (2007). Beyond grasping: Representation of action in human anterior intraparietal sulcus. Neuroimage, 36, T77-T86.

Uchimura, M., Nakano, T., Morito, Y., Ando, H., & Kitazawa, S. (2015). Automatic representation of a visual stimulus relative to a background in the right precuneus. Eur J Neurosci, 42(1), 1651-1659.

Valyear, K. F., Gallivan, J. P., McLean, D. A., & Culham, J. C. (2012). fMRI repetition suppression for familiar but not arbitrary actions with tools. Journal of Neuroscience, 32(12), 4247-4259.

Van Der Werf J, Jensen O, Fries P, Medendorp WP. 2008. Gamma-band activity in human posterior parietal cortex encodes the motor goal during delayed prosaccades and antisaccades. J Neurosci. 28(34):8397-8405.

Van Der Werf J, Jensen O, Fries P, Medendorp WP. 2010. Neuronal synchronization in human posterior parietal cortex during reach planning. J Neurosci. 30(4):1402-1412.

van Donkelaar, P. (1998). Saccade amplitude influences pointing movement kinematics. Neuroreport, 9(9), 2015-2018.

van Donkelaar, P., & Adams, J. (2005). Gaze-dependent deviation in pointing induced by transcranial magnetic stimulation over the human posterior parietal cortex. Journal of Motor Behavior, 37(2), 157-163.

van Donkelaar, P., Lee, J. H., & Drew, A. S. (2000). Transcranial magnetic stimulation disrupts eye-hand interactions in the posterior parietal cortex. Journal of Neurophysiology, 84(3), 1677-1680.

van Donkelaar, P., Lee, J. H., & Drew, A. S. (2002). Eye-hand interactions differ in the human premotor and parietal cortices. Human Movement Science, 21(3), 377-386.

Vesia M, Crawford JD. 2012. Specialization of reach function in human posterior parietal cortex. Exp brain Res. 221:1–18.

Vesia M, Monteon JA, Sergio LE, Crawford JD. 2006. Hemispheric asymmetry in memory-guided pointing during single-pulse transcranial magnetic stimulation of human parietal cortex. J Neurophysiol. 96(6):3016-3027.

Vesia M, Prime SL, Yan X, Sergio LE, Crawford JD. 2010. Specificity of human parietal saccade and reach regions during transcranial magnetic stimulation. J Neurosci. 30:13053–13065.

Vesia, M., Yan, X., Henriques, D. Y., Sergio, L. E., & Crawford, J. D. (2008). Transcranial magnetic stimulation over human dorsal-lateral posterior parietal cortex disrupts integration of hand position signals into the reach plan. Journal of Neurophysiology, 100(4), 2005-2014.

Wardak, C., Ibos, G., Duhamel, J. R., & Olivier, E. (2006). Contribution of the monkey frontal eye field to covert visual attention. Journal of Neuroscience, 26(16), 4228-4235.

Wardak, C., Olivier, E., & Duhamel, J. R. (2002). Saccadic target selection deficits after lateral intraparietal area inactivation in monkeys. Journal of Neuroscience, 22(22), 9877-9884.

Wardak, C., Olivier, E., & Duhamel, J. R. (2004). A deficit in covert attention after parietal cortex inactivation in the monkey. Neuron, 42(3), 501-508.

Weinrich M, Wise SP. 1982. The premotor cortex of the monkey. J Neurosci. 2(9):1329-1345.

Westendorff S, Klaes C, Gail A. 2010. The cortical timeline for deciding on reach motor goals. J Neurosci. 30:5426–5436.

Wise, S. P., Boussaoud, D., Johnson, P. B., & Caminiti, R. (1997). Premotor and parietal cortex: Corticocortical connectivity and combinatorial computations. Annual Review of Neuroscience, 20, 25-42.

Wise, S. P., & Mauritz, K. H. (1985). Set-related neuronal-activity in the premotor cortex of rhesus-monkeys - effects of changes in motor set. Proceedings of the Royal Society Series B-Biological Sciences, 223(1232), 331-354.

Zhang M, Barash S. 2000. Neuronal switching of sensorimotor transformations for antisaccades. Nature. 408(6815):971-975.

Appendix A: Chapter Two Supplementary Figures

Supplementary Figure 1

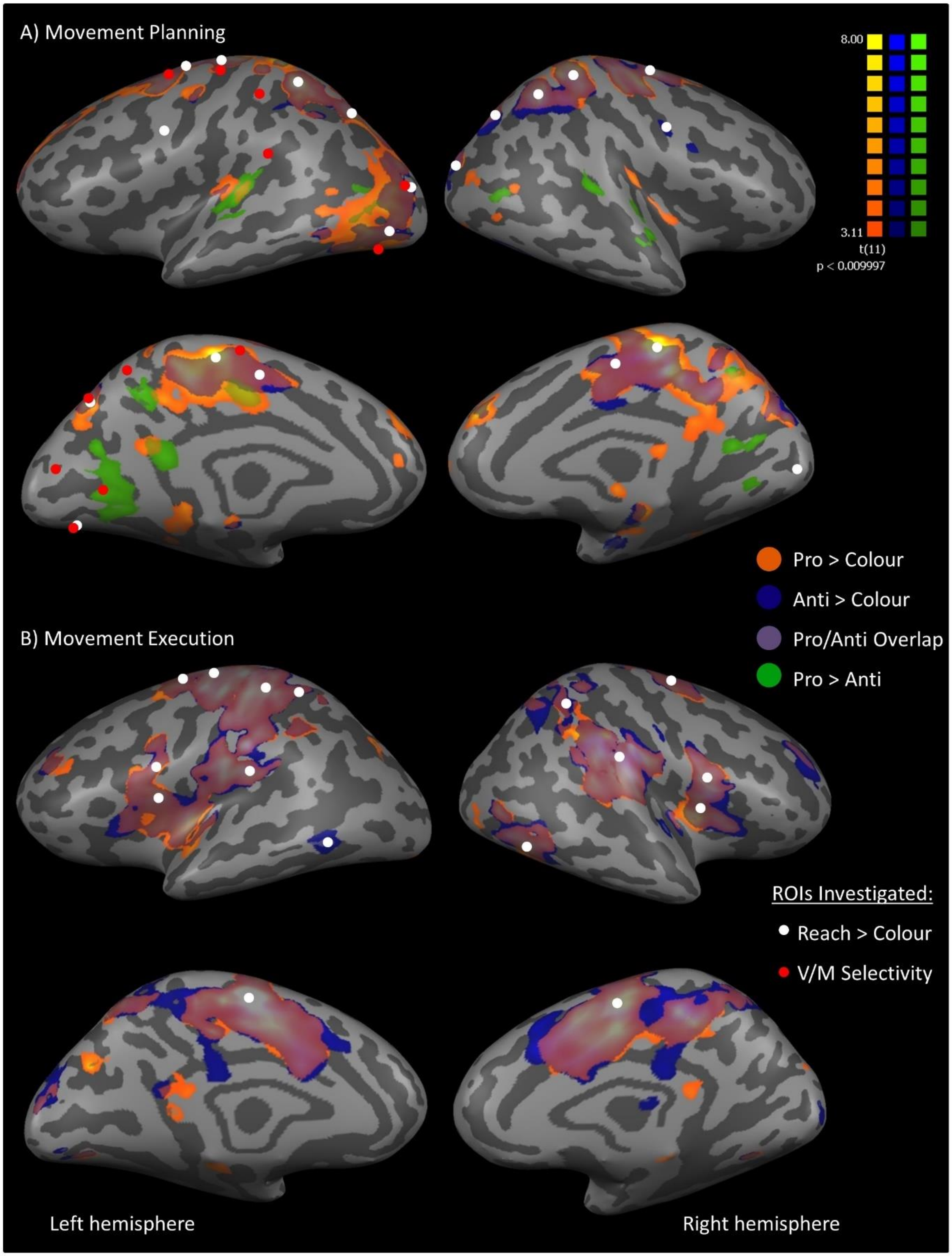

Supplementary Figure 1. Voxelwise statistical maps obtained from the RFX GLM for the contrasts Pro-Reach > Color report (orange scale), Anti-Reach > Color Report (blue scale), and Pro-Reach > Anti-Reach (green scale) during the motor planning (A) and motor execution (B) phases. Event-related group activation maps are displayed on the inflated brain of one representative subject for target representation. The leftward inflated brains represent the left hemisphere, and the rightward brains represent the right hemisphere. In A and B, the top figures show a lateral view and the bottom figures show the medial view. Highlighted areas show significantly higher activation than control data with a $p>0.01$ with cluster threshold corrections. Note the large amount of overlap between pro-reach > colour and anti-reach > colour. In both A and B, white dots represent the approximate location of the peak voxel for the ROIs from the motor planning and execution phases (respectively) form the reach > colour contrasts. In A, red dots indicate the approximate location of the peak voxels for the motor and visual directionally selective contrasts. For Movement Planning, of the general reach ROIs that we investigated in Figure 3 (white dots), bilateral PMd, mIPS, pIPS, SMA, CMA, and SOG, as well as left SPOC, M1, and IOG and Right S1 fell within areas of overlap. Bilateral PMv and LG fell within regions that only reached significance with combined anti and pro data (and thus do not appear here). For the left hemisphere visual or movement selective areas shown in Figure 5, PMd, M1S1, SOG, LG, & SPOC fell within areas of overlap. V1 fell within a region that showed greater pro-reach activation than anti and Cuneus, PCu, aIPS, and AG within regions that only reached significance with combined anti and pro data (and thus do not appear here). For Movement execution, bilateral PMd, PMv, mIPS, SMG, IFG, and SMA as well as right IOG and left M1 and S1 fell within areas of overlap. Left IOG fell within an area that showed greater activation for only anti-reach>colour.

Supplementary figure 2

A) Stimulus Representation

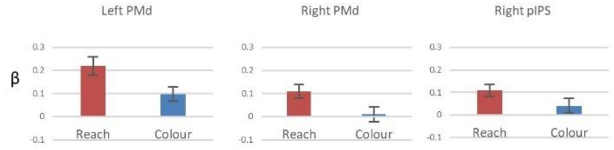

B) Movement Planning

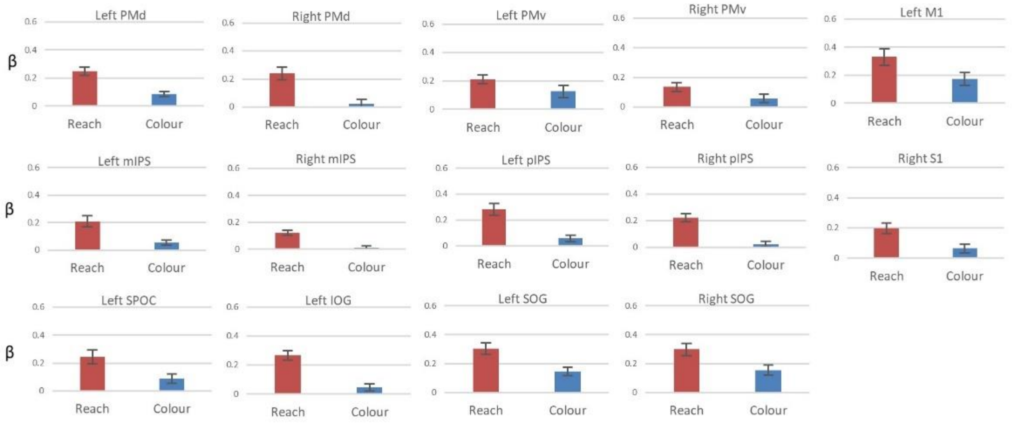

C) Movement Execution

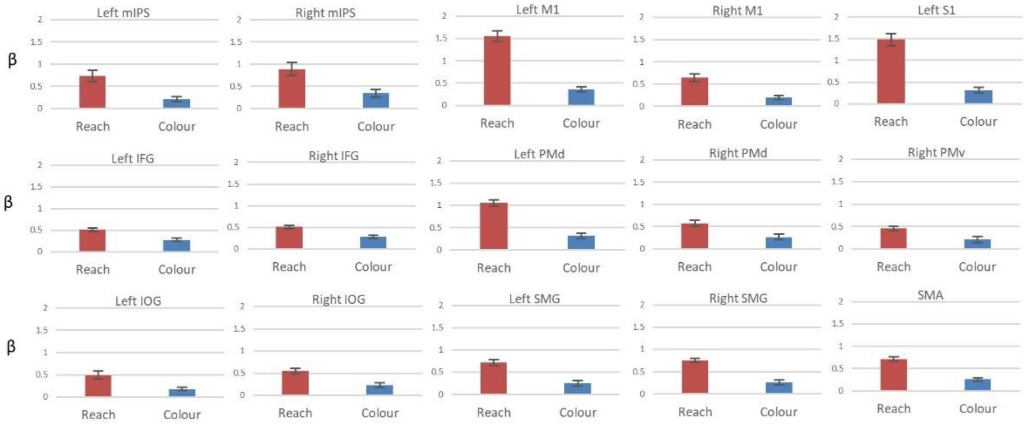

Supplementary Figure 2. A) Bar graphs represent the β weights for the reach (pro + anti) and colour conditions for each area showing target representation related activation, independent of target direction. ***B)*** Bar graphs represent the β weights for the reach (pro + anti) and colour conditions for each area showing motor planning related activation. ***C).*** Bar graphs represent the β weights for the reach (pro + anti) and colour conditions for each area showing motor execution related activation.

Supplementary Figure 3

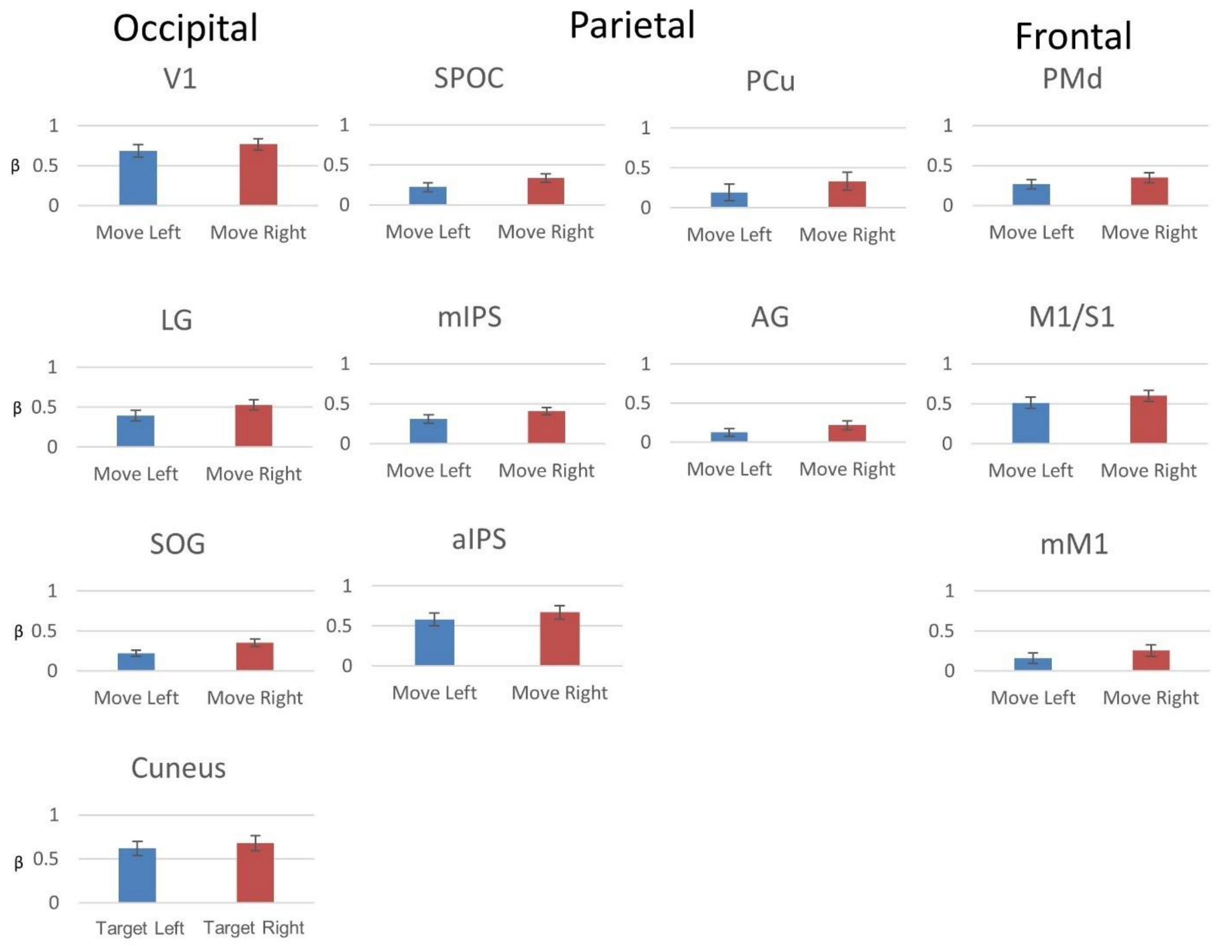

Supplementary Figure 3. Bar graphs represent the β weights related to the contrast for each area showing visual target (for Cuneus) or movement (for V1, LG, SOG, SPOC, mIPS, aIPS, PCu, AG, PMd, M1/S1, and mM1) related directional activation for the brain areas identified in contrast 4 and 5, respectively.

Supplementary Figure 4

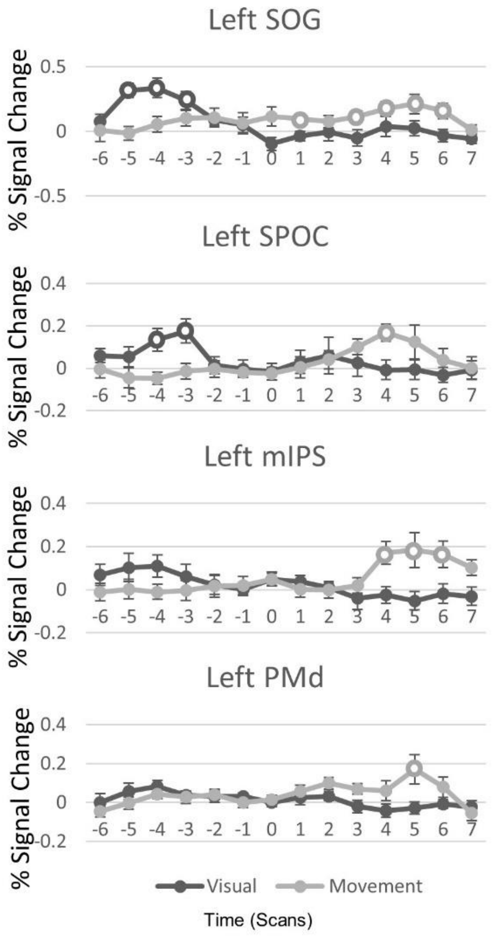

Supplementary Figure 4. A plot of the time course of visual and motor selectivity for left SOG, SPOC, mIPS, and PMd regions of interest taken from the motor planning phase from contrast 2. This figure follows the same conventions as figure 6.

Supplementary Figure 5

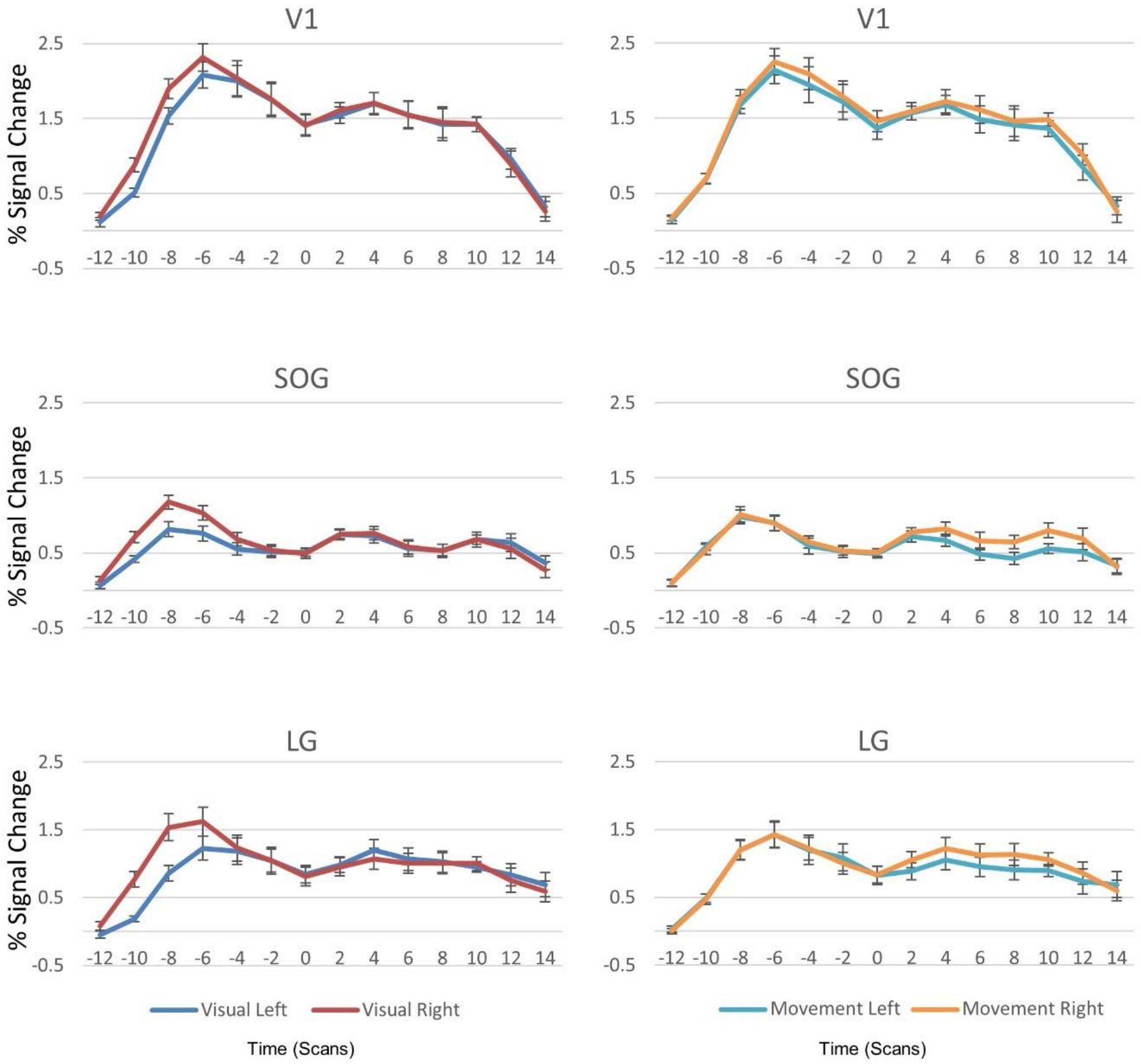

Supplementary Figure 5. A plot of the time course for visual left (pro-left + anti-left), visual right (pro-right + anti-right), motor left (pro-left + anti-right), and motor right (pro-right + anti-left) activation in occipital brain regions V1, SOG, and LG. These brain areas were taken from the regions of interest identified from contrasts 4 and 5 and shown in figure 5. Subtractions of these time courses produce the data for Figure 5. Error bars are SEM across subjects.

Supplementary Figure 6

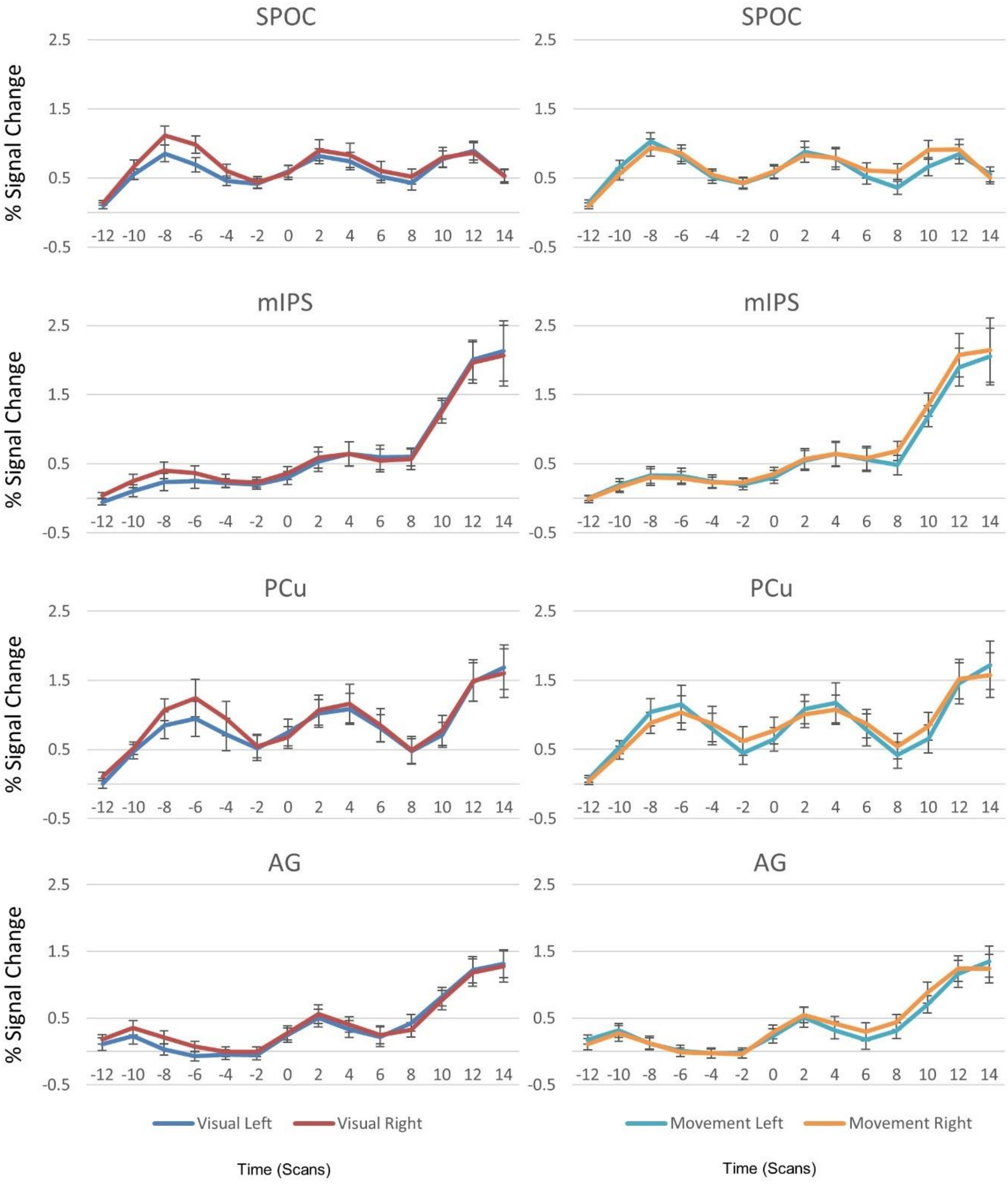

Supplementary Figure 6. A plot of the time course for visual left (pro-left + anti-left), visual right (pro-right + anti-right), motor left (pro-left + anti-right), and motor right (pro-right + anti-left) activation in parietal brain regions SPOC, mIPS, PCu, and AG. These brain areas were taken from the regions of interest identified from contrasts 4 and 5 and shown in figure 4. Subtractions of these time courses produce the data for Figure 5. Error bars are SEM across subjects.

Supplementary Figure 7

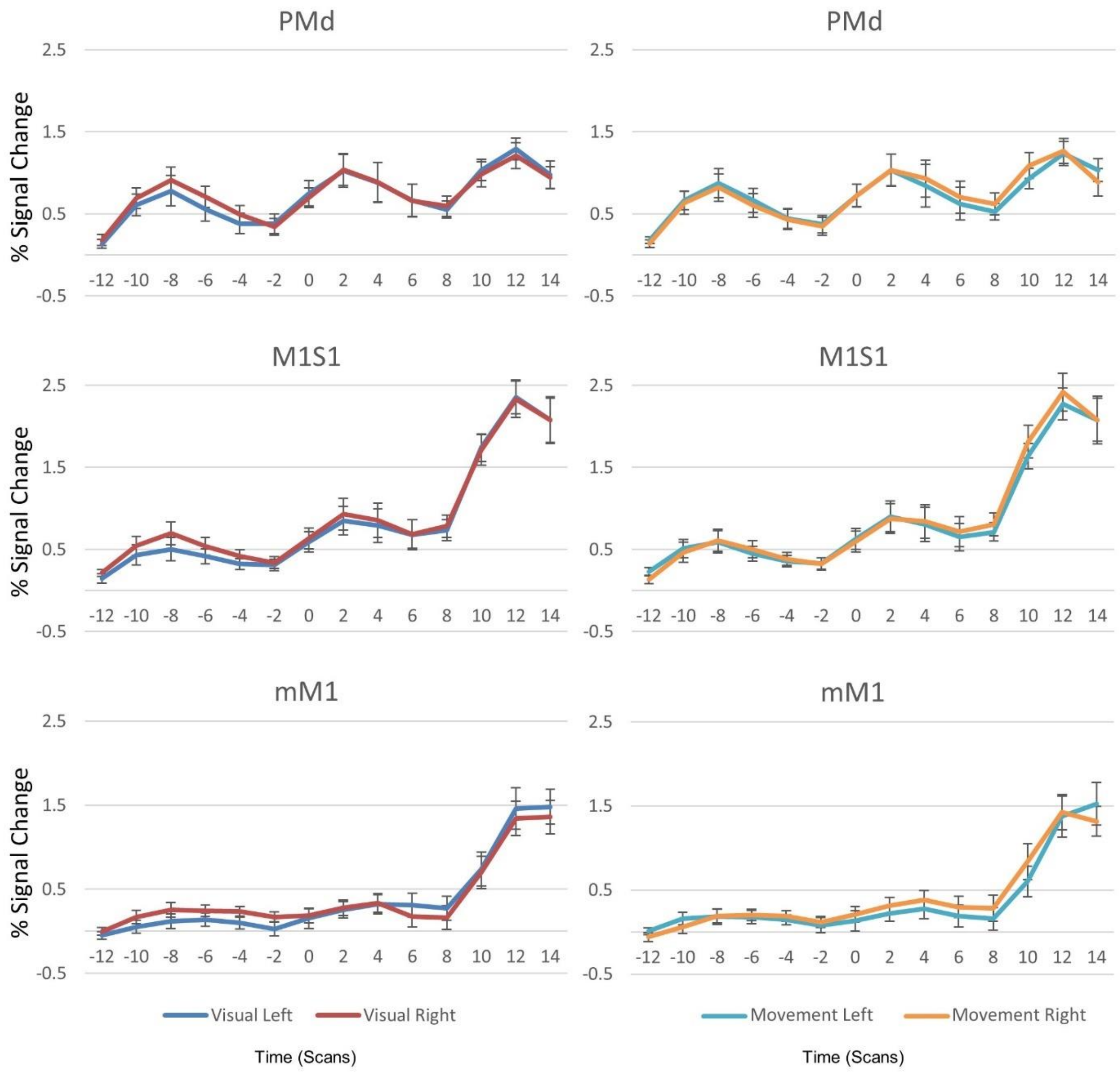

Supplementary Figure 7. A plot of the time course for visual left (pro-left + anti-left), visual right (pro-right + anti-right), motor left (pro-left + anti-right), and motor right (pro-right + anti-left) activation in frontal brain regions PMd, M1S1, and mM1. These brain areas were taken from the regions of interest identified from contrasts 4 and 5 and shown in figure 4. Subtractions of these time courses produce the data for Figure 5. Error bars are SEM across subjects.

Supplementary Figure 8

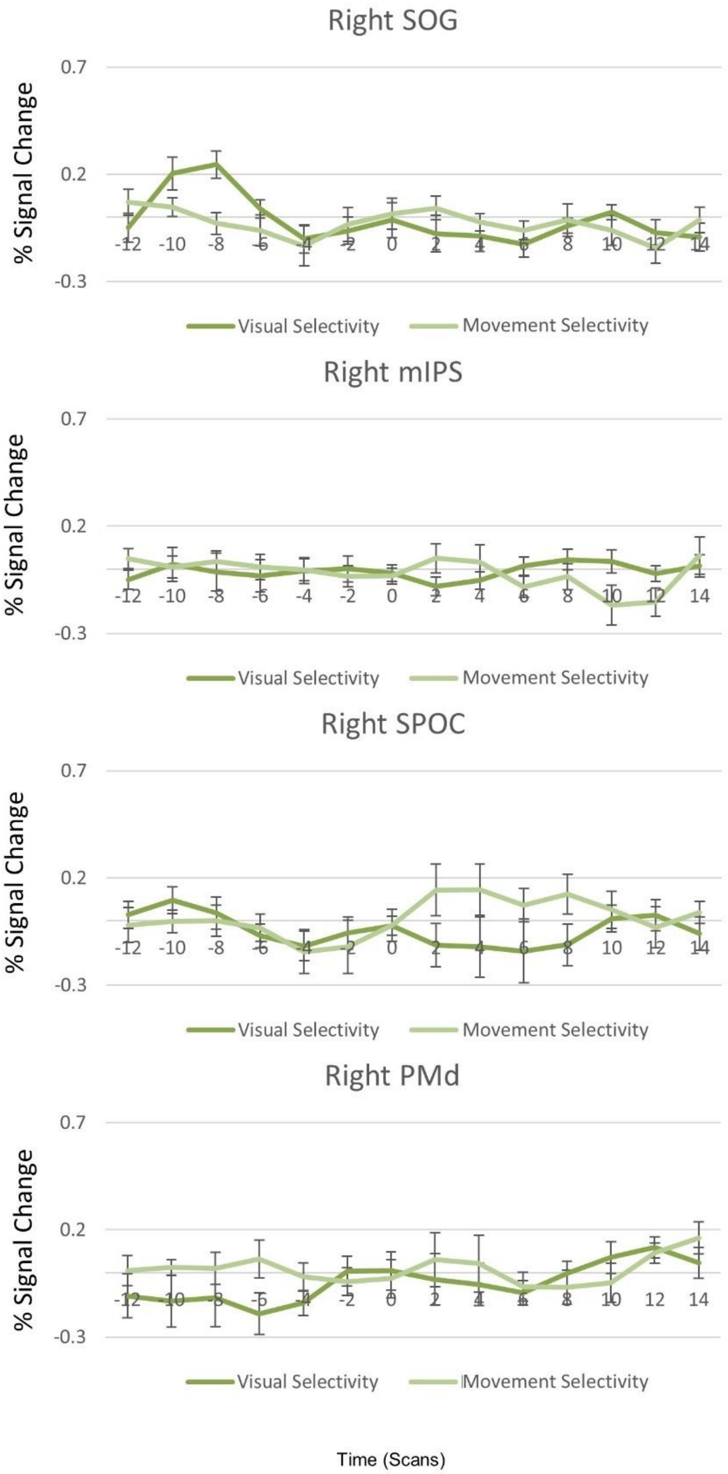

Supplementary Figure 8. Time courses showing visual and motor selectivity for right SOG, mIPS, SPOC, and PMd. This data was produced by creating volumes of interest in the right hemisphere by flipping the sign of the Talariach ‘x’ coordinate for these respective regions of interest identified by contrast 5 and creating a 5mm sphere ROI. Error bars are SEM across subjects.

Appendix B: Author Contributions

Chapter Two:

- Hypothesis generation: David Cappadocia and Doug Crawford
- Study design: David Cappadocia, Doug Crawford, and Simona Monaco
- Data collection and analysis: David Cappadocia
- Data interpretation and manuscript writing: All authors, with David Cappadocia as the primary author

Chapter Three:

- Hypothesis generation: David Cappadocia and Doug Crawford
- Study design: David Cappadocia, Doug Crawford, and Simona Monaco
- Data collection and analysis: David Cappadocia
- Data interpretation and manuscript writing: All authors, with David Cappadocia as the primary author